QCD on a small circle

Kyle Aitken, Aleksey Cherman, Erich Poppitz, and Laurence G. Yaffe

Phys. Rev. D **96**, 096022 — Published 27 November 2017

DOI: 10.1103/PhysRevD.96.096022

INT-PUB-17-026

QCD on a small circle

Kyle Aitken,[a] **Aleksey Cherman,**[b] **Erich Poppitz,**[c] **Laurence G. Yaffe**[a]

[a] *Department of Physics, University of Washington, Seattle, WA 98195-1560, USA*

[b] *Institute for Nuclear Theory, University of Washington, Seattle, WA 98195-1560, USA*

[c] *Department of Physics, University of Toronto, Toronto, ON M5S 1A7, Canada*

E-mail: kaitken17@gmail.com, aleksey.cherman.physics@gmail.com, poppitz@physics.utoronto.ca, yaffe@phys.washington.edu

Abstract: QCD-like theories can be engineered to remain in a confined phase when compactified on an arbitrarily small circle, where their features may be studied quantitatively in a controlled fashion. Previous work has elucidated the generation of a non-perturbative mass gap and the spontaneous breaking of chiral symmetry in this regime. Here, we study the rich spectrum of hadronic states, including glueball, meson, and baryon resonances. We find an exponentially growing Hagedorn density of states, as well as the emergence of non-perturbative energy scales given by iterated exponentials of the inverse Yang-Mills coupling g^2.

1 Introduction

There are few ways to analytically study the low temperature and density behavior of QCD-like quantum field theories.[1] Near the chiral limit (in theories containing light fermions), chiral perturbation theory may be used to systematically characterize the low energy consequences of spontaneously broken chiral symmetry using a small number of low energy parameters. (See, e.g., Ref. [1] for a review.) But the demonstration of chiral symmetry breaking and determination of these low energy constants requires other methods, such as large scale lattice gauge theory simulations or input of experimental data. Gauge-gravity duality [2] has provided insight into some 4D confining gauge theories [3–8], but is usefully applicable primarily in theories which are strongly coupled at all scales, not asymptotically free, and have a large number N of colors. For 4D confining, asymptotically free gauge theories, analytic methods based on controlled approximations are generally unavailable.

In this paper, we study properties of 4D confining QCD-like theories, at finite N, in a regime which allows controlled analytic calculations. Specifically, we consider theories on $\mathbb{R}^3 \times S^1$, with one dimension compactified on a circle of circumference L which is small compared to the inverse strong scale of the theory, $L \ll \Lambda^{-1}$ (and henceforth denoted S^1_L). This is a very old idea (see, e.g., Ref. [9] for a review) but interest has been renewed in recent years with the realization that a wide range of QCD-like theories may be engineered to possess a phase diagram in which the small-L regime is continuously connected to the large-L or decompactified regime. Achieving such "adiabatic compactification" requires non-thermal boundary conditions and suitable matter content (or the addition of double trace deformations) [10–15].

Compactifying one direction on a small circle does, obviously, change properties of a theory. Lorentz invariance is reduced from $SO(1,3)$ to $SO(1,2)$ and physical quantities will depend on the newly introduced scale L. But if one can engineer compactifications where the L dependence is smooth ("adiabatic"), then studies of the small-L regime may teach one qualitative lessons which remain valid in the large-L limit. Previous work [12–35] has examined symmetry realizations at small L and studied the properties of the very lightest excitations. One finds that it is possible to prevent the spontaneous breaking of the $\mathbb{Z}_N$ center symmetry of pure Yang-Mills (YM) theory, which would signal a deconfinement transition. With massless quarks present, one finds that chiral symmetry is spontaneously broken. The mechanism of confinement, the generation of a non-perturbative mass gap (without massless quarks), and the spontaneous breaking

[1] By "QCD-like" we mean 4D asymptotically free $SU(N)$ gauge theories, possibly containing fermions but without light fundamental scalar fields. We assume that the fermion content is such that the theory, when defined on $\mathbb{R}^4$, has a confining phase characterized by some strong scale Λ.

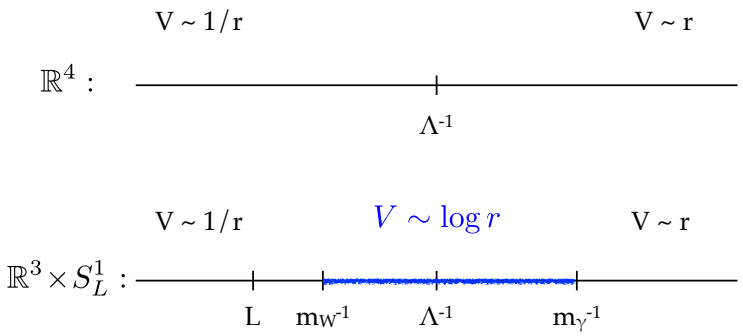

Figure 1. Characteristic length scales in the static potential $V(r)$ for a heavy quark and antiquark separated by a distance r in Yang-Mills theory on $\mathbb{R}^4$ (top), and in adiabatically compactified YM theory on $\mathbb{R}^3 \times S^1_L$ (bottom). On $\mathbb{R}^4$ there is only one intrinsic length scale Λ^{-1} which separates the short ($V \sim 1/r$) and long ($V \sim r$) distance regimes. In the small-L regime of adiabatically compactified YM theory on $\mathbb{R}^3 \times S^1_L$, there is a parametrically large intermediate regime, $m_{\rm W}^{-1} \ll r \ll m_\gamma^{-1}$, in which the potential is logarithmic, $V \sim \ln r$. Here $m_{\rm W}^{-1} \sim NL$ and $m_\gamma^{-1} \sim NL\,\eta^{-11/6}$ with $\eta \equiv NL\Lambda \ll 1$. (See Eq. (2.14) below for details.)

of chiral symmetry (with massless quarks) all may be nicely understood in the small-L regime using semiclassical methods. All evidence supports the view that these center-stabilized compactifications are, indeed, adiabatic.[2]

Given the weight of evidence that adiabatic compactifications exist, it is interesting to use these calculable settings to explore properties of QCD-like theories in more detail. In this paper we initiate efforts in this direction by investigating qualitatively, and where possible quantitatively, the spectrum and properties of glueballs, mesons, and baryons in the small-L regime of adiabatically compactified theories. Some of the hadronic states we find are stable, but naturally most are resonances. In the weakly coupled small-L regime, hadronic resonances are narrow with parametrically small decay widths. Portions of the spectrum have interesting parallels with what one obtains from naive quark models, but in a context where the dynamics of the quantum field theory are under systematic theoretical control.

We mention here two especially curious aspects of our results. First, we find that the lightest glueballs (or dual photons in the small-L description) form bound states whose binding energies are given by iterated exponentials of the Yang-Mills coupling,

[2]Consistency of symmetry realizations between small and large L is, of course, necessary but not sufficient for physics to be smooth in L. Phase transitions not involving any change in symmetry realization could always be present at some intermediate value of L. For center-stabilized QCD, with light quarks, the careful lattice studies which would be needed to rule out this possibility are not yet available. In the absence of any evidence to the contrary, we proceed assuming that for the compactifications we study below, physical properties are smooth in L.

$\Delta E \sim \exp(-Ag^k \exp(B/g^2))$. Second, we find that the density of states of both glueballs and mesons exhibits Hagedorn (or exponential) growth with energy, but this growth has an unusual origin. Hagedorn scaling of the density of mesonic states is typically attributed to the fluctuations of a long, highly excited confining string, and can only be established systematically in the large N limit where mesons cannot decay. The origin of Hagedorn scaling in our context is quite different. The extra scale L introduced by the adiabatic compactification modifies the potential experienced by heavy test quarks separated by a distance r, and introduces a parametrically large regime where the potential is logarithmic, as illustrated in Fig. 1. The compactified theory has many narrow resonances which can be described using non-relativistic quantum mechanics with this logarithmic potential, leading to a Hagedorn spectrum. The fact that stringy dynamics are not the only way to obtain a Hagedorn spectrum, and in particular that such a spectrum arises in ordinary quantum mechanics with logarithmic potentials does not seem to be widely appreciated.[3]

To make our presentation reasonably self-contained, we begin in Section 2 with a summary of center-stabilized adiabatic compactifications. Section 3 discusses the light sector of the compactified theory, with a focus on the spectrum of bound states. In Section 4, we formulate the 3D non-relativistic effective field theory (EFT) which efficiently describes the dynamics of heavy quark and gluon degrees of freedom. Section 5 describes how the various symmetries of the underlying 4D gauge theory act within our 3D effective field theory. In Section 6 we examine the resulting spectrum of heavy bound states, while Section 7 discusses decay processes. We summarize our findings in Section 8 and discuss some of their consequences, including large N scaling relations and implications for the thermodynamics of QCD-like theories. Several appendices contain technical details.

2 Adiabatic compactification

Consider $SU(N)$ Yang-Mills theory compactified on $\mathbb{R}^3 \times S^1$, with the spatial circle having circumference L,

$$S_{\rm YM} = \frac{1}{4g^2} \int_{\mathbb{R}^3 \times S^1} d^4x \, \left(F^a_{\mu\nu}\right)^2 . \tag{2.1}$$

If all matter fields added to the theory transform in the adjoint representation of the gauge group, then the theory has a $\mathbb{Z}_N$ center symmetry. (We discuss below the addition

[3] However, the notion of a limiting temperature for systems with exponential densities of states was first introduced by Rumer in 1960 [36], precisely in quantum mechanics with a logarithmic potential, several years before Hagedorn's suggestion [37] that such a density of states may arise in hadronic physics.

of fundamental representation fermions.) Order parameters for center symmetry are built from the holonomy of the gauge field in the compact direction (or "Polyakov loop"),

$$\Omega \equiv \mathcal{P}\, e^{i\int_0^L dx_3\, A_3}\,. \tag{2.2}$$

Center symmetry transformations multiply the (fundamental representation) trace of the holonomy by a phase factor equal to an N'th root of unity. The defining transformation is

$$\mathrm{tr}\,\Omega \to \omega\ \mathrm{tr}\,\Omega\,, \qquad \omega \equiv e^{2\pi i/N}\,. \tag{2.3}$$

At large L center symmetry is unbroken, implying that $\langle \mathrm{tr}\,\Omega^n\rangle = 0$ for all integer $n \neq 0 \mod N$. This is a hallmark of a confining phase. At small L the realization of center symmetry is analytically calculable [38, 39]. We require that the theory is engineered to prevent spontaneous breaking of the $\mathbb{Z}_N$ center symmetry in the $L \to 0$ limit, so that the theory is *not* in a deconfined plasma phase at small L. This can be achieved by adding suitable double trace deformations of the form $|\mathrm{tr}\,\Omega|^2$ (plus higher windings) to the action of pure Yang-Mills theory [12, 40]. Alternatively, the center symmetry at small L can be stabilized by the addition of massless or sufficiently light adjoint representation fermions [15, 18, 41–43].[4] If the adjoint fermions are massive, center stabilization for small L requires that their mass $m_{\rm adj}$ satisfy the constraint $m_{\rm adj} \lesssim 2\pi/NL$ [15].

With center symmetry stabilized, the one-loop effective potential $V_{\rm eff}(\Omega)$ for the holonomy, obtained by integrating out field modes with non-zero Kaluza-Klein (KK) momentum in the compact direction, has a unique (up to gauge equivalence) $\mathbb{Z}_N$ symmetric minimum,

$$\Omega = \omega^{-(N-1)/2}\,\mathrm{diag}\,(1,\omega,\omega^2,\cdots,\omega^{N-1})\,. \tag{2.4}$$

For sufficiently small L, the gauge coupling at the compactification scale is weak and quantum fluctuations are suppressed. Hence, one may regard the holonomy Ω as a nearly constant $SU(N)$ matrix with eigenvalues which are all N'th roots of unity for N odd, and all N'th roots of -1 for N even. The holonomy acts like an adjoint representation Higgs field, "breaking" the non-Abelian gauge symmetry (using typical sloppy perturbative language) down to the $U(1)^{N-1}$ Cartan subgroup. We will refer to the $N-1$ diagonal Cartan components of the gauge field as "photons." The off-diagonal

[4] If center symmetry is stabilized with adjoint fermions, we assume that $2 \le n_A \le 5$ species of adjoint Majorana fermions are added, so the theory is asymptotically free but non-supersymmetric (in the massless limit). We also take the adjoint fermion mass $m_{\rm adj}$ to be large compared to the mass gap scale m_γ discussed below.

components of gauge field (charged under the Cartan subgroup) will be termed "W-bosons" and receive masses given by positive integer multiples of

$$m_{\rm W} \equiv 2\pi/(NL)\,. \tag{2.5}$$

Fluctuations in the eigenvalues of the holonomy will have an effective mass m_Ω whose value depends on the details of the center symmetry stabilization. One may regard $m_\Omega \sim \sqrt{\lambda}\, m_{\rm W}$ as a characteristic fiducial value, with $\lambda \equiv g^2 N$ the usual 't Hooft coupling. This is the typical size resulting from modifications to the one-loop effective potential for the holonomy, unless one fine-tunes the stabilization mechanism, for instance by considering a nearly supersymmetric limit of the theory.

The dynamical Higgs mechanism and resulting Abelianization induced by the center-symmetric holonomy is the key feature responsible for the analytic tractability of the theory at small L. All charged degrees of freedom have masses of order $m_{\rm W}$ or more, so the 4D 't Hooft coupling λ does not continue to run below the scale $m_{\rm W}$. If $m_{\rm W} \gg \Lambda$, or equivalently

$$\eta \equiv NL\Lambda \ll 1\,, \tag{2.6}$$

then the long-distance value of the 't Hooft coupling will be small, $\lambda(m_{\rm W}) \ll 1$. We focus on this regime in what follows and, unless stated otherwise, the value of g^2 is taken at the scale $m_{\rm W}$.

Previous work on adiabatically compactified QCD-like theories has focused exclusively on the lightest subsector in the small L limit, with characteristic energies and momenta much less than $m_{\rm W}$ and m_Ω. On these scales, the physics can be described by an effective field theory of $N-1$ Abelian photons living in three dimensions. Non-perturbative monopole-instanton effects generate small but relevant interactions between the photons. The Euclidean action for the diagonal components of the gauge field has the schematic form[5]

$$S_{\rm light} = L \int d^3x \, \left[\tfrac{1}{4g^2} (F^a_{\mu\nu})^2 + \mathcal{L}^{\rm monopole}_{\rm int} \right]. \tag{2.7}$$

A three-dimensional Abelian duality transformation leads to the Coulomb gas repre-

[5]Perturbative corrections generate photon mixing terms (as well as higher derivative terms which are irrelevant at long distances). The photon mixing matrix has been calculated in $\mathcal{N} = 1$ SYM theory to first order in λ [29]. This photon mixing is diagonalized by the same $\mathbb{Z}_N$ Fourier transform mentioned below, and does not affect the following discussion.

sentation,[6]

$$S_{\rm light} = \int d^3x \left[\frac{\lambda m_{\rm W}}{16\pi^3} (\nabla \boldsymbol{\sigma})^2 - \zeta \sum_{i=1}^{N} \cos(\boldsymbol{\alpha}_i \cdot \boldsymbol{\sigma} + \theta/N) \right]. \tag{2.8}$$

The field $\boldsymbol{\sigma} = \{\sigma^i\}$ is an N-component compact scalar field; in our basis it is independently periodic in every component with period 2π. The fundamental domain of $\boldsymbol{\sigma}$ is the unit cell of the weight lattice, generated by the shifts $\boldsymbol{\sigma} \to \boldsymbol{\sigma} + 2\pi\boldsymbol{\mu}_i$ where $\{\boldsymbol{\mu}_i\}$ are the fundamental weight vectors of $SU(N)$ and $\{\boldsymbol{\alpha}_i\}$ are the corresponding root vectors. The "fugacity"

$$\zeta = A\, m_{\rm W}^3\, \lambda^{-2}\, e^{-8\pi^2/\lambda}\,, \tag{2.9}$$

where A is an $\mathcal{O}(1)$ coefficient which depends on the choice of regularization scheme. Although not immediately apparent, the action (2.8) is invariant, as it must be, under shifts in the QCD θ angle by multiples of 2π.

To obtain an expression for the masses of the dual photons, note that the potential $V = -\zeta \sum_{i=1}^{N} \cos(\boldsymbol{\alpha}_i \cdot \boldsymbol{\sigma} + \theta/N)$ has N extrema in the unit cell of the weight lattice located at $\langle \boldsymbol{\sigma} \rangle_k = \frac{2\pi k}{N} \boldsymbol{\rho}$ for $k = 0, \cdots, N-1$, where $\boldsymbol{\rho} = \sum_{i=1}^{N-1} \boldsymbol{\mu}_i$ is the Weyl vector.[7] For $\theta = 0$ the minimum lies at $k = 0$. For general θ, the vacuum energy density is given by

$$\epsilon_0 = -N^2 \frac{m_{\rm W}}{2\pi} \zeta \max_k \Big(\cos \frac{2\pi k + \theta}{N} \Big). \tag{2.10}$$

Expanding the potential around each of the N extrema and diagonalizing the curvature (via a $\mathbb{Z}_N$ Fourier transform) yields the θ-dependent mass spectrum in each of the N extrema (not all of which are minima). At the lowest-energy minimum, which determines the physical mass spectrum, one finds

$$m_p^2 = m_\gamma^2 \sin^2 \frac{\pi p}{N} \max_k \Big(\cos \frac{2\pi k + \theta}{N} \Big), \tag{2.11}$$

for $p = 1, 2, \cdots, N-1$, with

$$m_\gamma \equiv C\, m_{\rm W}\, \lambda^{-3/2}\, e^{-4\pi^2/\lambda}\,. \tag{2.12}$$

The $\mathcal{O}(1)$ coefficient C is determined in terms of the coefficient A in the fugacity (2.9). The label p can be viewed as the charge under $\mathbb{Z}_N$ center symmetry transformations; this

[6] A redundant field component has been introduced in this representation, as if the original gauge group were $U(N)$ instead of $SU(N)$. The unphysical components, $\sum_{a=1}^{N} F_{\mu\nu}^a$ and $\sum_{a=1}^{N} \sigma^a$, exactly decouple and can be ignored. See, e.g., Ref. [12] for more detailed discussion. Appendix B contains details of our conventions, normalizations, and duality transformation.

[7] To see this, use $\boldsymbol{\alpha}_i \cdot \boldsymbol{\rho} = 1$ for $i = 1, \cdots, N-1$, together with $\boldsymbol{\alpha}_N \cdot \boldsymbol{\rho} = 1-N$.

is discussed in Sec. 5. One may also show that expectation values of large fundamental representation Wilson loops (not wrapping the compactified direction) have area law behavior, with a string tension [12]

$$T = C' \lambda m_{\rm W} m_\gamma \,, \tag{2.13}$$

with C' another $\mathcal{O}(1)$ coefficient.

The dual photon mass m_γ can be expressed in terms of the strong scale Λ by using the renormalization group to relate λ at the scale of $m_{\rm W}$ to Λ. The specific form of this relation depends on the value of the beta function, and hence on whether center symmetry is stabilized by double trace deformations, or by the addition of adjoint fermions. If center symmetry is stabilized by a double trace deformation, then parametrically [12]

$$m_\gamma \sim \Lambda (N L \Lambda)^{5/6} = \mathcal{O}(\Lambda \, \eta^{5/6}) \,, \tag{2.14}$$

and $m_\gamma / m_{\rm W} = \mathcal{O}(\eta^{11/6})$.[8]

2.1 Addition of fundamental quarks

We will consider center-stabilized adiabatically compactified QCD in addition to pure Yang-Mills theory. This entails adding $n_{\rm f}$ flavors of quarks — fundamental representation Dirac fermions. We restrict our discussion to $n_{\rm f} \leq N$ and, for simplicity, focus on the massless quark limit,

$$m_q = 0 \,, \tag{2.15}$$

where the uncompactified theory has an $SU(n_{\rm f})_L \times SU(n_{\rm f})_R \times U(1)_V$ continuous chiral symmetry.[9] When compactifying the theory on $\mathbb{R}^3 \times S^1$, one must specify the boundary conditions on the quark fields. Instead of simply choosing periodic, or antiperiodic, boundary conditions for all quark flavors, we will consider flavor-twisted boundary conditions, or equivalently introduce a non-dynamical flavor holonomy $\Omega_F \in U(n_{\rm f})_V$. If one regards the quark fields q as an $N \times n_{\rm f}$ matrix of spinors, then in $A_3 = 0$ gauge (where the gauge holonomy becomes encoded in boundary conditions), the boundary conditions on quarks are

$$q(t, \mathbf{x}, L) = \Omega \, q(t, \mathbf{x}, 0) \, \Omega_F^\dagger \,. \tag{2.16}$$

We specifically choose the flavor holonomy Ω_F to have a set of eigenvalues which are invariant under $\mathbb{Z}_{n_{\rm f}}$ cyclic permutations. The symmetry structure of QCD with such

[8] If center symmetry is stabilized by the addition of n_A light adjoint Majorana fermions with mass comparable to $m_{\rm W}$, then $m_\gamma / m_{\rm W} = \mathcal{O}(\eta^{(11-2n_A)/6})$.

[9] For $n_{\rm f} > N$, it is not currently known how to ensure that chiral symmetry realizations coincide at large and small L.

boundary conditions was discussed in Ref. [44] (see also Refs. [45–53]). To preserve reflection (in the compactified direction) and charge conjugation symmetries, we also require that complex conjugation leave this set of eigenvalues unchanged. These two conditions imply that the eigenvalues of Ω_F are either given by all $n_{\rm f}$'th roots of $+1$, or by all $n_{\rm f}$'th roots of -1. Finally, to simplify our discussion and leave unchanged the relevant degrees of freedom in the non-perturbative analysis of the light sector, we want all flavors of quarks to receive non-zero effective masses from the compactification. This requires that no eigenvalue of the gauge holonomy coincide with an eigenvalue of the flavor holonomy.

Solutions to these just-stated constraints depend on the values of N and $n_{\rm f}$, in particular whether N is even or odd and (when N is even) whether N and $n_{\rm f}$ have common divisors. For simplicity of exposition we will henceforth assume that N is odd, unless stated otherwise, so that the eigenvalues (2.4) of the gauge holonomy Ω are N'th roots of unity. To avoid coinciding gauge and flavor eigenvalues, this implies that the flavor holonomy eigenvalues must equal $n_{\rm f}$'th roots of -1. Consequently, we choose

$$\Omega_F = \text{diag}\,(\xi^{\frac{1}{2}}, \xi^{\frac{3}{2}}, \cdots, \xi^{n_{\rm f}-\frac{1}{2}})\,, \qquad \xi \equiv e^{2\pi i/n_{\rm f}}\,. \tag{2.17}$$

When the gauge holonomy is encoded in a non-zero value of A_3 (so that the gauge field satisfies simple periodic boundary conditions), the resulting quark boundary conditions are

$$q^A(t, \mathbf{x}, L) = \xi^{\frac{1}{2}-A}\, q^A(t, \mathbf{x}, 0)\,, \tag{2.18}$$

where $A = 1, \cdots, n_{\rm f}$ is a flavor index. The effect of these boundary conditions is to shift the moding (i.e., the allowed values of the momentum in the compact direction), in a flavor-dependent fashion which is detailed below. The boundary conditions (2.18) reduce the non-Abelian flavor symmetry to the Abelian subgroup[10]

$$U(1)_L^{n_{\rm f}-1} \times U(1)_R^{n_{\rm f}-1} \times U(1)_V\,. \tag{2.19}$$

Note that this residual flavor symmetry of our compactified theory contains the axial subgroup $U(1)_A^{n_{\rm f}-1}$ which differentially rotates the phases of left and right handed quarks in a flavor-dependent fashion.

In the center-stabilized regime of YM theory, the addition of massless quarks with the boundary conditions (2.18) produces fermion zero modes localized on the monopole-instantons. The presence of these zero modes modifies the non-perturbative long distance dynamics. After a 3D duality transformation, one may show that $n_{\rm f}-1$ of the

[10] More precisely, the unbroken subgroup is $U(1)_L^{n_{\rm f}-1} \times U(1)_R^{n_{\rm f}-1} \times U(1)_V/\mathbb{Z}_{n_{\rm f}}$. Henceforth, we will not be explicit with the discrete identification needed to avoid double counting $\mathbb{Z}_{n_{\rm f}}$ phase rotations.

dual scalar fields remain exactly massless [35], while the remaining $N-n_{\rm f}$ dual scalar fields develop non-perturbative masses just as in center-stabilized YM theory without fundamental quarks. The mechanism causing $n_{\rm f}-1$ dual scalars to become massless in the presence of fermion zero modes involves their acquisition of non-trivial transformation properties under the anomaly-free $U(1)_A^{n_{\rm f}-1}$ axial symmetry, as explained in Ref. [35]. Consequently, these exactly-massless fields are precisely the expected Nambu-Goldstone bosons (or 'neutral pions') produced by spontaneous breaking of the chiral symmetry (2.19) down to the diagonal vector-like $U(1)_V^{n_{\rm f}}$ subgroup [35].

If a small quark mass m_q is added to the theory, then some of the dual photons, or neutral pions, become massive. For example, when $n_{\rm f}=N$ one finds [35] (at $\theta=0$) that

$$m_p = C\sqrt{m_{\rm W} m_q}\, e^{-4\pi^2/\lambda} \sin\frac{\pi p}{N}\,. \tag{2.20}$$

(Here p is the charge of the pion under cyclic flavor permutations.) One may again relate m_p to the strong scale Λ by taking into account the contribution of the fundamental fermions to the running of the coupling at the scale $m_{\rm W}$. With the pure-YM center symmetry stabilized via double trace deformations and $n_{\rm f}=N$, one finds

$$m_p = \mathcal{O}\big(\eta\sqrt{m_q\Lambda}\big)\,, \tag{2.21}$$

where, once again, $\eta \equiv NL\Lambda$.

3 Light sector bound states

As noted in the introduction, when the color holonomy has the center symmetric form (2.4), a rich spectrum of hadronic states is present in the small-L regime of the compactified theory. These states fall into two categories based on the scale of their rest masses. One set of states have rest masses of order of the light scale m_γ, while the other set has rest masses of order of the heavy scale $m_{\rm W}$. As will be shown below, in both sectors the binding momenta are small compared to the rest masses of constituents, so the most efficient way to describe each sector of the theory involves constructing an appropriate non-relativistic effective field theory. In this section we describe the effective field theory for the light 'dual photon' sector and discuss the resulting light bound state spectrum.

3.1 $N=2$ bound states

To illustrate the relevant physics in the simplest setting, consider adiabatically compactified pure YM theory with $N=2$ and $\theta=0$. The relativistic 3D effective theory

describing interactions of the single (physical) dual photon field $\sigma \equiv \sigma_1 - \sigma_2$, to leading non-trivial order in the semiclassical expansion, is

$$S_{\rm 3D,rel} = \int d^3x \, \left[\frac{\lambda m_{\rm W}}{32\pi^3} \, (\partial_\mu \sigma)^2 - 2\zeta \cos(\sigma) \right] . \tag{3.1}$$

Introducing a canonically normalized field $\tilde{\sigma} \equiv \sigma \left(\frac{\lambda m_{\rm W}}{16\pi^3}\right)^{1/2}$, and expanding the potential, one finds

$$S_{\rm 3D,rel} = \int d^3x \, \left[\tfrac{1}{2} (\partial_\mu \tilde{\sigma})^2 + \tfrac{1}{2} m_\gamma^{\,2} \, \tilde{\sigma}^2 - \tfrac{2}{3} \epsilon \, m_\gamma \, \tilde{\sigma}^4 + \tfrac{16}{45} \epsilon^2 \, \tilde{\sigma}^6 - \tfrac{32}{315} \epsilon^3 \, m_\gamma^{-1} \, \tilde{\sigma}^8 + \cdots \right] , \tag{3.2}$$

where

$$\epsilon \equiv \frac{\pi^3 m_\gamma}{\lambda m_W} = \mathcal{O}\big(\lambda^{-5/2} \, e^{-4\pi^2/\lambda}\big) . \tag{3.3}$$

At first glance it is tempting to assume that the interaction terms in (3.2) have negligible consequences. To our knowledge, effects of these weak interactions have not previously been considered, either in the literature on adiabatically compactified 4D theories starting with Ref. [12], or in the original literature on the Polyakov model in three dimensions [54]. As we now discuss, this presumption overlooks interesting physics.

The $\tilde{\sigma}^8$ and higher terms in the action (3.2) are irrelevant and can be ignored when focusing on the long distance behavior of the theory. The $\tilde{\sigma}^4$ coupling is relevant, but its coefficient is exponentially small in units of the σ mass. The $\tilde{\sigma}^6$ coupling is marginal and infrared-free [55–58]. It is also exponentially small and stops running below the mass gap scale m_γ. These considerations might naively be interpreted to imply that all interaction effects in the low energy theory (3.2) are tiny. But consider interactions of $\tilde{\sigma}$ modes with low momenta $p \ll m_\gamma$. Such interactions can be described by a non-relativistic effective field theory. Writing $\tilde{\sigma} = (2m_\gamma)^{-1/2} e^{-i m_\gamma t} \, \Sigma + (\text{h.c.})$, where Σ is the non-relativistic field, and integrating out rapidly oscillating terms leads to the non-relativistic description,[11]

$$S_{\rm 3D,NR} = \int dt \, d^2x \left[\Sigma^\dagger \left(i\partial_t + \frac{\nabla^2}{2m_\gamma} \right) \Sigma + \frac{\epsilon}{m_\gamma} \, (\Sigma^\dagger)^2 \, \Sigma^2 - \frac{8\epsilon^2}{9 m_\gamma^3} \, (\Sigma^\dagger)^3 \, \Sigma^3 + \cdots \right] . \tag{3.4}$$

The scaling dimension assignments appropriate to non-relativistic theories in spacetime dimension d are $[t] = -2$, $[x] = -1$, $[\Sigma] = \frac{d-1}{2}$, and $[m_\gamma] = 0$. This implies that the

[11] Here and in Eq. (3.10) below, we flip the overall sign so that the nonerelativistic action $S_{\rm 3D,NR}$ has the conventional $T-V$ form.

coefficients of the $(\Sigma^\dagger\Sigma)^2$ and $(\Sigma^\dagger\Sigma)^3$ interactions have dimensions $d{-}3$ and $2(d{-}2)$, respectively. In $d{=}3$, this shows that the two particle $(\Sigma^\dagger\Sigma)^2$ interaction becomes *marginal* in non-relativistic dynamics, while the three particle $(\Sigma^\dagger\Sigma)^3$ interaction becomes irrelevant. In fact, the $(\Sigma^\dagger\Sigma)^2$ coupling ϵ runs logarithmically with scale [59, 60], as may be seen (for example) by calculating the two particle scattering amplitude. Consequently, the definition (3.3) should be interpreted as the value of the running interaction strength ϵ at the UV momentum cutoff $\mu_{\rm UV} \sim m_\gamma$. In the non-relativistic limit the only diagrams which contribute to the renormalization group (RG) evolution of ϵ beyond tree level are iterated bubble diagrams. Summing them yields the exact beta function for ϵ. Using dimensional regularization, one simply finds [60]

$$\mu \frac{d\,\epsilon(\mu)}{d\mu} = -\frac{1}{\pi}\,\epsilon(\mu)^2\,. \tag{3.5}$$

When the initial coupling $\epsilon(\mu_{\rm UV})$ is positive, corresponding to an attractive interaction, $\epsilon(\mu)$ diverges at the momentum scale $\Lambda_{\rm IR} = \mu_{\rm UV}\exp\left[-\pi/(\epsilon(\mu_{\rm UV}))\right]$. As a function of momentum, the two particle scattering amplitude $\mathcal{A}(k)$ becomes singular at $k^2 = -\Lambda_{\rm IR}^2$. A pole develops at this position, indicating that $\Lambda_{\rm IR}$ can be interpreted as the binding momentum for a two-body bound state of dual photons.[12] The two particle binding energy is thus

$$\Delta E_2 = -\frac{k^2}{m_\gamma} = -\frac{\mu_{\rm UV}^2}{m_\gamma}\,e^{-2\pi/\epsilon(\mu_{\rm UV})} = -\tfrac{1}{4}\,c^2\,m_\gamma\,e^{-2\lambda m_{\rm W}/\pi^2 m_\gamma}\,. \tag{3.6}$$

In the final form we used the bare value (3.3) of ϵ and set the ultraviolet cutoff to the reduced mass $\frac{1}{2}m_\gamma$ times an $\mathcal{O}(1)$ coefficient c, whose determination requires a more careful matching calculation and is left for future work. The two dual photon bound state has a rest mass

$$m_2 = 2m_\gamma + \Delta E_2 = m_\gamma\left(2 - \tfrac{1}{4}\,c^2\,e^{-2\lambda m_W/\pi^2 m_\gamma}\right). \tag{3.7}$$

Expressed in terms of the original gauge coupling, the fractional binding energy involves a non-perturbative double exponential,

$$\frac{\Delta E_2}{2m_\gamma} = -\tfrac{1}{4}\,c^2\,\exp\left(-\tfrac{2}{\pi^2 C}\,\lambda^{5/2}\,e^{4\pi^2/\lambda}\right), \tag{3.8}$$

whose appearance is quite peculiar in the context of the 4D gauge theories.[13]

[12] One may also directly solve the quantum mechanical problem a particle of reduced mass $\frac{1}{2}m_\gamma$ moving in the attractive potential $-\frac{2\epsilon}{m_\gamma}\,\delta^{(2)}(\mathbf{x})$. The bound state wave function equals $K_0(r/r_B)$, with the bound state size $r_B = |m_\gamma\,\Delta E_2|^{-1/2}$ and ΔE_2 equaling the binding energy (3.6).

[13] However, the existence of double-exponential non-perturbative scales in gauge theory has been previously advocated [61], based on quite different considerations from those discussed here.

In addition to a two particle bound state, an attractive two-body interaction in two space dimensions also binds higher multi-body bound states. (See, for example, Refs. [59, 62].) The magnitude of the k-body binding energy ΔE_k increases exponentially with k, with $\Delta E_{k+1}/\Delta E_k \sim 8.6$ for large k [59]. In our context, we thus deduce the presence of a very large number of bound states of dual photons, one slightly below each k-particle threshold at $E = km_\gamma$ for $k = 2, 3, \cdots$, with fractional binding energies proportional to the non-perturbative double exponential (3.8).[14]

3.2 $N > 2$ bound states

We now briefly consider the generalization to arbitrary N, still with $\theta = 0$. Using a $\mathbb{Z}_N$ Fourier transform to diagonalize the mass terms, $\sigma_i \equiv \left(\frac{\lambda m_{\rm W}}{8\pi^3}\right)^{-1/2} \sum_{p=1}^{N-1} \omega^{ip}\, \tilde\sigma_p/\sqrt{N}$ (with $\tilde\sigma_p^* = \tilde\sigma_{N-p}$), the generalization of the action (3.2) is

$$S_{\rm 3D} = \int d^3x \sum_{p=1}^{N-1} \tfrac{1}{2}\left(|\partial_\mu \tilde\sigma_p|^2 + m_p^2 |\tilde\sigma_p|^2\right) - \frac{4\epsilon\, m_\gamma}{3N} \sum_{p_1 \cdots p_4 = 1}^{N-1} \delta_{p_1+p_2+p_3+p_4,0}\, e^{i\pi(p_1+p_2+p_3+p_4)/N} \times \left[\prod_{i=1}^{4} \sin\left(\frac{\pi p_i}{N}\right)\right] \tilde\sigma_{p_1}\tilde\sigma_{p_2}\tilde\sigma_{p_3}\tilde\sigma_{p_4} + \mathcal{O}(\tilde\sigma^6)\,, \quad (3.9)$$

where all center charges $\{p_k\}$ are understood to be defined modulo N. The masses $\{m_p\}$ and coupling ϵ are given by Eqs. (2.11) and (3.3), respectively. [Recall that the field $\tilde\sigma_0 \propto \sum_i \sigma_i$ decouples, and is omitted. Expression (3.9) reduces to the earlier form (3.2) for $N = 2$, as it should.]

The sign of the quartic interaction depends on the values of the center charges of the particles under consideration. For elastic scattering of dual photons with arbitrary charges p_1 and p_2, the relevant piece of the quartic interaction has an overall minus sign, which corresponds to attraction. The effective theory which follows from a non-relativistic reduction of the action (3.9), and generalizes the earlier form (3.4) to arbitrary N, is

$$S_{\rm 3D,NR} = \int dt\, d^2x \left[\sum_{p=1}^{N-1} \Sigma_p^\dagger \left(i\partial_t + \frac{\nabla^2}{2m_p}\right)\Sigma_p + \frac{2\epsilon}{N}\frac{m_p^2}{m_\gamma^3}\,(\Sigma_p^\dagger)^2\,\Sigma_p^2 + \sum_{p_1<p_2} \frac{8\epsilon}{N}\frac{m_{p_1} m_{p_2}}{m_\gamma^3}\,\Sigma_{p_1}^\dagger \Sigma_{p_2}^\dagger \Sigma_{p_2}\Sigma_{p_1} + \cdots\right], \quad (3.10)$$

[14] This weak coupling non-relativistic description breaks down when $k\,(\ln 8.6)$ becomes exponentially large and comparable to $2\lambda m_{\rm W}/\pi^2 m_\gamma \sim \lambda^{5/2} e^{+4\pi^2/\lambda}$.

where we have included only those terms contributing to elastic $2 \leftrightarrow 2$ scattering.[15] Note the factor of 4 difference in the coefficients of the quartic terms responsible for scattering of identical vs. non-identical particles.

Applying the earlier analysis (either solving the two-particle Schrödinger equation with a delta function potential, or resumming bubble diagrams and locating the resulting pole in the scattering amplitude) to states containing particles of center charge p_1 and p_2, one finds the binding energy

$$\Delta E_2^{p_1 \neq p_2} = -2c^2\, m\, \exp\left(-\frac{\pi N}{4\epsilon}\,\frac{m_\gamma^3}{m_{p_1} m_{p_2} m}\right), \tag{3.11}$$

if $p_1 \neq p_2$. Here $m \equiv (m_{p_1}^{-1} + m_{p_2}^{-1})^{-1}$ is the reduced mass of the two constituents. If the two constituents are identical, then the result is

$$\Delta E_2^{p_1 = p_2} = -c^2\, m_{p_1}\, \exp\left(-\frac{\pi N}{\epsilon}\,\frac{m_\gamma^3}{m_{p_1}^3}\right). \tag{3.12}$$

Bound states composed of equal mass constituents can have either equal or opposite charge constituents. For the first case, with charges $p_1 = p_2 = p$, the identical particle binding energy (3.12) gives a total mass

$$m_2^{p,p} = m_p \left[2 - c^2\, e^{-\frac{\pi N}{\epsilon}(m_\gamma/m_p)^3}\right]. \tag{3.13}$$

For opposite charges, p and $N-p$, the non-identical binding energy (3.11) with $m_{p_1} = m_{p_2} = 2m = m_p$ gives total mass

$$m_2^{p,N-p} = m_p \left[2 - c^2\, e^{-\frac{\pi N}{2\epsilon}(m_\gamma/m_p)^3}\right] \tag{3.14}$$

(except for the special case of $p = N/2$ with N even, where the first result (3.13) applies). In other words, the fractional binding energy for non-identical particles is $\mathcal{O}\big(e^{-\frac{\pi N}{2\epsilon}(m_\gamma/m_p)^3}\big) = \mathcal{O}\big(e^{-\frac{\pi N}{2\epsilon}|\sin\frac{\pi p}{N}|^{-3}}\big)$, while bound states of identical constituents have twice the exponential suppression in their binding energy.

[15] The interaction (3.9) also includes charge exchange processes which lead to mixing among bound states with differing constituents but the same total center charge. For generic values of N and choices of p_1 and p_2 the effects of such interaction terms on binding energies are suppressed in the non-relativistic limit, because the masses of the dual photons depend on their center charge. Charge exchange processes can only become relevant if states with differing constituents and the same total charge also have the same total constituent mass. Such mixing will deepen the binding of the lowest energy bound states of a given total charge. We defer a complete multi-channel treatment to future work.

4 Heavy sector effective field theory

We now consider states with rest masses of order $m_{\rm W}$ and above, and characteristic binding momenta p in the range

$$m_\gamma \ll p \ll m_{\rm W}\,. \tag{4.1}$$

This section describes the construction of a non-relativistic effective theory suitable for the description of such states. We begin with the effective theory characterizing pure gauge, or glueball, dynamics, and then discuss the addition of fundamental representation quarks.

4.1 Gauge field contributions

The center-symmetric holonomy (2.4) may equivalently be regarded as a non-vanishing constant diagonal gauge field in the compact direction, A_3, together with conventional periodic boundary conditions. The $\mathrm{tr}\,[A_3, \boldsymbol{A}]^2$ term in the classical Yang-Mills action generates tree-level masses of order $m_{\rm W}$ for the charged W-bosons. The efficient description of the interactions of these massive charged degrees of freedom with the Cartan photons is provided by a non-relativistic effective field theory with action:

$$\begin{aligned} S_{\rm heavy} = &\sum_{a,b=1}^{N} {\sum_{n=-\infty}^{\infty}}' \int dt\, d^2x \left[(\vec{\phi}_n^{ab})^\dagger\, i\partial_t\, \vec{\phi}_n^{ab} - M_n^{ab}\, |\vec{\phi}_n^{ab}|^2 - \frac{|\boldsymbol{\nabla}\vec{\phi}_n^{ab}|^2}{2m_n^{ab}} \right] \\ &+ \frac{\lambda m_{\rm W}}{4\pi} \sum_{a=1}^{N} \int dt\, d^2x\, d^2y\, \rho^a(t,\mathbf{x})\, G(\mathbf{x}{-}\mathbf{y})\, \rho^a(t,\mathbf{y})\,, \end{aligned} \tag{4.2}$$

where

$$G(\mathbf{x}{-}\mathbf{y}) \equiv \tfrac{1}{2\pi}\, \ln(\mu|\mathbf{x}{-}\mathbf{y}|) \tag{4.3}$$

is the two dimensional Laplacian Green's function. The derivation of this effective theory is detailed in appendix A. Higher order (in λ) corrections, such as magnetic moment interactions, are omitted for simplicity.

The two-dimensional vector fields $\vec{\phi}_n^{ab}$ are the non-relativistic reduction of the n'th Fourier component (in the compact direction) of the (ab) component of the $SU(N)$ gauge field, viewed as an $N \times N$ Hermitian matrix. The color (or 'Cartan') indices a, b run from 1 to N, and the Kaluza-Klein index n is an arbitrary integer. In the action (4.2), the prime on the sum over n is an indication to omit the $n = 0$ term when $a = b$, but not otherwise. The vector field $\vec{\phi}_n^{ab}$ annihilates W-bosons with charges $(+1, -1)$ with respect to the a'th and b'th unbroken $U(1)$ gauge groups. The spatial gradient $\boldsymbol{\nabla}$ is a two-dimensional $U(1)^N$ covariant derivative defined by

$$(\boldsymbol{\nabla})_i(\phi_n^{ab})_j \equiv \left[\nabla_i - ig_3(A_i^a{-}A_i^b)\right](\phi_n^{ab})_j\,. \tag{4.4}$$

Here $i, j = 1, 2$ label the two non-compact spatial directions and $\{\vec{A}^a\}$ are N independent spatial gauge fields. We have introduced N Abelian gauge fields, instead of $N-1$, as if the original gauge group were $U(N)$ instead of $SU(N)$. This simplifies notation, and makes no difference as the unphysical extra photon, $\bar{A}_i \equiv \sum_a A_i^a$, will exactly decouple from all physical states. We have also reverted to a perturbative normalization for the gauge fields, with a dimensionless gauge coupling g_3 appearing inside the covariant derivative, and a corresponding 3D Maxwell action given by $L \int d^3x \, \frac{1}{4}(F_{ij}^a)^2$. The 3D gauge coupling is, to lowest order, just the 4D gauge coupling evaluated at the scale $m_{\rm W}$,

$$g_3^2 \equiv g_4^2(m_{\rm W})\,. \tag{4.5}$$

Due to the non-trivial holonomy Ω, momentum in the compact direction carried by individual field components is quantized in units of $m_{\rm W}$, not $N m_{\rm W} = 2\pi/L$. The Kaluza-Klein reduction of the (ab) component of the gauge field yields a sum of modes with momentum

$$p_3 = m_{\rm W}\, k\,, \tag{4.6a}$$

where

$$k = a - b + nN\,, \qquad n \in \mathbb{Z}. \tag{4.6b}$$

For any given value of $a = 1, \cdots, N$ specifying a row of the $SU(N)$ gauge field, there is a one-to-one mapping between the momentum index k and the corresponding values of the column b and KK index n,

$$b - 1 = (k - a + 1) \bmod N\,, \qquad n = (k - a + b)/N\,. \tag{4.7}$$

In the following, we will sometimes write expressions involving the relabeled field

$$\vec{\phi}_k^{\,a} \equiv \vec{\phi}_n^{\,ab}\,, \tag{4.8}$$

with the implicit understanding that momentum index k is related to the (antifundamental) column and KK indices $\{b, n\}$ via relations (4.7). The momentum index k may take on any integer value other than zero. For charged W-bosons, $k \bmod N \neq 0$. The "diagonal" operators $\vec{\phi}_n^{\,aa}$ with $n \neq 0$ annihilate the neutral (uncharged under $U(1)^N$) gauge bosons carrying non-zero KK momentum. These gauge bosons form the Kaluza-Klein tower whose $n = 0$ modes (excluded from $S_{\rm heavy}$) are the $U(1)^N$ light Abelian photons.

The rest and kinetic mass parameters appearing in the effective theory (4.2) only depend on the Cartan and KK indices via the combination k, and equal the magnitude

of the compact momentum p_3, up to higher order radiative corrections. In other words,

$$M_n^{ab} = M_k \equiv m_{\rm W}\left(|k| + \mathcal{O}(\lambda)\right) = m_{\rm W}|a-b+nN| + \mathcal{O}(\lambda m_{\rm W})\,, \tag{4.9a}$$

$$m_n^{ab} = m_k \equiv m_{\rm W}\left(|k| + \mathcal{O}(\lambda)\right) = m_{\rm W}|a-b+nN| + \mathcal{O}(\lambda m_{\rm W})\,. \tag{4.9b}$$

Although they coincide at lowest order, the kinetic and rest masses appearing as parameters in our 3D non-relativistic effective field theory (4.2), or any other non-relativistic EFT, may differ when subleading corrections are included, even when the underlying theory retains full 2+1 dimensional Lorentz invariance.

In the effective action (4.2), the time components of the $U(1)^N$ Abelian gauge fields have been integrated out, producing non-local Coulomb interactions. The operators

$$\rho^a \equiv \sum_{b=1}^{N} {\sum_{n=-\infty}^{\infty}}' \left[(\vec{\phi}_n^{ab})^\dagger \cdot \vec{\phi}_n^{ab} - (\vec{\phi}_n^{ba})^\dagger \cdot \vec{\phi}_n^{ba}\right], \tag{4.10}$$

are the $U(1)^N$ charge densities. (Note that $\bar{\rho} \equiv \sum_a \rho^a$ vanishes identically.) The conserved charges defined by spatial integrals of these charge densities must vanish,

$$Q^a \equiv \int d^2x\, \rho^a(\mathbf{x}) = 0\,, \tag{4.11}$$

when acting on any physical, gauge invariant state. Because of this, the dependence of the 2D Laplacian Green's function (4.3) on the arbitrary scale μ inside the logarithm cancels in any physical state, since the variation of the Lagrangian with respect to μ is proportional to $(Q^a)^2$.

The non-relativistic effective theory (4.2) describes the dynamics of all modes of the non-Abelian gauge field which are charged under the $U(1)^N$ Cartan subgroup, namely W-bosons, plus the uncharged gauge field modes which carry non-zero KK momentum, which we will term "heavy photons." However, we have not included any fields describing fluctuations of the eigenvalues of the holonomy in the effective field theory. These could easily be included as $N-1$ additional neutral scalar fields (not 2D vectors like $\vec{\phi}_n^{ab}$) with $\mathcal{O}(\sqrt{\lambda}m_{\rm W})$ masses whose precise values depend on the matter content or double trace deformations used to stabilize the center symmetry. These scalar fields only interact with $\vec{\phi}_n^{ab}$ via higher dimension local operators, suppressed by powers of λ. For the physics we choose to focus on, holonomy fluctuation fields will not play any significant role and may be neglected. If adjoint fermions are used to stabilize the center symmetry, then these fermions are also missing from our non-relativistic effective theory. They could be easily included but, for simplicity, we will limit our attention to states where adjoint fermions (and eigenvalue fluctuations) play no significant role.

Reading off the quantum Hamiltonian from the effective action (4.2) is trivial, except for one UV subtlety. The Hamiltonian of the second quantized non-relativistic theory (with rest energies included) is

$$\begin{aligned}\hat{H} = &\sum_{a,b=1}^{N} {\sum_{n=-\infty}^{\infty}}' \int d^2x\, \phi_n^{ab}(\mathbf{x})_i^\dagger \left[-\frac{\boldsymbol{\nabla}^2}{2m_k} + M_k(\mu)\right] \phi_n^{ab}(\mathbf{x})_i \\ &- \sum_{a,b,c=1}^{N} {\sum_{m,n=-\infty}^{\infty}}' \int d^2x\, d^2y\, \frac{\lambda m_{\rm W}}{8\pi^2} \ln(\mu|\mathbf{x}-\mathbf{y}|) \times \\ &\qquad \times \Big[\phi_n^{ab}(\mathbf{x})_i^\dagger \left(\phi_m^{ac}(\mathbf{y})_j^\dagger\, \phi_m^{ac}(\mathbf{y})_j - \phi_m^{ca}(\mathbf{y})_j^\dagger\, \phi_m^{ca}(\mathbf{y})_j\right) \phi_n^{ab}(\mathbf{x})_i \\ &\qquad - \phi_n^{ba}(\mathbf{x})_i^\dagger \left(\phi_m^{ac}(\mathbf{y})_j^\dagger\, \phi_m^{ac}(\mathbf{y})_j - \phi_m^{ca}(\mathbf{y})_j^\dagger\, \phi_m^{ca}(\mathbf{y})_j\right) \phi_n^{ba}(\mathbf{x})_i\Big]\,. \end{aligned} \tag{4.12}$$

where the field operators satisfy canonical commutation relations,

$$\left[\phi_n^{ab}(\mathbf{x})_i,\, \phi_{n'}^{cd}(\mathbf{y})_j\right] = 0\,, \quad \left[\phi_n^{ab}(\mathbf{x})_i, \phi_{n'}^{cd}(\mathbf{y})_j^\dagger\right] = \delta^{ac}\,\delta^{bd}\,\delta_{nn'}\,\delta_{ij}\,\delta^2(\mathbf{x}-\mathbf{y})\,. \tag{4.13}$$

In the Hamiltonian (4.12) we have written out the charge densities ρ^a explicitly and normal ordered the results. In the quartic terms, normal ordering removes the UV sensitive self-energy of each charged W-boson. The price of that removal is that the μ dependence of the Coulomb interaction terms no longer vanishes identically. Instead, this unphysical dependence on the scale μ is canceled by explicit dependence on μ which has been introduced into the bare rest masses (of charged W's only),

$$\mu\frac{d}{d\mu}\, M_k(\mu) = -\frac{\lambda m_{\rm W}}{4\pi^2}\,(1 - \delta^0_{k \bmod N})\,. \tag{4.14}$$

The effective action (4.2), and corresponding Hamiltonian (4.12), depend on the 3D gauge coupling g_3, or equivalently the 't Hooft coupling λ, both in the coefficient of the Coulomb interactions and inside the spatial covariant derivatives. But when considering phenomena for which the coupling to the transverse Cartan gauge fields $\{\vec{A}^a\}$ may be neglected, the remaining dependence on λ takes a very simple form. To see this, rescale all spatial coordinates, $\mathbf{x} \to \mathbf{x}'/s$, $\mathbf{y} \to \mathbf{y}'/s$, and then redefine $\vec{\phi}_k^{\,a}(\mathbf{x}'/s) = s\,\vec{\varphi}_k^{\,a}(\mathbf{x}')$. This is a unitary transformation; the rescaled operators $\{\vec{\varphi}_k^{\,a}(\mathbf{x})\}$ satisfy the same canonical commutation relations as the original operators $\{\vec{\phi}_k^{\,a}(\mathbf{x})\}$. In the Hamiltonian, the effect of this rescaling is to change the relative coefficients of the kinetic and Coulomb energy terms. Let

$$\hat{N}_n^{ab} \equiv \int d^2x\, \vec{\phi}_n^{\,ab}(\mathbf{x})^\dagger \cdot \vec{\phi}_n^{\,ab}(\mathbf{x}) \tag{4.15}$$

denote the number operator which counts the number of constituents of the indicated type, and define

$$\hat{H}_{\rm NR}(\lambda;\mu) \equiv \hat{H}\Big|_{\vec{A}^a=0} - \sum_{a,b=1}^{N} \sum_{n=-\infty}^{\infty}{}' \; M_k(\mu)\, \hat{N}_n^{ab} \tag{4.16}$$

as the non-relativistic Hamiltonian with rest energy contributions removed, the spatial Abelian gauge fields set to zero, and dependence on λ and the scale μ made explicit. If one chooses $s = \sqrt{\lambda}$, then a short exercise shows that

$$\hat{H}_{\rm NR}(\lambda;\mu) \cong \lambda\, \hat{H}_{\rm NR}(1,\mu/\sqrt{\lambda}) = \lambda\, \hat{H}_{\rm NR}(1,\mu) - \frac{\lambda \ln \lambda}{8\pi^2}\, m_{\rm W} \hat{N}_{\rm W}\,, \tag{4.17}$$

where $\cong$ denotes unitary equivalence and

$$\hat{N}_{\rm W} \equiv \sum_{\substack{a,b=1 \\ a\neq b}}^{N} \sum_{n=-\infty}^{\infty}{}' \; \hat{N}_n^{ab} \tag{4.18}$$

is the total number of charged W-bosons. The scaling relation (4.17) shows that the spectrum of the 2D Coulomb Hamiltonian $\hat{H}_{\rm NR}(\lambda;\mu)$ is simply proportional to the 't Hooft coupling λ, up to an overall additive shift proportional to $\lambda \ln \lambda$ times the number of charged constituents. This relation may equivalently be expressed as

$$\frac{1}{\lambda}\, \hat{H}_{\rm NR}(\lambda;\mu) \cong \frac{1}{\lambda'}\, \hat{H}_{\rm NR}(\lambda';\mu) - \frac{m_{\rm W}}{8\pi^2}\, \ln(\lambda/\lambda')\, \hat{N}_W\,. \tag{4.19}$$

4.2 Quark contributions

The quark fields modify the light and heavy sectors of the theory in several ways. In addition to their effects on the non-perturbative large distance dynamics, already mentioned in the previous section, the compactified quark fields contain massive degrees of freedom which play a role in physics on the scale of $m_{\rm W}$ and above. Specifically, every flavor and color component of a fundamental representation Dirac fermion leads, in a non-relativistic description, to a pair of two-component spinor fields which we will denote as ψ_n^{aA} and χ_n^{aA}. The field ψ_n^{aA} annihilates quarks of flavor A which have charge $+1$ under the a'th $U(1)$ gauge group (and are neutral with respect to all other $U(1)$ gauge group factors). The field χ_n^{aA} annihilates antiquarks of flavor A and charge -1 under the a'th $U(1)$ gauge group (and are neutral with respect to the other $U(1)$ gauge group factors). It will be convenient to define quark KK indices as half-integers, $n \in \mathbb{Z} + \frac{1}{2}$. These fields satisfy canonical anticommutation relations,

$$\left\{\psi_n^{aA}(\mathbf{x})_s,\, \psi_{n'}^{bB}(\mathbf{y})_{s'}^\dagger\right\} = \left\{\chi_n^{aA}(\mathbf{x})_s,\, \chi_{n'}^{bB}(\mathbf{y})_{s'}^\dagger\right\} = \delta^{ab}\, \delta^{AB}\, \delta_{nn'}\, \delta_{ss'}\, \delta^2(\mathbf{x}-\mathbf{y})\,, \tag{4.20}$$

where $s, s' = \pm$ are spin-1/2 spinor indices. All other anticommutators vanish. To describe the dynamics of the quarks, one must add another set of terms to the effective theory (4.2) describing W-bosons, namely

$$S_{\rm quark} = \sum_{a=1}^{N} \sum_{A=1}^{n_{\rm f}} \sum_{n \in \mathbb{Z}+\frac{1}{2}} \int dt\, d^2x \left[(\psi_n^{aA})^\dagger\, i\partial_t\, \psi_n^{aA} - M_n^{aA} |\psi_n^{aA}|^2 - \frac{|\boldsymbol{\nabla} \psi_n^{aA}|^2}{2m_n^{aA}} \right.$$
$$\left. + (\chi_n^{aA})^\dagger\, i\partial_t\, \chi_n^{aA} - M_n^{aA} |\chi_n^{aA}|^2 - \frac{|\boldsymbol{\nabla} \chi_n^{aA}|^2}{2m_n^{aA}} \right], \qquad (4.21)$$

where the covariant spatial gradients acting on fermions are defined by

$$(\boldsymbol{\nabla})_i\, \psi_n^{aA} \equiv [\nabla_i - i g_3 A_i^a]\, \psi_n^{aA}\,, \qquad (\boldsymbol{\nabla})_i\, \chi_n^{aA} \equiv [\nabla_i + i g_3 A_i^a]\, \chi_n^{aA}\,. \qquad (4.22)$$

The compact momentum p_3 carried by a quark created by $(\psi_n^{aA})^\dagger$ is

$$p_3 = m_{\rm W} \big[(a - \tfrac{1}{2}) - (A - \tfrac{1}{2})\, N/n_{\rm f} + nN \big]\,, \qquad (4.23)$$

while the antiquark created by $(\chi_n^{aA})^\dagger$ carries the opposite momentum $-p_3$. The rest and kinetic quark masses equal $|p_3|$, the magnitude of the compact momentum, up to higher order radiative corrections,

$$M_n^{aA} = |p_3|\, (1 + \mathcal{O}(\lambda))\,, \quad m_n^{aA} = |p_3|\, (1 + \mathcal{O}(\lambda))\,. \qquad (4.24)$$

Note that these fermion masses in the effective theory have nothing to do with chiral symmetry breaking quark masses in the underlying 4D theory, which we have assumed vanish. Our EFT fully respects the chiral symmetry (2.19) of the compactified theory. Nevertheless, the non-relativistic quark masses (4.24) are non-vanishing for all values of $n \in \mathbb{Z} + \frac{1}{2}$, $a = 1, \cdots, N$, and $A = 1, \cdots, n_{\rm f}$. (Recall that we have assumed that N is odd.) Our explicit calculations in Sec. 6 will focus on the special case of $n_{\rm f} = N$, for which the allowed values of the compact momentum of a quark become half-integers (times $m_{\rm W}$),

$$p_3 = m_{\rm W}\, k\,, \qquad \text{with } k \equiv a - A + nN\,. \qquad (4.25)$$

For a given Cartan index a, relation (4.25) gives a one-to-one mapping between the flavor and KK indices $\{A, n\}$ and the quantized momentum index k. When discussing the $n_{\rm f} = N$ theory, it will often be convenient to use the momentum index $k \in \mathbb{Z} + \frac{1}{2}$ in place of the (equivalent) values of the the flavor and KK indices and relabel the quark fields as

$$\psi_k^a \equiv \psi_n^{aA}\,, \quad \chi_k^a \equiv \chi_n^{aA}\,, \qquad (4.26)$$

with the implicit understanding that the flavor, KK and momentum indices are connected via relation (4.25). In other words, ψ_k^a annihilates a quark with compact momentum $p_3 = m_{\rm W} k$ and charge $+1$ under the a'th $U(1)$ gauge group, while χ_k^a annihilates an antiquark with compact momentum $p_3 = -m_{\rm W} k$ and charge -1 under the a'th $U(1)$ group.

In addition to the above quark kinetic terms, the Abelian charge densities ρ^a appearing in the Coulomb interactions of the effective theory (4.2) must be augmented to include the quark contributions,

$$\rho^a \equiv \sum_{b=1}^{N} {\sum_{n\in\mathbb{Z}}}' \left[(\vec{\phi}_n^{\,ab})^\dagger \cdot \vec{\phi}_n^{\,ab} - (\vec{\phi}_n^{\,ba})^\dagger \cdot \vec{\phi}_n^{\,ba} \right] + \sum_{A=1}^{n_{\rm f}} \sum_{n\in\mathbb{Z}+\frac{1}{2}} \left[(\psi_n^{aA})^\dagger \psi_n^{aA} - (\chi_n^{aA})^\dagger \chi_n^{aA} \right], \tag{4.27}$$

and the form of the Coulomb interactions appearing in the action (4.2) must now have the contribution from the unwanted extra $U(1)$ gauge group removed,

$$S_{\rm Coulomb} = \frac{\lambda m_{\rm W}}{4\pi} \int dt\, d^2x\, d^2y\, G(\mathbf{x}-\mathbf{y}) \left[\sum_{a=1}^{N} \rho^a(t,\mathbf{x})\, \rho^a(t,\mathbf{y}) - \frac{1}{N} \sum_{a,b=1}^{N} \rho^a(t,\mathbf{x})\, \rho^b(t,\mathbf{y}) \right]. \tag{4.28}$$

(Without the subtraction of the second term in this expression, the Coulomb energy would be that of a $U(N)$ gauge theory instead of $SU(N)$.) With quarks added to the theory, all the conserved Abelian charges Q^a, when acting on physical states, equal the baryon number,

$$Q^a = N_B \equiv \frac{1}{N} \sum_{a,A,n} \int d^2x \left[(\psi_n^{aA})^\dagger \psi_n^{aA} - (\chi_n^{aA})^\dagger \chi_n^{aA} \right]. \tag{4.29}$$

Conversion of the effective action for quarks (4.21) to the corresponding quark contribution of the non-relativistic Hamiltonian proceeds as described earlier. As with the W-bosons, normal ordering the Coulomb interactions induces logarithmic dependence on the scale μ in the quark rest masses,

$$\mu \frac{d}{d\mu} M_n^{aA}(\mu) = -\frac{\lambda m_{\rm W}}{8\pi^2} \left(1 - \tfrac{1}{N}\right). \tag{4.30}$$

In the presence of quarks the rescaling relation (4.19) becomes

$$\frac{1}{\lambda}\, \hat{H}_{\rm NR}(\lambda;\mu) \cong \frac{1}{\lambda'}\, \hat{H}_{\rm NR}(\lambda',\mu) - \frac{m_{\rm W}}{16\pi^2} \ln(\lambda/\lambda') \left[2\hat{N}_{\rm W} + \left(1 - \tfrac{1}{N}\right) \hat{N}_{\rm q+\bar{q}} \right], \tag{4.31}$$

where

$$\hat{H}_{\rm NR}(\lambda;\mu) \equiv \hat{H}\Big|_{\vec{A}^a=0} - \sum_{a,b=1}^{N} {\sum_{n\in\mathbb{Z}}}' M_n^{ab}(\mu)\, \hat{N}_n^{ab} - \sum_{a=1}^{N} \sum_{A=1}^{n_{\rm f}} \sum_{n\in\mathbb{Z}+\frac{1}{2}} M_n^{aA}(\mu)\, \hat{N}_n^{aA} \tag{4.32}$$

is the non-relativistic Hamiltonian with all rest energies removed,

$$\hat{N}_n^{aA} \equiv \int d^2x \, \left[\psi_n^{ab}(\mathbf{x})^\dagger \psi_n^{ab}(\mathbf{x}) + \chi_n^{ab}(\mathbf{x})^\dagger \chi_n^{ab}(\mathbf{x})\right] \tag{4.33}$$

counts the number of quarks plus antiquarks of the specified type, and the operator $\hat{N}_{\mathrm{q}+\bar{\mathrm{q}}} \equiv \sum_{A=1}^{n_{\mathrm{f}}} \sum_{a=1}^{N} \sum_{n \in \mathbb{Z}+\frac{1}{2}} \hat{N}_n^{aA}$ is the total number of quarks plus antiquarks.

5 Symmetries

As already noted, physical states in an $SU(N)$ gauge theory must be gauge invariant. In the compactified theory, this is trivially enforced dynamically: gauge invariant states are those which do not have divergent Coulomb energies. This is equivalent to the just-stated condition (4.29) that all $U(1)$ changes equal the baryon number, $Q^a = N_B$. To see this connection more explicitly, it may be helpful to note that our effective W-boson fields, $\vec{\phi}_n^{ab}$, which were described earlier in a basis-dependent fashion as coming from a specified row and column of the 4D gauge field — when the holonomy has the specific form (2.4) — could have been introduced in a manifestly basis-independent fashion by first defining the operators

$$\mathcal{P}_a \equiv \frac{1}{N} \sum_{n=0}^{N-1} \omega^{-(a-\frac{1}{2}(N+1))n} \, \Omega^n \,, \qquad a = 1, \cdots, N. \tag{5.1}$$

The operators (5.1) are mutually orthogonal Hermitian projection operators, $\mathcal{P}_a \, \mathcal{P}_b = \delta_{ab} \, \mathcal{P}_a$, when Ω lies at the center-symmetric minimum (2.4) and the eigenvalues of Ω are all N'th roots of -1 or $+1$. Our effective 3D fields correspond to pieces of the original 4D fields extracted by these projection operators,[16]

$$F_{\mu\nu}^a \propto \mathrm{tr}\,(\mathcal{P}_a F_{\mu\nu}) \,, \quad \vec{\phi}_n^{ab} \propto \mathcal{P}_a \vec{D} \, \mathcal{P}_b \,, \quad \psi_n^{aA} \propto \mathcal{P}_a \, q^A \,, \quad \chi_n^{aA} \propto \bar{q}^A \mathcal{P}_a \,, \tag{5.2}$$

(neglecting details of the KK decomposition, spinor structure, etc.). This highlights the point that the Cartan gauge fields are associated with manifestly gauge invariant 4D operators, while the W-boson and quark fields are gauge covariant, as one would expect. With the aid of such expressions, it is easy to see that composite operators in the 3D theory which map onto manifestly gauge invariant 4D operators are precisely those satisfying the condition $Q^a = N_B$. As examples, the operators

$$G^{ab} \equiv \vec{\phi}_0^{ab} \cdot \vec{\phi}_0^{ba} \qquad \sim \mathrm{tr}\,(D_i \, \mathcal{P}_b \, D_i \, \mathcal{P}_a) \,, \tag{5.3a}$$

$$M_{AB}^a \equiv \chi_{1/2}^{aA} \, \psi_{1/2}^{aB} \qquad \sim \bar{q}^B \mathcal{P}_a \, q^A \,, \tag{5.3b}$$

$$B_A \equiv \psi_{1/2}^{1,A} \, \psi_{1/2}^{2,A} \cdots \psi_{1/2}^{N,A} \sim (\mathcal{P}_1 q^A) \, (\mathcal{P}_2 q^A) \cdots (\mathcal{P}_N q^A) \,, \tag{5.3c}$$

[16] These are leading order relations. As with any effective field theory, field redefinitions and matching corrections complicate higher order relations between fields in the effective and original theories.

(with no implied sums on Cartan indices, and extraneous structure suppressed) are prototypical glueball, meson, and baryon operators, respectively.

The global symmetries which are respected by our compactification and under which eigenstates of the Hamiltonian may be classified include the spacetime symmetries of 2+1 dimensional Minkowski space, leading to conserved total 2D spatial momentum ($\vec{P}$) and angular momentum (J_z). States with vanishing J_z may be further classified by their behavior under 2D spatial reflections.[17] Translation invariance in the compactified direction implies conservation of the total compact momentum,

$$P_3 \equiv \int d^2x \left\{ \sum_{a,b=1}^{N} \sum_{n\in\mathbb{Z}} m_{\rm W}(a-b+nN)\, (\vec{\phi}_n^{ab})^\dagger \vec{\phi}_n^{ab} \right. \\ \left. + \sum_{a=1}^{N} \sum_{A=1}^{n_{\rm f}} \sum_{n\in\mathbb{Z}+\frac{1}{2}} m_{\rm W}\big((a-\tfrac{1}{2}) - \tfrac{N}{n_{\rm f}}(A-\tfrac{1}{2}) + nN\big) \left[(\psi_n^{aA})^\dagger \psi_n^{aA} - (\chi_n^{aA})^\dagger \chi_n^{aA}\right] \right\}. \quad (5.4)$$

As discussed earlier, our individual fields carry compact momentum quantized in units of $m_{\rm W}$ (for $\vec{\phi}_n^{ab}$) or linear combinations of $m_{\rm W}$ and $(N/n_{\rm f})\, m_{\rm W}$ (for ψ_n^{aA} and χ_n^{aA}). Physical glueball and flavor singlet mesons states must have total compact momentum equal to an integer multiple of $2\pi/L = N m_{\rm W}$, as these states remain invariant when translated once around the compact dimension. Due to our flavor-twisted boundary conditions for quarks, flavor non-singlet mesons can have P_3 equal to integer multiples of $2\pi/(n_{\rm f}L)$. The allowed values of P_3 for flavor singlet (non-singlet) baryons are integer or half-integer multiples of $2\pi/L$ (or $2\pi/(n_{\rm f}L)$) depending on whether N is even or odd.

When quarks are present, the unbroken $U(1)_V^{n_{\rm f}}$ flavor symmetry transformations are generated by the conserved flavor charges

$$N^A \equiv \int d^2x \sum_{a=1}^{N} \sum_{n\in\mathbb{Z}+\frac{1}{2}} \left[(\psi_n^{aA})^\dagger \psi_n^{aA} - (\chi_n^{aA})^\dagger \chi_n^{aA}\right]. \quad (5.5)$$

The sum of these flavor charges equals the total number of quarks minus antiquarks, or N times the baryon number N_B.

Axial $U(1)_A^{n_{\rm f}}$ flavor symmetry transformations act as spin rotations on the EFT fermions and are generated by the axial charges

$$N_5^A \equiv \int d^2x \sum_{a=1}^{N} \sum_{n\in\mathbb{Z}+\frac{1}{2}} \left[(\psi_n^{aA})^\dagger \sigma_3\, \psi_n^{aA} + (\chi_n^{aA})^\dagger \sigma_3\, \chi_n^{aA}\right]. \quad (5.6)$$

[17] Reflections are only a symmetry of the theory when $\theta = 0$ (or π), but the violation of reflection symmetry induced by a non-zero θ only affects the long distance non-perturbative physics. For a more thorough discussion of the action of various symmetry transformations in the 3D effective theory, refer to Appendix C.

The perturbative dynamics conserves these charges but the long range non-perturbative dynamics violates conservation of $\overline{N}_5 \equiv \sum_A N_5^A$ (and the non-perturbative vacuum is not annihilated by the other axial charges).

In the absence of quarks, the compactified theory is invariant under the $\mathbb{Z}_N$ center symmetry which, by construction, remains unbroken. The defining center symmetry transformation (2.3) multiplies the holonomy by an N'th root of unity, $\Omega \to \omega\,\Omega$. This permutes the projection operators (5.1), $\mathcal{P}_a \to \mathcal{P}_{a-1}$ (with $\mathcal{P}_0 \equiv \mathcal{P}_N$), and also acts as a cyclic permutation on our 3D fields,

$$\sigma^a \to \sigma^{a-1}\,, \quad \vec{\phi}_k^{\,a} \to \vec{\phi}_k^{\,a-1}\,. \tag{5.7}$$

Here, Cartan indices are to be understood to be defined modulo N (so $a-1 \equiv N$ when $a=1$). Glueball operators such as $G_k^a \equiv \vec{\phi}_k^{\,a} \cdot \vec{\phi}_{-k}^{\,a-q}$ (with $k \bmod N \equiv q$) are likewise cyclically permuted by center symmetry transformations. To diagonalize center symmetry, one must perform a discrete $\mathbb{Z}_N$ Fourier transform and define, for example,

$$\tilde{\sigma}^p \equiv \frac{1}{\sqrt{N}} \sum_{a=1}^{N} \omega^{ap}\,\sigma^a\,, \quad \widetilde{G}_k^p \equiv \frac{1}{\sqrt{N}} \sum_{a=1}^{N} \omega^{ap}\,G_k^a\,. \tag{5.8}$$

These operators now have definite center symmetry charge $p = 0, \cdots, N-1$, meaning that under the center symmetry transformation (2.3) they transform into themselves multiplied by the eigenvalue $\omega^p = e^{2\pi i p/N}$.

Adding fundamental representation quarks to the theory generally breaks the $\mathbb{Z}_N$ center symmetry. However, in the special case of $n_{\rm f} = N$, the theory retains an intertwined $\mathbb{Z}_N$ color-flavor center symmetry (see, e.g., Refs. [44, 45]).[18] This symmetry combines the usual center transformation (2.3) with a cyclic permutation of quark flavors. In terms of our 3D fields, this flavor-intertwined center symmetry acts as

$$\sigma^a \to \sigma^{a-1}\,, \quad \vec{\phi}_k^{\,a} \to \vec{\phi}_k^{\,a-1}\,, \quad \psi_k^a \to \psi_k^{a-1}\,, \quad \chi_k^a \to \chi_k^{a-1}\,, \tag{5.9}$$

and again may be diagonalized by a discrete $\mathbb{Z}_N$ Fourier transform.

Because the sets of eigenvalues (2.4) and (2.17) of the gauge holonomy Ω and our chosen flavor holonomy Ω_F are invariant under complex conjugation, both charge conjugation and reflection of the compactified dimension ($x_3 \to -x_3$) remain symmetries of theory provided they are combined with global gauge and flavor transformations which suitably permute the Cartan and flavor indices. The ordering (2.4) of the eigenvalues

[18] More generally, if $d \equiv \gcd(n_{\rm f}, N) > 1$, then a $\mathbb{Z}_d$ color-flavor center symmetry remains [44]. For simplicity, we will focus on the case of $n_{\rm f} = N$.

of the gauge holonomy was chosen so that the required global gauge transformation V is just a permutation which flips Cartan indices, $a \to N{+}1 - a$, reflecting the fact that

$$\Omega^* = V\,\Omega\,V^\dagger\,, \tag{5.10}$$

with $V \equiv \|\delta_{a+b,N+1}\|$ an anti-diagonal transposition. Similarly, given the order (2.17) of the flavor holonomy eigenvalues, the required flavor transformation V_F also corresponds to a simple flip of flavor indices, $A \to n_{\rm f}{+}1 - A$, since

$$\Omega_F^* = V_F\,\Omega_F\,V_F^\dagger\,, \tag{5.11}$$

with $V_F \equiv \|\delta_{A+B,n_{\rm f}+1}\|$. This redefined charge conjugation symmetry acts on the fields of our our dimensionally reduced EFT as

$$\sigma^a \to -\sigma^{\bar a}\,, \qquad\qquad \psi_n^{aA} \to \chi_{-n}^{\bar a\bar A}\,, \tag{5.12a}$$

$$\vec\phi_n^{\,ab} \to -\vec\phi_n^{\,\bar b\bar a}\,, \qquad\qquad \chi_n^{aA} \to \psi_{-n}^{\bar a\bar A}\,, \tag{5.12b}$$

where $\bar a \equiv N{+}1 - a$, $\bar A \equiv n_{\rm f}{+}1 - A$.[19] Note that center symmetry does not commute with charge conjugation. In choosing a basis for degenerate levels of the Hamiltonian, one must choose between specifying center symmetry charge, or the sign under the (appropriately redefined) charge conjugation symmetry; we will generally opt for the former.

Finally, reflection in the compact direction, x_3 $to - x_3$, when combined with the same global gauge and flavor transformations V and V_F, remains a symmetry. This redefined reflection symmetry acts on our 3D EFT fields as

$$\sigma^a \to \sigma^{\bar a}\,, \qquad\qquad \psi_n^{aA} \to -i\sigma_2\,\psi_{-n}^{\bar a\bar A}\,, \tag{5.13a}$$

$$\vec\phi_n^{\,ab} \to \vec\phi_{-n}^{\,\bar a\bar b}\,, \qquad\qquad \chi_n^{aA} \to i\sigma_2\,\chi_{-n}^{\bar a\bar A}\,. \tag{5.13b}$$

The combined symmetry of charge conjugation times x_3 reflection does not involve any global gauge or flavor transformations and acts as

$$\sigma^a \to -\sigma^a\,, \qquad\qquad \psi_n^{aA} \to i\sigma_2\,\chi_n^{aA}\,, \tag{5.14a}$$

$$\vec\phi_n^{\,ab} \to -\vec\phi_{-n}^{\,ba}\,, \qquad\qquad \chi_n^{aA} \to -i\sigma_2\,\psi_n^{aA}\,. \tag{5.14b}$$

This is the same as a CP transformation times a 180° rotation in the uncompactified directions.

[19] The form of this transformation relies on our simplifying assumption that N is odd, so that eigenvalues of Ω are roots of $+1$ and Ω_F eigenvalues are roots of -1. If N is even then both ±1 can be eigenvalues of the flavor holonomy Ω_F for some values of $n_{\rm f} \le N$. When two eigenvalues of Ω_F are real, the required flavor transformation V_F which must be combined with the naive action of charge conjugation no longer corresponds to the simple flip $A \to \bar A$ of flavor indices.

6 Heavy sector spectrum

6.1 Overview

Three basic types of bound states can be formed from the constituents of our non-relativistic effective theory: glueballs, mesons, and baryons. Here, "bound state" means either a genuine single particle eigenstate of the full theory, or a narrow resonance whose fractional decay width vanishes in the $L \to 0$ (and correspondingly $\lambda \to 0$) limit. In this section, we neglect the coupling to the Abelian gauge fields contained in the spatial covariant derivatives, as well as higher dimension operators not shown explicitly in our effective theories (4.2) and (4.21). Effects of these terms are discussed in Sec. 7 which discusses decay processes.

By glueballs we mean bound states of two or more charged W-bosons, and no quarks or antiquarks. Mesons are, of course, bound states of a quark and antiquark, possibly containing additional W-bosons, while baryons are bound states of N quarks (perhaps with additional charged W-bosons). In our weakly coupled small-L regime, mixing between glueballs and flavor singlet mesons is suppressed, so they are clearly distinguishable. Manifestly gauge invariant interpolating operators for simple examples of such states were shown in Eq. (5.3). Further possibilities, which we will not focus on in this paper, include multi-meson or multi-glueball "molecules" and multi-baryon bound states.

As discussed above, all physical (gauge invariant) states must satisfy $Q^a = N_B$. Hence, glueballs and mesons must be composed of combinations of constituents for which all $U(1)^N$ charges sum to zero. The simplest glueballs are two-body bound states of a W-boson and its oppositely charged antiparticle, created by operators such as

$$(\vec{\phi}_0^{\,ab})^\dagger \cdot (\vec{\phi}_0^{\,ba})^\dagger \,, \tag{6.1}$$

with $a \neq b$. Two different $U(1)$ gauge group factors contribute to the logarithmic interaction between these constituents, giving an attractive interaction of relative strength 2. The explicit two-body Hamiltonian, and its spectrum, is examined in Sec. 6.2.2 below. Bound states of more than two W-bosons can also form. States of this type which cannot be decomposed into two or more separately gauge invariant glueballs consist of W-bosons whose charge assignments lead to a ring-like color structure with nearest-neighbor logarithmic interactions. Examples of operators creating such states are

$$(\phi_0^{ab})_i^\dagger (\phi_0^{bc})_j^\dagger (\phi_0^{ca})_k^\dagger \,, \quad (\phi_0^{ab})_i^\dagger (\phi_0^{bc})_j^\dagger (\phi_0^{cd})_k^\dagger (\phi_0^{da})_l^\dagger \,, \tag{6.2}$$

etc., with up to N constituents and Cartan indices $a, b, c, \cdots$ all distinct. We will refer to these as "closed string" glueballs. These are all single trace operators when

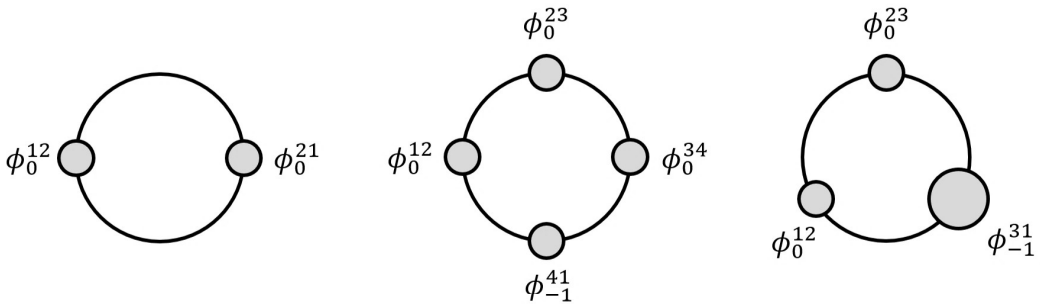

Figure 2. Examples of glueball states when $N = 4$. Filled circles represent the charged W-bosons, with larger circles indicating more massive constituents. Lines connecting the constituents indicate attractive logarithmic interactions (of relative strength 1).

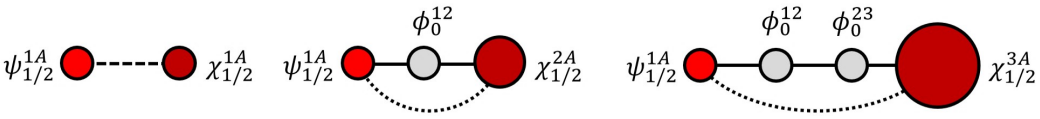

Figure 3. Examples of meson states (with $N \geq 3$). Filled circles represent the charged constituents. Solid lines connecting constituents indicate attractive logarithmic interactions of relative strength 1, dashed lines represent attractive interactions of strength $1-\frac{1}{N}$, and dotted lines represent repulsive logarithmic interactions of strength $1/N$.

expressed in terms of the original 4D fields (as in Eq. (5.3)). In these multi-body states, a single $U(1)$ factor generates an attractive logarithmic interaction (of relative strength 1) between each pair of neighboring constituents in the cyclic list. This is illustrated schematically in Fig. 2. We note that there is an amusing similarity between these states and the picture advocated long ago in Ref. [63].

The situation with mesons is similar. The simplest mesons are two-body bound states, created by operators such as

$$(\chi_{1/2}^{aA})^\dagger (\psi_{1/2}^{aB})^\dagger \,. \tag{6.3}$$

The attractive logarithmic interaction between the quark and antiquark has relative strength of $(1-\frac{1}{N})$, with the reduction from 1 coming from the subtraction of the unwanted "extra" $U(1)$ contribution in the Coulomb interaction (4.28). There are also mesons in which one or more additional W-bosons are present. States of this type which cannot be decomposed into meson-glueball products have charge assignments implying an "open string" color structure. Examples of operators creating such states include

$$(\chi_{1/2}^{aA})^\dagger (\phi_0^{ab})_i^\dagger (\psi_{1/2}^{bB})^\dagger \,, \quad (\chi_{1/2}^{aA})^\dagger (\phi_0^{ab})_i^\dagger (\phi_0^{bc})_j^\dagger (\psi_{1/2}^{cB})^\dagger \,, \tag{6.4}$$

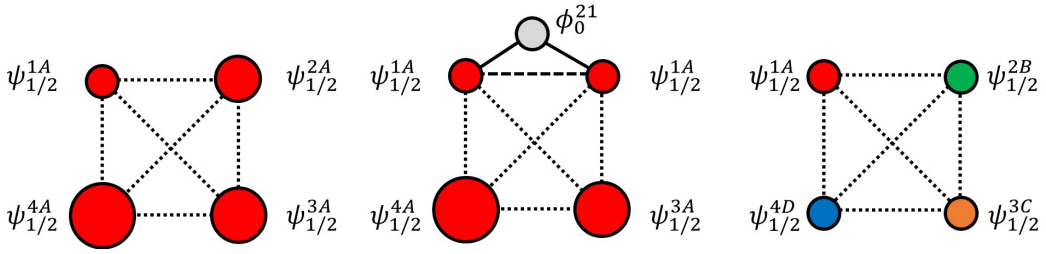

Figure 4. Examples of baryon states when $N=4$. Filled circles represent the charged constituents, with larger circles indicating more massive constituents. Dotted lines represent attractive logarithmic interactions of strength $1/N$, dashed lines represent repulsive interactions of strength $1-\frac{1}{N}$, and solid lines show attractive interactions of strength 1. In the single flavor example (left), each quark constituent has a different mass due to their differing Cartan indices. The multi-flavor example (right) shows the special case with $n_{\rm f}=4$ where all constituents have equal mass.

etc, with up to $N-1$ W-bosons inserted between the quark and antiquark and Cartan indices $a, b, c, \cdots$ all distinct. There are attractive logarithmic interactions of relative strength 1 between each pair of neighboring constituents, along with a repulsive logarithmic interaction of strength $1/N$ between the quark and antiquark (with differing Cartan charges). This is illustrated schematically in Fig. 3.

Finally, baryons containing N quarks, potentially with additional W-bosons as well, are present as finite energy bound states because our gauge group is $SU(N)$, not $U(N)$. The simplest non-exotic baryons are created by operators like

$$(\psi^{1,A}_{1/2})^\dagger(\psi^{2,B}_{1/2})^\dagger(\psi^{3,C}_{1/2})^\dagger\cdots(\psi^{N,Z}_{1/2})^\dagger\,. \tag{6.5}$$

In such states, every pair of quarks has an attractive logarithmic interaction of relative strength $1/N$. Several such baryon states, as well as baryon states containing additional W-bosons, are illustrated schematically in Fig. 4.

The stability of these various hadronic states will depend on their relative energy differences and the resulting radiative transition and short distance annihilation rates. These are discussed below in Sec. 7.

6.2 Two-body states

Neglecting couplings to the spatial Abelian gauge fields (which are relevant for radiative decays but not the leading order spectrum), the dynamics of all two-body sectors of our effective theory (4.12), namely glueballs composed of oppositely charged W-bosons,

quark-antiquark mesons, and diquark baryons in the special case of $N=2$, are described by a common first-quantized two-dimensional non-relativistic Hamiltonian,

$$\hat{H} = \frac{\mathbf{p}_1^2}{2m_1} + \frac{\mathbf{p}_2^2}{2m_2} + \kappa\, \ln(\mu|\mathbf{x}_1 - \mathbf{x}_2|)\,, \tag{6.6}$$

with a logarithmic potential and positive interaction strength, $\kappa > 0$. Before discussing our specific application to glueball, meson, and $N=2$ baryons in compactified QCD, we first summarize properties of the spectrum of this quantum theory.

6.2.1 2D logarithmic QM

Starting with the two particle Hamiltonian (6.6), separating the center of mass motion and working in the center-of-mass frame leads to a one-body Hamiltonian for the relative motion,

$$\hat{H}_{\text{relative}} = \frac{\mathbf{p}^2}{2m} + \kappa\, \ln(\mu|\mathbf{x}|)\,, \tag{6.7}$$

where $m \equiv m_1 m_2/(m_1+m_2)$ is the reduced mass. Non-relativistic dimensional analysis (with $\hbar \equiv 1$) shows that $\kappa m/\mu^2$ is the only dimensionless combination of parameters appearing in the Hamiltonian (6.7), so its eigenvalues must have the form $E = \kappa\, f(\kappa m/\mu^2)$ for some univariate function f. The manifestly trivial μ dependence, $\partial E/\partial \mu = \kappa/\mu$, then implies that the energy eigenvalues of $\hat{H}_{\text{relative}}$ are given by

$$E = \kappa\Big[\epsilon - \tfrac{1}{2} \ln \frac{\kappa m}{\mu^2}\Big], \tag{6.8}$$

where ϵ is an eigenvalue of the theory with $\kappa = m = \mu \equiv 1$. Introducing a dimensionless radial variable $r = \sqrt{\kappa m}\,|\mathbf{x}|$, eigenstates with orbital angular momentum $L_z \equiv \ell = 0, \pm 1, \pm 2, \cdots$ satisfy the one-dimensional radial Schrödinger equation,

$$\left[-\tfrac{1}{2}\frac{d^2}{dr^2} + V_\ell(r)\right] \chi(r) = \epsilon\, \chi(r)\,, \tag{6.9}$$

with effective radial potential

$$V_\ell(r) \equiv \frac{\ell^2 - \frac{1}{4}}{2r^2} + \ln r\,. \tag{6.10}$$

Solutions to the Schrödinger equation (6.9) are not expressible in terms of familiar special functions. The equation was analyzed numerically over 40 years ago [64] (see also Refs. [36, 65]), but we will present our own more accurate and extensive results. Calculations of low-lying energy levels are fairly straightforward using variational methods and a suitable basis set, or alternatively using pseudo-spectral methods [66] with

n	$\lvert\ell\rvert = 0$	1	2	3	4	5	6	7	8	9
0	0.179935	1.03961	1.49780	1.81127	2.04971	2.24214	2.40348	2.54238	2.66432	2.77301
1	1.31468	1.66290	1.92929	2.14154	2.31731	2.46710	2.59753	2.71299	2.81656	2.91044
2	1.83061	2.04777	2.23348	2.39248	2.53070	2.65265	2.76163	2.86008	2.94982	3.03224
3	2.16887	2.32609	2.46790	2.59439	2.70781	2.81028	2.90360	2.98920	3.06819	3.14152
4	2.42105	2.54403	2.65839	2.76311	2.85901	2.94717	3.02859	3.10416	3.17460	3.24054
5	2.62222	2.72309	2.81873	2.90790	2.99083	3.06805	3.14015	3.20770	3.27118	3.33102
6	2.78959	2.87502	2.95712	3.03466	3.10761	3.17622	3.24085	3.30185	3.35957	3.41429
7	2.93290	3.00696	3.07882	3.14735	3.21239	3.27407	3.33257	3.38814	3.44101	3.49138
8	3.05822	3.12356	3.18740	3.24875	3.30740	3.36337	3.41677	3.46776	3.51650	3.56314
9	3.16956	3.22799	3.28541	3.34092	3.39428	3.44548	3.49457	3.54165	3.58684	3.63024

Table 1. The first ten eigenvalues $\epsilon_{n,\ell}$ of the radial Schrödinger equation (6.9), for $|\ell| = 0, 1, \cdots, 9$. All digits shown are accurate.

a Gauss-Laguerre grid for the semi-infinite radial domain.[20] The first ten levels, for each $|\ell| = 0, \cdots, 9$, are listed in Table 1. The spectrum is shown graphically in Fig. 5. Notice that levels at neighboring values of ℓ are interleaved, $\epsilon_{n,|\ell|} < \epsilon_{n,|\ell|+1} < \epsilon_{n+1,|\ell|}$.

As $|\ell|$ increases, the minimum of the potential moves to larger values, with $r_{\min} \sim |\ell| + \mathcal{O}(\ell^{-2})$. When $|\ell| \gg 1$, a quadratic approximation to the potential is sufficient to find low-lying states. For fixed level number n (starting from 0),

$$\epsilon_{n,\ell} = \ln(|\ell|) + \tfrac{1}{2} + \frac{2n+1}{\sqrt{2}\,|\ell|} + \mathcal{O}(\ell^{-2})\,. \tag{6.11}$$

Standard WKB methods may be used to study more highly excited states. When the energy ϵ is large compared to $\max(1, \ln|\ell|)$, the classically allowed region of the Schrödinger equation (6.9) extends out to a turning point at $r_* \equiv \exp(\epsilon)$. For $r > r_*$, the WKB solution which decays as $r \to \infty$ is

$$f_{\rm I}(r) = \big[\ln(r)/\epsilon - 1\big]^{-1/4} \exp\big[-\sqrt{2\epsilon}\,|Q_0(r)| + \mathcal{O}(\epsilon^{-1/2})\big], \tag{6.12}$$

[20] A simple choice of basis for a variational calculation consists of 2D harmonic oscillator eigenstates with definite angular momentum ℓ. Given a suitable adjustment of the scale of the harmonic oscillator basis functions, a truncated basis of 40 harmonic oscillator states is sufficient to find the lowest energy level of the logarithmic Hamiltonian (6.7) to an accuracy of a few parts in 10^4. However, pseudo-spectral discretization using a Laguerre grid turns out to provide significantly better accuracy for a given basis size. (This is because harmonic oscillator wavefunctions with their Gaussian envelope decrease too rapidly at large r; as discussed below eigenstate wavefunctions in a logarithmic potential decrease much more slowly.) To obtain the eigenvalues shown in Table 1 and compute transition matrix elements for radiative decays, discussed in Sec. 7, we used Gauss-Laguerre grids with 100–200 points. To avoid excessive precision loss in the evaluation of the spectral differentiation matrices and the resulting eigenvalue computation, we used extended precision arithmetic with slightly over twice as many digits as the number of grid points.

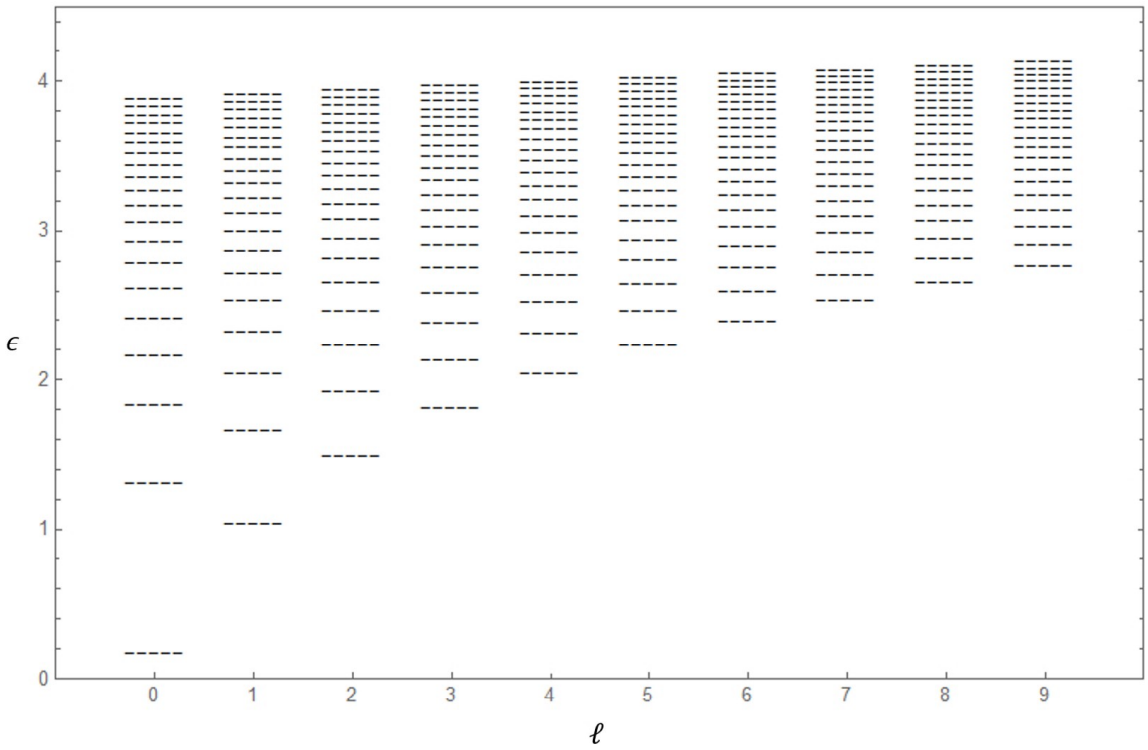

Figure 5. Energy spectrum of the radial Schrödinger equation (6.9).

where

$$Q_0(r) \equiv \int_r^{r_*} dr' \, \sqrt{1-\ln(r')/\epsilon} \, . \tag{6.13}$$

The usual Airy function matching across the turning point (or analytic continuation around the turning point) shows that this solution matches onto the allowed region WKB solution

$$f_{\rm II}(r) = [1-\ln(r)/\epsilon]^{-1/4} \, \cos\left[\sqrt{2\epsilon}\, Q_0(r) - \tfrac{\pi}{4} + \mathcal{O}(\epsilon^{-1/2})\right]. \tag{6.14}$$

This WKB approximation is valid down to $r = \mathcal{O}(1)$, where

$$f_{\rm II}(r) \sim \cos\left[\sqrt{2\epsilon}\, r - I(\epsilon) + \tfrac{\pi}{4} + \mathcal{O}(\epsilon^{-1/2})\right] \times (1 + \mathcal{O}(\epsilon^{-1})) \, , \tag{6.15}$$

with

$$I(\epsilon) \equiv \sqrt{2\epsilon}\, Q_0(0) = \sqrt{\tfrac{\pi}{2}}\, \exp(\epsilon) \, . \tag{6.16}$$

For parametrically small values of r, the centrifugal term in the potential cannot be neglected but the logarithmic term is subdominant. In this region, the appropriate solution satisfying regularity at the origin is

$$f_{\rm III}(r) = (\tfrac{1}{2}\epsilon)^{1/4} \sqrt{\pi r}\, J_{|\ell|}(\sqrt{2\epsilon}\, r) \, . \tag{6.17}$$

When $r \gg \epsilon^{-1/2}$, $f_{\rm III}(r) \sim \cos(\sqrt{2\epsilon}\, r - \frac{\pi}{2}\,|\ell| - \frac{\pi}{4}) + \mathcal{O}\big((\sqrt{\epsilon} r)^{-1}\big)$. For $\mathcal{O}(1)$ values of r, this matches onto the the classically allowed WKB solution (6.14) provided

$$I(\epsilon) = \tfrac{1}{2}(2n+|\ell|+1)\,\pi + \mathcal{O}(\epsilon^{-1/2})\,, \tag{6.18}$$

for some integer n. Inserting the result (6.16), one finds that eigenvalues $\epsilon_{n,\ell}$ of the radial Schrödinger equation (6.9) are given by

$$\epsilon_{n,\ell} = \ln(2n+|\ell|+1) + \tfrac{1}{2}\ln\tfrac{\pi}{2}\,, \tag{6.19}$$

up to corrections vanishing faster than $\mathcal{O}(1/n)$. One may verify that n equals the number of nodes in this solution, so n is level number when counting from 0.

Numerically, the accuracy of the WKB approximation (6.19) to energy levels is surprisingly good for modest values of the level number n. For $\ell = 0$ and $n = 10$, the difference between our numerical and WKB results is less than 2 parts in 10^4. The relative deviation grows with increasing ℓ at fixed n, reaching 2% for $\ell = n = 10$.

The WKB result (6.19) shows that the level spacing (at fixed ℓ) decreases with increasing level number, $d\epsilon/dn = 2/(2n+|\ell|+1)$. Inverting this relation, one finds that the asymptotic density of states with fixed orbital angular momentum ℓ rises exponentially with energy,

$$\frac{\partial n_\ell}{\partial \epsilon} \sim \frac{e^\epsilon}{\sqrt{2\pi}}\,. \tag{6.20}$$

(This neglects any spin degeneracy of the constituents.) The integral of this density of states gives the total number of quantum states, with fixed ℓ, below a given energy, and asymptotically equals the area of the classically allowed region in phase space (in units of $2\pi\hbar$),

$$\begin{aligned} n_\ell(\epsilon) &= \int \frac{dp}{2\pi}\, dr\, \Theta(\epsilon - \tfrac{1}{2}p^2 - V_\ell(r)) = \frac{\sqrt{2}}{\pi}\int_{r_{\rm min}}^{r_{\rm max}} dr\, \sqrt{\epsilon - V_\ell(r)} \\ &= \frac{\sqrt{2}}{\pi}\left[\int_0^{e^\epsilon} dr\, \sqrt{\epsilon - \ln r}\right] + \mathcal{O}(|\ell|^{-\frac{1}{2}}) = \frac{e^\epsilon}{\sqrt{2\pi}} + \mathcal{O}(|\ell|^{-\frac{1}{2}})\,. \end{aligned} \tag{6.21}$$

The total number of states below energy ϵ (with vanishing total momentum, but no projection onto definite ℓ), $N(\epsilon) = \sum_\ell n_\ell(\epsilon)$, coincides asymptotically with the classically allowed phase space volume of the 2D relative dynamics. This grows exponentially at twice the rate of the fixed-ℓ result,

$$N(\epsilon) = \int \frac{d^2p}{(2\pi)^2}\, d^2r\, \Theta(\epsilon - \tfrac{1}{2}p^2 - \ln r) = \int_0^{e^\epsilon} r\, dr\, (\epsilon - \ln r) = \tfrac{1}{4}\, e^{2\epsilon}\,. \tag{6.22}$$

This exponential growth is a direct consequence of the slow increase of the confining logarithmic potential with distance. Bound states spread over rapidly growing spatial

regions as their energy increases. The exponential behavior (6.21) of the fixed-ℓ number of states is nothing but linear dependence on the turning point radius r_*, while the total number of states (6.22) is, up to a factor of $1/(4\pi)$, just the spatial area of the allowed region, πr_*^2.

6.2.2 Glueballs

For every pair of oppositely charged W-bosons there is a manifold of bound states described by the two-body logarithmic interaction Hamiltonian (6.6) with interaction strength

$$\kappa = \frac{\lambda m_{\rm W}}{2\pi^2}\,. \tag{6.23}$$

This is analogous to the ro-vibrational states associated with each electronic level in molecular spectroscopy. For a pair of W-bosons with compact momentum indices k and k' (defined by the relation (4.6) and satisfying the constraint $k + k' = 0 \bmod N$ so that the W-bosons have opposite Cartan charges), the resulting bound state energies are given by

$$E_{WW} = M_k(m_{\rm W}) + M_{k'}(m_{\rm W}) + \frac{\lambda m_{\rm W}}{2\pi^2}\Big(\epsilon_{n,\ell} - \tfrac{1}{2}\ln\frac{\lambda\, m_{kk'}}{2\pi^2 m_{\rm W}}\Big), \tag{6.24}$$

where the reduced mass $m_{kk'} \equiv m_k\, m_{k'}/(m_k{+}m_{k'})$, and we have chosen to set the arbitrary scale μ equal to $m_{\rm W}$. The lightest glueballs are composed of W-bosons with one unit of compact momentum, $|k| = |k'| = 1$, and tree-level constituent mass $m_{\rm W}$, leading to glueball energies

$$E = 2M_1(m_{\rm W}) + \frac{\lambda m_{\rm W}}{2\pi^2}\Big(\epsilon_{n,\ell} - \tfrac{1}{2}\ln\frac{\lambda}{4\pi^2}\Big). \tag{6.25}$$

Neglecting higher order relativistic corrections, as well as non-perturbative physics on the scale of m_γ, two-body glueball states have a degeneracy of $4N$ if they are $\ell = 0$ and CP self-conjugate. (Center symmetry gives a factor of N, and there is a spin degeneracy of 4 since each massive W-boson has two spin states.) There is an additional factor of 2 degeneracy for states with non-zero orbital angular momentum (corresponding to positive and negative values of ℓ, which are exchanged by 2D spatial reflections), and a separate additional factor of 2 degeneracy for states which are not CP self-conjugate. The lightest glueball level (6.25) contains CP self-conjugate $\ell = 0$ states, and hence has the minimal degeneracy of $4N$.

Relativistic corrections to the above results contribute $\mathcal{O}(\lambda^2 m_{\rm W})$ energy shifts, or relative $\mathcal{O}(\lambda)$ corrections to binding energies. Spin-orbit corrections give an energy shift proportional to $\ell\, S_z$ (where $S_z \equiv s_z^{(1)} + s_z^{(2)}$), with a positive coefficient. In our

dimensionally reduced effective theory, spin-spin (or hyperfine) interactions are local and proportional to $s_z^{(1)} s_z^{(2)}\, \delta^2(\mathbf{x})$, also with a positive coefficient.[21] This spin-spin correction only has a non-zero expectation value in $\ell = 0$ states. Hence, first order relativistic corrections produce an energy shift of the form

$$\Delta E_{\text{fine-structure}} = \lambda^2 m_{\text{W}} \left[A\, \ell\, S_z + B\, \delta_\ell^0\, (S_z^2 - 2) \right], \tag{6.26}$$

where A and B are positive $\mathcal{O}(1)$ coefficients (depending on n and $|\ell|$). For a given n and $\ell \neq 0$, the spin-orbit correction splits the four possible spin states, $\{|\uparrow\uparrow\rangle,\ |\uparrow\downarrow \pm \downarrow\uparrow\rangle,\ |\downarrow\downarrow\rangle\}$, into three sublevels with the $S_z = -2\ell/|\ell|$ state moving lower in energy, the $S_z = +2\ell/|\ell|$ state moving higher, and the two $S_z = 0$ states unchanged. For $\ell = 0$ levels, the spin-spin interaction produces two sublevels, with the energy of the $S_z = \pm 2$ states shifted upward, and the $S_z = 0$ states downward. The degeneracy between the spin symmetric and antisymmetric $S_z = 0$ states, $|\uparrow\downarrow \pm \downarrow\uparrow\rangle$, is not lifted by these leading relativistic corrections, but should be removed at higher orders.

Short distance effects will also induce higher order corrections to the rest and kinetic masses, leading to further spin-independent $\mathcal{O}(\lambda^2 m_{\text{W}})$ energy shifts. Operators producing $\mathcal{O}(\lambda^2 m_{\text{W}})$ corrections are listed in Appendix A, which discusses the relevant power counting rules. The structure of higher dimensional operators that appear in our non-relativistic EFT follow the same pattern known, for example, from studies of hydrogenic spectra or heavy quark physics in QCD [67], but quantitative evaluation of these higher order effects is left to future work.

The factor of N degeneracy associated with center symmetry would be lifted by the non-perturbative long distance physics on the scale of m_γ but, more importantly, this degeneracy is first lifted by one loop perturbative corrections which generate photon mixing terms (mentioned earlier in footnote 5). Such mixing arises from vacuum polarization corrections which are sensitive to the differing masses M_n^{ab} of the charged virtual W-bosons. This mixing (when rediagonalized) induces $\mathcal{O}(\lambda)$ variations in the coupling strengths of different light photons. Eigenstates of bound W-bosons will have definite center charge and are constructed by a $\mathbb{Z}_N$ Fourier transform, as in Eq. (5.8). The energies of states with differing values of center charge will be split by $\mathcal{O}(\lambda^2 m_{\text{W}})$, or in other words additional $\mathcal{O}(\lambda)$ relative corrections to binding energies.

6.2.3 Mesons

Differences between the two-body meson and glueball spectra arise from the differing constituent masses and the strength of the logarithmic interaction. For an oppositely

[21] In two spatial dimensions, spin-spin interactions do not have a long range dipolar form since the magnetic field produced by a current loop is localized inside the loop.

charged quark-antiquark pair, the interaction strength is given by

$$\kappa = (1-\tfrac{1}{N})\,\frac{\lambda m_{\rm W}}{4\pi^2}\,. \tag{6.27}$$

The allowed values of compact momentum (4.23) depend on both N and $n_{\rm f}$. As mentioned earlier, a particularly simple case which we will focus on is $n_{\rm f} = N$. For this number of flavors the tree-level constituent quark masses (4.24) become half-integers times $m_{\rm W}$,

$$M_n^{aA} = M_k \equiv m_{\rm W}(|k| + \mathcal{O}(\lambda))\,, \qquad m_n^{aA} = m_k \equiv m_{\rm W}(|k| + \mathcal{O}(\lambda))\,, \tag{6.28}$$

with $k = a - A + nN$ and $n \in \mathbb{Z} + \frac{1}{2}$. The resulting bound state energies are given by

$$E_{\bar{q}q} = M_k(m_{\rm W}) + M_{k'}(m_{\rm W}) + (1-\tfrac{1}{N})\frac{\lambda m_{\rm W}}{4\pi^2}\Big(\epsilon_{n,\ell} - \tfrac{1}{2}\ln\frac{(1-\frac{1}{N})\lambda\, m_{kk'}}{4\pi^2 m_{\rm W}}\Big), \tag{6.29}$$

where, once again, $m_{kk'}$ is the reduced mass. The lightest mesons have $|k| = |k'| = \frac{1}{2}$, leading to

$$E_{\bar{q}q} = 2M_{1/2}(m_{\rm W}) + (1-\tfrac{1}{N})\frac{\lambda m_{\rm W}}{4\pi^2}\Big(\epsilon_{n,\ell} - \tfrac{1}{2}\ln\frac{(1-\frac{1}{N})\lambda}{16\pi^2}\Big). \tag{6.30}$$

Neglecting higher order relativistic corrections, the lightest two-body meson levels (6.30) have a degeneracy of $16N$ if they have $\ell = 0$, with an additional factor of 2 if $\ell \neq 0$. (Four factors of 2 coming from the choice of spin for quark and antiquark, plus the choice of sign of each momentum index, and a factor of N from one choice of flavor, or equivalently from the choice of which $U(1)$ photon provides the binding.) Higher order spin-orbit, spin-spin and other radiative effects partially lift this degeneracy in the same manner discussed above for glueballs.

6.2.4 $N = 2$ baryons

Finally, in the special case of two-color QCD, the simplest baryons are bound states of two quarks (with no additional W-bosons). The interaction strength κ equals $\frac{1}{N}\lambda m_{\rm W}/(4\pi^2)$ which, for $N = 2$, coincides with the quark-antiquark interaction strength. Consequently, the resulting diquark baryon spectrum is identical to the meson spectrum (6.29) and (6.30) given above, when specialized to $N = 2$. The degeneracy of the lightest baryon levels (neglecting relativistic corrections) is 16 for $\ell = 0$ states, with an additional factor of two for $\ell \neq 0$.

6.3 Multi-body states

6.3.1 Glueballs

As noted in the overview, in addition to two-body W-boson bound states, multi-body bound states containing three or more W-bosons with a ring-like color structure can

also form, such as those illustrated in Fig. 2. The spectrum of such "closed string" states is quite rich.

The rest mass of W-bosons is given by Eq. (4.9), reproduced here for convenience,

$$M_n^{ab} = M_k \equiv m_{\rm W}|k| = m_{\rm W}\,|a - b + nN|, \tag{6.31}$$

up to $\mathcal{O}(\lambda m_{\rm W})$ corrections. To form a physical (gauge invariant) bound state, the $U(1)^N$ Cartan charges of all W-bosons in the bound state must sum to zero. For closed-string glueball states which are not decomposable into multiple separate glueballs, this means that each neighboring pair of W's in the ring is bound together by a distinct Abelian gauge interaction. Bound states containing $3 \le P \le N$ constituents having compact momentum indices $\{k_1,\, k_2,\, \cdots, k_P\}$ exist, consistent with this constraint, provided that

$$\sum_{i=1}^{P} k_i = 0 \bmod N\,. \tag{6.32}$$

For this state to be non-decomposable, no partial sum of the momentum indices should vanish modulo N. In addition to specifying the momentum index of each constituent, one may specify one Cartan index of a single constituent; together this information completely determines the Cartan and KK indices of all constituents around the cycle. The tree-level mass of such a closed string state is just

$$M_{\rm tot} = m_{\rm W} \sum_{i=1}^{P} |k_i|\,. \tag{6.33}$$

"Near extremal" states: An interesting subset of states are those with non-zero compact momentum P_3 and whose tree-level mass equals the minimal value consistent with this compact momentum,

$$M = |P_3|\,. \tag{6.34}$$

This implies that the momentum indices of all constituents have the same sign. One simple case, satisfying the constraint (6.32) (plus non-decomposability), are "pearl necklace" bound states containing N W-bosons, all with momentum indices equal to unity, $k_i = 1$, or all equal to minus one, $k_i = -1$. For these states $P_3 = m_{\rm W}\sum_i k_i = \pm N\, m_{\rm W} = \pm 2\pi/L$ and the (tree level) rest mass $M = |P_3| = N m_{\rm W}$. The middle example in Fig. 2 illustrates this type of pearl necklace state (with $P_3 = -2\pi/L$) in the case of $N = 4$. Such a state is created by the N-body operator

$$A^{i_1 i_2 \cdots i_N}\, (\phi^1_{-1})^\dagger_{i_1}\, (\phi^2_{-1})^\dagger_{i_2} \cdots (\phi^{N-1}_{-1})^\dagger_{i_{N-1}}\, (\phi^N_{-1})^\dagger_{i_N}\,, \tag{6.35}$$

where the coefficients $\{A^{i_1\cdots i_N}\}$ (defining a rank-N 2D spatial tensor) determine the spin wavefunction.

There are also near-extremal states with fewer constituents. One can imagine fusing together any neighboring pair of constituents in the operator (6.35) and replacing them with a single W-boson having the same Cartan charges and compact momentum as the pair. Or doing the same fusing process with a neighboring triplets of constituents, etc. The resulting states are also near-extremal, and are created by $N-1$ or $N-2$ body operators such as

$$A^{i_1 i_2\cdots i_{N-1}}\,(\phi^1_{-1})^\dagger_{i_1}\,(\phi^2_{-1})^\dagger_{i_2}\cdots(\phi^{N-1}_{-2})^\dagger_{i_{N-1}}\,, \tag{6.36a}$$

or

$$A^{i_1 i_2\cdots i_{N-2}}\,(\phi^1_{-1})^\dagger_{i_1}\,(\phi^2_{-1})^\dagger_{i_2}\cdots(\phi^{N-2}_{-3})^\dagger_{i_{N-2}}\,. \tag{6.36b}$$

Continuation of this fusing process leads to near-extremal states with any number of constituents from N down to 1. Three and two body examples are

$$A^{i_1 i_2 i_3}\,(\phi^1_{-1})^\dagger_{i_1}\,(\phi^2_{-1})^\dagger_{i_2}\,(\phi^3_{-(N-2)})^\dagger_{i_3}\,, \tag{6.37a}$$

and

$$A^{i_1 i_2}\,(\phi^1_{-1})^\dagger_{i_1}\,(\phi^2_{-(N-1)})^\dagger_{i_2}\,, \tag{6.37b}$$

while the endpoint of this process is a neutral "heavy photon" state created by a one-body operator such as

$$A^{i}\,(\phi^1_{-N})^\dagger_{i}\,. \tag{6.38}$$

More generally, ignoring spin and center degeneracies there are $\binom{N}{P-\delta^P_1}$ distinct categories of near-extremal states containing P constituents associated with different contiguous fusing of the fields in the N-body operator (6.35), or altogether 2^N-N types of non-decomposable near-extremal states having the same value of $P_3 = \pm N m_{\rm W}$.

"Non-extremal" states: Bound states containing constituents with oppositely signed momentum indices are "non-extremal." Such states have rest masses which exceed their compact momentum, $M > |P_3|$, by an $\mathcal{O}(m_{\rm W})$ amount or more. This includes all bound states of W-bosons having vanishing total compact momentum, $P_3 = 0$, such as the lightest glueballs (6.25).

Binding energies: Calculating the $\mathcal{O}(\lambda m_{\rm W})$ binding energies of multi-body glueball states requires one to find eigenvalues of the first-quantized Hamiltonian which describes the sector of the theory (4.12) with the chosen number of constituents. For "closed string" bound states composed of $P \leq N$ W-bosons, this is

$$\hat{H} = \sum_{i=1}^{P}\left[\frac{\mathbf{p}_i^2}{2m_i} + \frac{\lambda m_{\rm W}}{4\pi^2}\ln(\mu|\mathbf{x}_i - \mathbf{x}_{i-1}|)\right], \tag{6.39}$$

with the understanding that $\mathbf{x}_0 \equiv \mathbf{x}_P$. The scaling relation (4.19) allows one to remove the dependence on λ, but eigenvalues will be non-trivial functions of constituent mass ratios,

$$E_{\text{binding}} = \frac{P\lambda m_{\text{W}}}{8\pi^2}\left[f(\{m_i/m_j\}) - \ln(\lambda\widetilde{m}m_{\text{W}}/\mu^2)\right], \tag{6.40}$$

where f is a dimensionless $\mathcal{O}(1)$ function (depending on the chosen energy level as well as mass ratios), and $\widetilde{m}$ is the harmonic mean of the constituent masses.

For modest values of P (three or four), an accurate variational calculation should be feasible despite the fact that computational effort will rise as a rather high power of the number of single particle states included in the truncated basis. We leave such calculations to future work.

An interesting limiting case partially amenable to analytic analysis concerns low-lying states with large orbital angular momentum, $\ell \gg 1$, and constituents all having the same mass m. Such states include rotating "pearl necklace" configurations in which each constituent contributes equally to the total orbital angular momentum. A semi-classical analysis of such states is straightforward. The classical Hamiltonian (for fixed ℓ) has a local minimum in which the constituents lie at the vertices of a regular P-sided polygon whose circumscribed circle has radius $r = 2\pi\ell/(P\sqrt{\lambda m m_{\text{W}}})$, rotating at angular velocity $\Omega = \ell/(P\,mr^2) = P\lambda m_{\text{W}}/(4\pi^2\ell)$. Semiclassical quantization of vibrations about this configuration leads to energy levels whose binding energies (ignoring center of mass motion) are given by

$$E_{\text{binding}} = \frac{P\lambda m_{\text{W}}}{4\pi^2}\left[\tfrac{1}{2} + \ln\left(\frac{4\pi\ell\mu\sin(\pi/P)}{P\sqrt{\lambda m m_{\text{W}}}}\right)\right] + \sum_{i=-(P-2)}^{P-2}(n_i+\tfrac{1}{2})\,\omega_{|i|} + \mathcal{O}(\ell^{-2}), \tag{6.41}$$

where the $P-1$ vibrational frequencies $\{\omega_i\}$ are $\mathcal{O}(\lambda m_{\text{W}}/\ell)$.[22]

The result (6.41) grows logarithmically with increasing angular momentum ℓ, with a coefficient of $P\lambda m_{\text{W}}/4\pi^2$ proportional to the number of constituents. This linear increase with P implies that these semiclassical "pearl necklace" states are not the minimal energy states with a given large orbital angular momentum. "Core-halo" states will exist in which $P-1$ constituents are clumped together in a region of size $\sqrt{P/\lambda m m_{\text{W}}}$ while a single constituent circles at a distance of order $\mathcal{O}(\ell/\sqrt{\lambda m m_{\text{W}}})$ and contributes (nearly) all the orbital angular momentum. The binding energy of such states will increase with ℓ just like the two-body case, namely $E_{\text{binding}} \sim (\lambda m_{\text{W}}/2\pi^2)\,\ln\ell$ as $\ell \to \infty$. Computing the sub-dominant ℓ-independent contribution coming from the core wavefunction requires a full quantum calculation.

[22] One mode, here labeled $i = 0$, is a uniform "breathing" mode with $\omega_0 = \sqrt{2}\,\Omega$. All other modes (present only for $P > 2$) are higher frequency doubly-degenerate asymmetric stretching modes. For $P = 2$, the form (6.41) agrees as it must with the prior results (6.24) and (6.11).

6.3.2 Mesons

Largely identical considerations apply to multi-body mesons. Focusing, once again, on the case of $n_{\rm f} = N$, bound states containing a quark and antiquark having half-integer compact momentum indices k_q and $k_{\bar{q}}$, plus P W-bosons with momentum indices $\{k_1, \cdots, k_P\}$, will have total compact momentum

$$P_3 = m_{\rm W}\big(k_q - k_{\bar{q}} + \sum_{i=1}^{P} k_i\big)\,. \tag{6.42}$$

For the state not to be decomposable into a glueball-meson molecule, no partial sum of the W-boson momentum indices should vanish modulo N. With tree-level mass $M_{\rm tot} = m_{\rm W}(|k_q| + |k_{\bar{q}}| + \sum_i |k_i|)$, it is immediate that $M_{\rm tot} \geq |P_3|$. Any of the multi-body "closed string" glueball states discussed above may be converted into an "open string" meson state by replacing any one of the W-boson constituents by a $q\bar{q}$ pair collectively having the same Cartan charges and compact momentum. As an example, one analogue of the near-extremal N-body glueball operator (6.35) is the near-extremal meson operator

$$B^{s_{\bar{q}} s_q\, i_1 i_2 \cdots i_{N-1}}\, (\chi^{\,1}_{+1/2})^\dagger_{s_{\bar{q}}} (\phi^{\,1}_{-1})^\dagger_{i_1}\, (\phi^{\,2}_{-1})^\dagger_{i_2} \cdots (\phi^{\,N-1}_{-1})^\dagger_{i_{N-1}}\, (\psi^{\,N}_{-1/2})^\dagger_{s_q}\,, \tag{6.43}$$

(with s_q and $s_{\bar{q}}$ denoting two-component spinor indices of the quark and antiquark, respectively), in which $N{-}1$ W-bosons are inserted between the quark and antiquark.

The $\mathcal{O}(\lambda m_{\rm W})$ binding energies of (non-decomposable) multi-body meson states containing P W-bosons are given by eigenvalues of the first-quantized Hamiltonian

$$\hat{H} = \sum_{i=0}^{P+1} \frac{\mathbf{p}_i^2}{2m_i} + \frac{\lambda m_{\rm W}}{4\pi^2}\Big[-\tfrac{1}{N}\ln(\mu|\mathbf{x}_0{-}\mathbf{x}_{P+1}|) + \sum_{i=1}^{P+1}\ln(\mu|\mathbf{x}_i{-}\mathbf{x}_{i-1}|)\Big], \tag{6.44}$$

where $\mathbf{x}_0 \equiv \mathbf{x}_{\bar{q}}$ and $\mathbf{x}_{P+1} \equiv \mathbf{x}_q$ refer to the antiquark and quark, respectively, and likewise for the momenta $\mathbf{p}_0$ and $\mathbf{p}_{P+1}$ and masses $m_0 \equiv m_{\bar{q}}$ and $m_{P+1} \equiv m_q$. The resulting energy levels have the form

$$E_{\rm binding} = (P + (1{-}\tfrac{1}{N}))\,\frac{\lambda m_{\rm W}}{8\pi^2}\left[f(\{m_i/m_j\}) - \ln(\lambda\widetilde{m} m_{\rm W}/\mu^2)\right], \tag{6.45}$$

with f some $\mathcal{O}(1)$ function, differing from the glueball case (6.40) just in the prefactor.

Just as with closed-string glueballs, it is interesting to consider open-string mesons with large orbital angular momentum, $\ell \gg 1$. Among such states are semiclassical "rotating wire" states. The classical Hamiltonian (for fixed orbital angular momentum ℓ) has local minima in which all constituents are arrayed along a straight line which

rotates uniformly with some angular velocity ω, with the positions of constituents along this line adjusted so that the sum of forces (falling with inverse separation) acting on each constituent provides the required centripetal acceleration, and the common angular velocity ω is suitably adjusted to yield the chosen angular momentum ℓ. Solving for this minimum analytically, for arbitrary P, is not easy, but a numerical determination for chosen values of P is straightforward. Semiclassical quantization of such a stationary configuration will lead to energy levels which, as in the glueball case (6.41), grow logarithmically with increasing ℓ, with a coefficient which increases with the number of constituents. Hence, for the same reasons discussed above, lower energy "core-halo" mesonic states will exist in which all but one constituent are clumped together and collectively carry little or no angular momentum while a single constituent (which may be either a quark or a W-boson) circles the core at a large $\mathcal{O}(\ell/\sqrt{\lambda m m_{\rm W}})$ distance and carries (nearly) all the orbital angular momentum.

6.3.3 Baryons

Baryonic bound states containing quarks with no additional W-bosons ("non-exotic baryons") may be formed from a collection of N quarks, each having a distinct color (Cartan) index. Focusing, once again, on the case of $n_{\rm f} = N$, the momentum indices $\{k_1, \cdots, k_N\}$ of the quarks are arbitrary half-integers (with k_i the momentum index of the quark with Cartan index i). The total compact momentum $P_3 = m_{\rm W} \sum_i k_i$ and the tree-level mass $M_{\rm tot} = m_{\rm W} \sum_{i=1}^N |k_i|$.

Note that, for large values of N, baryons which are composed of the lightest quark constituents with $\mathcal{O}(1)$ momentum indices will have a total mass $M_{\rm tot}$ which scales linearly with N. Such baryons contain quarks of (nearly) all N different flavors. Baryons which are solely composed of quarks of a single flavor will have a total mass which is at least $\mathcal{O}(N^2)$, because the momentum indices of quarks must, in this case, all be distinct and hence will, at a minimum, have magnitudes ranging from $\frac{1}{2}$ up to $\lfloor N/2 \rfloor$.

The strength of the attractive logarithmic interaction between two quarks of differing colors is $1/N$, so the first-quantized non-relativistic Hamiltonian for non-exotic baryons is

$$\hat{H} = \sum_{i=1}^{N} \frac{\mathbf{p}_i^2}{2m_i} + \frac{1}{N} \sum_{i<j=1}^{N} \frac{\lambda m_W}{4\pi^2} \ln\left(\mu |\mathbf{x}_i - \mathbf{x}_j|\right), \tag{6.46}$$

with $m_i = m_{\rm W}|k_i|$ the i'th constituent quark mass.

For the lightest class of baryons, each quark has momentum index $\pm\frac{1}{2}$ and the minimal constituent mass $m_i = m_q \equiv \frac{1}{2} m_{\rm W}$. Such states are created by operators of the form

$$C^{s_1 s_2 \cdots s_N} \left(\psi^1_{\pm 1/2}\right)^\dagger_{s_1} \left(\psi^2_{\pm 1/2}\right)^\dagger_{s_1} \cdots \left(\psi^N_{\pm 1/2}\right)^\dagger_{s_N}, \tag{6.47}$$

with s_i denoting the two-component spinor index of the ith quark. (Fig. 4 illustrates one such state for $N=4$.) For simplicity of presentation, we will focus our discussion on this lightest class of baryons.

For baryons with equal mass constituents, the Hamiltonian (6.46) is completely symmetric under permutations of constituents. The rescaling relation (4.31) implies that

$$\hat{H} \cong \frac{\lambda m_W}{4\pi^2}\left(\tfrac{1}{2}\sum_{i=1}^{N}\mathbf{p}_i^2 + \frac{1}{2N}\sum_{i\neq j=1}^{N}\ln|\mathbf{x}_i-\mathbf{x}_j|\right) - (N-1)\,\frac{\lambda m_W}{16\pi^2}\,\ln\left(\frac{\lambda m_{\rm W} m_q}{4\pi^2\mu^2}\right). \tag{6.48}$$

The spectrum of this Hamiltonian was already discussed in Sec. 6.2 in the special case of $N=2$. We now examine the opposite extreme, $N \gg 1$.

As discussed by Witten [68], a Hartree approximation to the many-body wavefunction is asymptotically accurate as $N \to \infty$. The appropriate N-body Hartree wavefunction for the ground state is just a product of identical one-body wavefunctions,

$$\Psi(\mathbf{x}_1,\cdots,\mathbf{x}_N) = \prod_{i=1}^{N}\psi(\mathbf{x}_i)\,, \tag{6.49}$$

with the one-body wavefunction $\psi(\mathbf{x})$ determined by minimizing the expectation value of the Hamiltonian (subject to the normalization constraint $\int d^2x\,|\psi(\mathbf{x})|^2 = 1$).[23] The resulting ground state baryonic mass grows linearly with N and is given by

$$E_{\rm baryon}/N = M_{1/2}(m_{\rm W}) + \frac{\lambda m_{\rm W}}{4\pi^2}\left(\bar{\epsilon} - \tfrac{1}{4}\ln\frac{\lambda m_q}{4\pi^2 m_{\rm W}}\right) + \mathcal{O}(1/N)\,, \tag{6.50}$$

where

$$\bar{\epsilon} \equiv \min_{\psi}\epsilon[\psi]\,, \qquad \epsilon[\psi] = \mathcal{T}[\psi] + \mathcal{V}[\psi]\,. \tag{6.51}$$

Here,

$$\mathcal{T}[\psi] \equiv \tfrac{1}{2}\int d^2\mathbf{x}\,|\nabla\psi(\mathbf{x})|^2 \Big/ \mathcal{N}[\psi]\,, \tag{6.52a}$$

$$\mathcal{V}[\psi] \equiv \tfrac{1}{2}\int d^2\mathbf{x}\,d^2\mathbf{x}'\,\ln|\mathbf{x}-\mathbf{x}'|\,|\psi(\mathbf{x})|^2\,|\psi(\mathbf{x}')|^2 \Big/ \mathcal{N}[\psi]^2\,, \tag{6.52b}$$

with $\mathcal{N}[\psi] \equiv \int d^2\mathbf{x}\,|\psi(\mathbf{x})|^2$. The ground state wavefunction which minimizes $\epsilon[\psi]$ satisfies the Hartree equation,

$$\left[-\tfrac{1}{2}\nabla^2 + U(\mathbf{x})\right]\psi(\mathbf{x}) = \lambda\,\psi(\mathbf{x})\,, \tag{6.53}$$

[23] A better approximation would project this state onto vanishing center-of-mass momentum. However, such projection only affects $\mathcal{O}(1)$ contributions to the total energy of the state, which we neglect.

with the self-consistent potential

$$U(\mathbf{x}) \equiv \int d^2\mathbf{x}' \, \ln|\mathbf{x}-\mathbf{x}'| \, |\psi(\mathbf{x}')|^2 \Big/ \mathcal{N}[\psi] \, . \tag{6.54}$$

This wavefunction is guaranteed to be nodeless, and hence is spherically symmetric, $\psi(\mathbf{x}) = \psi(|\mathbf{x}|)$. After angular averaging of the logarithm, the potential (6.54) becomes a convolution with the radial Green's function,

$$U(|\mathbf{x}|) \equiv \int_0^\infty r' \, dr' \, \ln\bigl(\max(|\mathbf{x}|, r')\bigr) \, \psi(r')^2 \Big/ \int_0^\infty r' \, dr' \, \psi(r')^2 \, . \tag{6.55}$$

We minimize the functional $\epsilon[\psi]$ numerically, using pseudospectral methods [66]. We write $\psi(r) = e^{-\mu r/2} f(r)$ and then represent the function f as an order $M-1$ polynomial determined by its values $\{f_k\}$ on the Gauss-Laguerre grid points $\{r_k\}$ which are the roots of the Laguerre polynomial $L_M(\mu r)$. This is equivalent to, but much more computationally convenient than using the coefficients $\{c_k\}$ in the orthogonal polynomial expansion $f(r) = \sum_{k=0}^{M-1} c_k \, L_k(\mu r)$. The radial integrals in expressions (6.52)–(6.55) are evaluated using M-point Gauss-Laguerre quadrature. Radial derivatives become dense $M \times M$ matrices acting on the M-component vector $\vec{f} \equiv (f_k)$, and the Hartree equation (6.53) becomes an M-dimensional linear eigenvalue equation. Starting with a simple pure exponential initial guess for $\psi(r)$, we compute the Hartree potential (6.55), solve for the lowest eigenvalue of the Hartree equation (6.53), and iterate these two steps until convergence.[24]

Due to the non-analyticity in the Green's function (6.55), the truncation error only falls with increasing basis size as $\mathcal{O}(1/M)$. Six points suffice for 5% accuracy, thirty points yield better than 1%, and several hundred are needed to achieve 0.1% accuracy. For large M, the spectral matrices become quite ill-conditioned and extended precision arithmetic with roughly $2M$ digits is needed to avoid precision loss. A very stable extrapolation in $1/M$ yields the result,

$$\bar{\epsilon} = 0.449558 \, . \tag{6.56}$$

The degeneracy of this lightest baryon level, before taking into account splittings due to higher order radiative corrections, is 4^N, growing exponentially as N increases. (For each quark, there is one factor of two for the choice of spin and another factor of two from the compact momentum $k = \pm\frac{1}{2}$.)

[24] Demanding stationarity of $\epsilon[\psi]$ under a rescaling $\psi(\mathbf{x}) \to \xi\psi(\xi\mathbf{x})$ at $\xi = 1$ shows that $\mathcal{T}[\psi] = \frac{1}{4}$ at extrema of ϵ. This is the analogue of the usual virial theorem for our logarithmic potential. Choosing the scale $\mu = \sqrt{2}$ in our spectral representation gives our initial guess this correct value of $\mathcal{T}$.

To compare our $N=2$ and $N\gg1$ results for ground state baryons in a coupling independent fashion, consider the binding energy scaled by $N-1$, with the exactly known $\lambda\ln\lambda$ contribution removed,

$$\delta E_{\rm binding}(N) \equiv \frac{1}{N-1}\left[E_{\rm baryon} - NM_{1/2}(m_{\rm W})\right] + \frac{\lambda m_{\rm W}}{16\pi^2}\ln\frac{\lambda}{8\pi^2}\,. \tag{6.57}$$

Our results,

$$\frac{\delta E_{\rm binding}(\infty)}{\delta E_{\rm binding}(2)} = \frac{\bar\epsilon}{\frac{1}{2}(\epsilon_{00}+\ln 2)} = 1.0298\,, \tag{6.58}$$

show stunningly little dependence on N. It would be interesting to see if this near-constancy is a coincidence, or remains true for other values of N.

At large N, the probability density to find a quark at position $\mathbf{x}$ relative to the baryon center of mass equals the square of the Hartree single particle wavefunction, $p(\mathbf{x}) = |\psi(\mathbf{x})|^2$. To compare this with the corresponding distribution in $N=2$ ground state baryons, recall that the Hamiltonian for relative motion (6.7) was expressed in terms of the separation between constituents, so the corresponding distribution relative to the center of mass is $p(\mathbf{x}) = 4|\psi_{\rm rel}(2\mathbf{x})|^2$. One finds that the single particle distribution is more highly concentrated at $N=2$ than at $N=\infty$. The mean square deviations differ by just about a factor of two,

$$\langle\mathbf{x}^2\rangle = \frac{8\pi^2}{\lambda m_{\rm W}^2}\times\begin{cases}1.0907\,, & N=2;\\ 2.0294\,, & N=\infty.\end{cases} \tag{6.59}$$

Fig. 6 compares the $N=\infty$ single particle radial probability density $|\mathbf{x}|\,p(\mathbf{x})$ with the corresponding $N=2$ distribution when distance is rescaled by a factor of $\sqrt{2}$, that is $\frac{1}{2}|\mathbf{x}|\,p(\mathbf{x}/\sqrt{2})$. As one sees from the figure, with this rescaling the two radial distributions are very similar.

Above the baryon ground state level there is a manifold of vibrationally excited baryon levels. For $N\gg1$, energy levels in which a small number of quarks are excited may be computed using a product wavefunction with a few of the factors in the ground state wavefunction (6.49) replaced by excited single particle wavefunctions. Low lying levels with a single excited quark may be labeled by the number of radial nodes n and orbital angular momentum ℓ of the excited quark, and have excitation energies

$$\Delta E_{n,\ell} = \frac{\lambda m_{\rm W}}{4\pi^2}\left(\lambda_{n,\ell}-\lambda_{0,0}\right), \tag{6.60}$$

where $\lambda_{n,\ell}$ is an eigenvalue of the Hartree equation (6.53) containing the mean field generated by all the unexcited quarks. The subtraction of $\lambda_{0,0}$ accounts for the decrease in the number of quarks in the lowest single particle level. Table 2 lists the eigenvalues

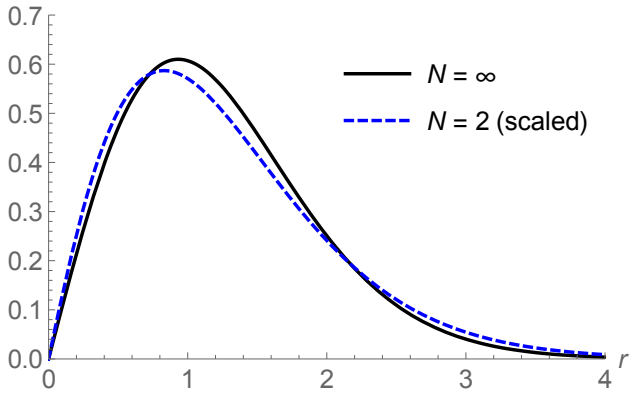

Figure 6. Single particle radial probability density $|\mathbf{x}|\,p(\mathbf{x})$ of ground state baryons at $N=\infty$ as a function of $r \equiv \sqrt{\lambda}\, m_{\rm W}|\mathbf{x}|/(4\pi)$ (solid curve) overlaid with the corresponding density for $N=2$ baryons as a function of $r' \equiv \sqrt{2\lambda}\, m_{\rm W}|\mathbf{x}|/(4\pi)$ (dashed curve).

n	$\lvert\ell\rvert = 0$	1	2	3
0	0.64911	1.1367	1.5182	1.8152
1	1.4448	1.7124	1.9450	2.1457
2	1.9018	2.0805	2.2458	2.3964
3	2.2169	2.3503	2.4780	2.5979
4	2.4569	2.5632	2.6669	2.7663

Table 2. Eigenvalues $\lambda_{n,\ell}$ of the Hartree equation (6.53), with the self-consistent potential for the lowest baryon level, for indicated values of the radial quantum number n and orbital angular momentum ℓ.

$\lambda_{n,\ell}$ for the lowest few levels. Excitation energies to baryon levels with multiple excited quarks are, up to $1/N$ corrections, just the sum of the individual excitation energies (provided the number of excited quarks is a negligible fraction of N).

Lastly, in the same manner discussed above for mesons, it is also possible to form exotic baryons containing N quarks plus one or more W-bosons. For the bound state to be non-decomposable into baryon-glueball molecules, no partial sum of the W-boson momentum indices should vanish. Such states can be progressively built from non-exotic baryons by replacing a quark with a quark plus one or more W-boson(s) which collectively have the same Cartan charge and compact momentum as the removed quark. One example of such a state is shown in Fig. 4. By suitably repeating this process one may, for example, build baryons in which all N quarks have the same color while $N-1$ W-bosons mediate attractive interactions between these quarks.

7 Decay processes

Higher order perturbative interactions turn most of the hadronic states discussed in the previous sections into narrow resonances. Examining the systematics of the various decay processes is our next topic. First, however, we detail those states which *cannot* decay.

7.1 Stable states

In the light sector of the quarkless theory, individual dual photons are exactly stable. Each dual photon has a non-zero center charge $p = 1, \cdots, N-1$, and is the lightest state with that value of center charge.[25] To see this, note that the mass formula (2.11) is a subadditive function of the center charge, $m_{p_1+p_2} < m_{p_1} + m_{p_2}$. This implies that any splitting of a dual photon into two or more photons with the same total center charge is kinematically forbidden. The formation of k-body light sector bound states discussed in Sec. 3 does not affect this conclusion, as the k-body binding energies are exponentially small compared to the relevant differences in photon masses. The two-body bound state of dual photons with center charges 1 and $N-1$, whose binding energy is given by Eq. (3.8), is the lightest center charge zero excitation and is likewise exactly stable.

If $\theta = 0$ then the theory is CP invariant.[26] Individual dual photons are CP odd. The lightest CP even states with non-zero center charge p are bound states of two dual photons with charges q and $p-q$ and minimal total mass $M_p = \min_q(m_q + m_{p-q})$. Specifically, these are the $(q, p-q)$ bound states with

$$q = \begin{cases} 1\,, & \text{for } p = 2, \cdots, \lfloor \frac{N}{2} \rfloor, \text{ or } p = N-1; \\ N-1\,, & \text{for } p = \lfloor \frac{N+1}{2} \rfloor, \cdots, N-2, \text{ or } p = 1. \end{cases} \tag{7.1}$$

Similarly, the lightest CP odd state with vanishing center charge is a bound state of three dual photons with charges $(1, 1, N-2)$ (or their conjugates). These bound states are necessarily stable at $\theta = 0$. Moreover, the charged two particle bound states (7.1) remain absolutely stable at $\theta \neq 0$ for purely kinematic reasons. These bound states are heavier than a single dual photon of the same total center charge, but are lighter than all other multiparticle bound states of the given charge, and hence have no allowed decay channels which can conserve both energy and momentum.

[25] Recall that a $p = 0$ dual photon was artificially added to the light sector effective theory (2.8) to simplify the presentation, but this extra degree of freedom exactly decouples from all physical degrees of freedom. The physical particles of the $SU(N)$ gauge theory do not include a $p = 0$ dual photon.

[26] This paragraph assumes that $N \geq 3$. Because $SU(2)$ is pseudo-real, charge conjugation is a distinct symmetry in $SU(N)$ pure YM theory only for $N > 2$.

Turning now to the theory with quarks, as discussed in Sec. 2.1 with $n_{\rm f} \leq N$ massless quark flavors, $n_{\rm f}-1$ of the dual photons become exactly massless and are the Goldstone bosons of spontaneously broken $U(1)_A^{n_{\rm f}-1}$ symmetry. When $n_{\rm f}=N$, this means all $N-1$ dual photons are massless. These massless Goldstone bosons are stable.

In the heavy sector, exactly stable states are those protected by conservation of the $U(1)_V^{n_{\rm f}}$ flavor charges (5.5) and/or compact momentum (5.4). With $n_{\rm f}=N$, mesons composed of a quark and antiquark having the minimal mass, $m_q = m_{\bar{q}} = \frac{1}{2}m_{\rm W}$, and opposite compact momentum indices, $k_q = -k_{\bar{q}} = \pm\frac{1}{2}$, have flavor charges $(+1,-1)$ under two different $U(1)$ flavor subgroups and non-vanishing total compact momentum $P_3 = \pm m_{\rm W}$. Such mesons (with vanishing vibrational and rotational excitations) are the lightest states with these flavor quantum numbers, and hence are stable.[27] These mesons are the small-L avatars of charged pions and kaons (in the chiral limit).

Baryons (or antibaryons) composed of N quarks (or antiquarks) all with mass $m_q = \frac{1}{2}m_{\rm W}$ are the lightest states with non-vanishing baryon number, and a subset of these states (those with minimal energy after including hyperfine interactions) are stable. Whether there are additional bound, and hence stable, di-baryons or higher multi-baryon states is an interesting open question.

Whether the heavy photons created by our EFT operators $\vec{\phi}^{aa}_{\pm N}$ are stable is also an interesting open question. These states have $P_3 = \pm N m_{\rm W}$ and tree-level mass $M = N m_{\rm W}$. This is the same value of P_3 and the same tree-level mass as a flavor singlet meson containing a quark and antiquark with $k_q = -k_{\bar{q}} = \pm N/2$, or of a collection of N lightest mesons each with identical values of $P_3 = \pm 1$ and flavor charges summing to zero, or a variety of other "near-extremal" flavor singlet multi-constituent states. Whether heavy photons decay into flavor singlet mesons, or collections of flavored mesons, or vice-versa, depends on which of these near-extremal states have the lowest energy. To determine this one must, at a minimum, take into account the leading $\mathcal{O}(\lambda m_{\rm W})$ perturbative energy shifts. These include the binding energies computed in Sec. 6.2.3 for two-body mesons. But $\mathcal{O}(\lambda m_{\rm W})$ energy shifts also include corrections to the tree-level constituent rest masses. Evaluation of such corrections requires an improved one-loop matching of the EFT parameters to the underlying 4D gauge theory, and this matching calculation has not yet been completed. Consequently, we are not yet able to determine which transitions among near-extremal states are kinematically allowed.

[27] More precisely, such mesons with opposite spins and total $S_z = 0$ are stable. As noted in Sec. 6.2, hyperfine interactions shift the $S_z = \pm 1$ mesons up in energy relative to the $S_z = 0$ states. A light $S_z = \pm 1$ meson can decay to its corresponding $S_z = 0$ partner via emission of a dual photon — the QCD analog of 21 cm radiation from hydrogen.

7.2 Light sector resonances

Light sector bound states other than those discussed above (which are stable due to the absence of any symmetry and kinematically allowed decay channels) will decay via emission of one of more dual photons. Such decays are induced by the cubic and higher order terms in the expansion of the effective Lagrangian (2.8) about its minimum. The relative decay widths of all of these states are doubly exponentially small. Not only are the non-linear couplings within the dual photon sector (3.2) exponentially small, $\mathcal{O}(e^{-4\pi^2/\lambda})$, more importantly the binding momentum (3.6) is so tiny that the probability for two constituents of a bound state to be within a Compton wavelength of each other is comparable to the relative binding energy (3.8). Consequently, the logarithm of the relative decay width is exponentially large and negative,

$$-\ln(\Gamma/m_\gamma) = \mathcal{O}(e^{4\pi^2/\lambda}) \tag{7.2}$$

(neglecting powers of λ). We have not attempted to compute any such decays quantitatively.

7.3 Heavy sector resonances

The primary decay processes for heavy sector resonances are direct analogues of familiar processes in QED and atomic physics: radiative decays and particle-antiparticle annihilations. The key differences are the reduced dimensionality, additional conserved quantities (compact momentum and center charge), and multiple $U(1)$ gauge groups. There are also more unusual decay processes involving splitting or joining of W-boson constituents within hadrons. These include, in particular, transitions among "near-extremal" states whose tree-level masses are identical. As noted above, understanding such processes requires a higher order determination of rest masses in the non-relativistic EFT. We leave explorations of such transitions to future work, and focus here on radiative and annihilation processes, specifically in two-body states.

7.3.1 Radiative decays

The relevant photon momenta for radiative decays will be in the range $m_\gamma \ll p \ll m_{\rm W}$, so the non-perturbative physics of the light sector may be wholly ignored and photons treated as massless. Excitation energies of low-lying heavy sector states are $\mathcal{O}(\lambda m_{\rm W})$. Photons of such energies have wavelengths parametrically large compared to the characteristic $\mathcal{O}(\lambda^{-1/2}\, m_{\rm W}^{-1})$ size of these states. Consequently, the usual multipole expansion of the photon field applies. The fastest radiative decays will be electric dipole transitions. Adapting the standard logic for hydrogenic decays to our 2D multi-photon

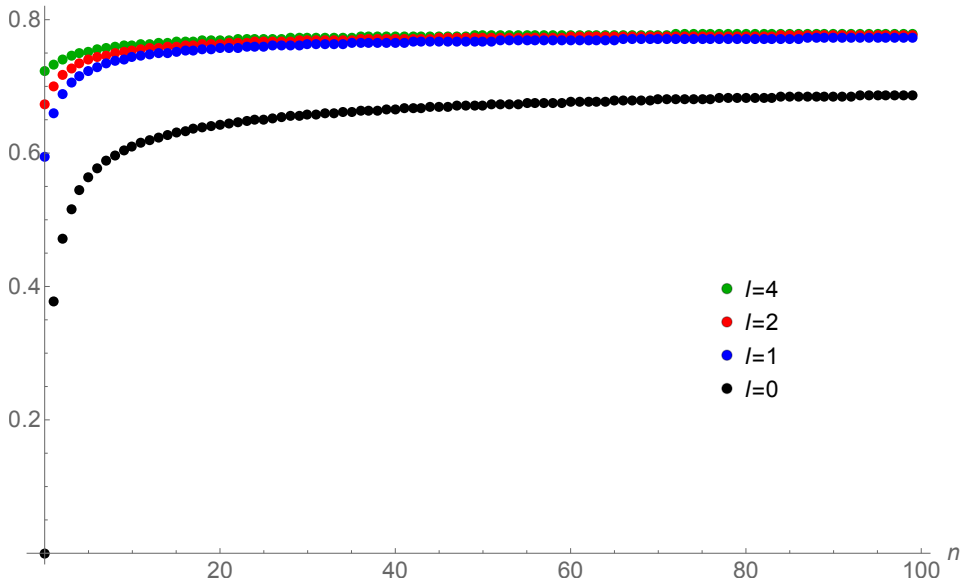

Figure 7. [Color online] Total radiative decay rates of two-body bound states in units of κ^2/m, as a function of the level number for the first 100 states with $\ell = 0, 1, 2$, and 4. Higher rows of points correspond to larger values of ℓ.

situation, one finds that the total dipole transition rate from some initial state $|I\rangle$ to lower energy final states $\{|F\rangle\}$ is given by

$$\Gamma_{\rm tot} = \tfrac{\pi}{2}\,\kappa \sum_F \Delta E_{IF}^2 \left|\langle F|\mathbf{x}|I\rangle\right|^2, \tag{7.3}$$

where $\Delta E_{IF} \equiv E_I - E_F$ and κ equals to the strength of the logarithmic potential binding the constituents, so $\kappa = \lambda m_{\rm W}/(2\pi^2)$ for glueballs and $(1-\frac{1}{N})\,\lambda m_{\rm W}/(4\pi^2)$ for mesons.

Parametrically, dipole decay rates for low-lying states are $\mathcal{O}(\lambda^2 m_{\rm W})$. To obtain quantitative results, including state dependence, one must evaluate the precise dipole matrix elements. We evaluated these matrix elements, for level numbers n up to 100, using radial wavefunctions computed using pseudo-spectral methods (as briefly described in footnote 20 and Sec. 6.3.3), with up to several hundred grid points. Figure 7 shows the resulting total dipole decay rates, in units of κ^2/m (with m the reduced mass of the two-body bound state), for orbital angular momentum $\ell = 0$, 1, 2 and 4. As seen in the figure, decay rates at fixed ℓ grow with increasing level number n and appear to asymptote to a finite limit. At fixed level number n, decay rates also grow with increasing ℓ, and quickly appear to reach a limiting value. Our numerical results are consistent with a limiting value of $\frac{\pi}{4}\,\kappa^2/m$ in either case, with subleading $\mathcal{O}(1/\ell)$ corrections if ℓ increases at fixed n, and $\mathcal{O}(n^{-1/2})$ corrections if n increases at fixed ℓ,

although this inverse power of n is not well-constrained by our data on the first 100 levels.

Consider states with positive orbital angular momentum, $\ell > 0$. The interleaving of energy levels, $\epsilon_{n,|\ell|} < \epsilon_{n,|\ell|+1} < \epsilon_{n+1,|\ell|}$, implies that the $|0,\ell\rangle$ minimal energy states (for a given angular momentum) decay down to the $|0,0\rangle$ ground level by sequential $|0,\ell\rangle \to |0,\ell{-}1\rangle$ transitions, with each emitted photon carrying off one unit of angular momentum. States with non-zero angular momentum and non-minimal energy, $n > 0$ and $\ell > 0$, have multiple possible dipole allowed final states, including both $\Delta\ell = +1$ and $\Delta\ell = -1$ transitions. Examining transition rates to specific final states, one finds that the total decay rates for states with $n, \ell > 0$ are highly dominated by decays to the nearest lower levels, either $|n,\ell\rangle \to |n,\ell{-}1\rangle$ or $|n,\ell\rangle \to |n{-}1,\ell{+}1\rangle$. Of these two decay channels, the decay decreasing ℓ is significantly more likely than the decay increasing ℓ. All other decays channels are smaller by one or more orders of magnitude. (The predominance of transitions decreasing $|\ell|$ over those increasing $|\ell|$ is visible in Fig. 7 as the smaller values of the $\ell = 0$ points compared to $\ell = 1$.) Consequently, an excited state $|n,\ell\rangle$ with $n \gg 1$ will cascade stepwise down to $n = 0$, with ℓ undergoing a random walk biased toward $\ell = 0$.

For high angular momentum, $\ell \gg 1$, one may regard the $n = 0$ eigenstate as a quasiclassical circular orbit. In two dimensions, the power radiated by an electric dipole of magnitude eR rotating at frequency ω is

$$P = \tfrac{1}{8}\, e^2\, R^2\, \omega^3\,. \tag{7.4}$$

For our high-ℓ bound states with $e^2 = 2\pi\kappa$, $R = \ell(\kappa m)^{-1/2}$, and orbital frequency $\omega = \kappa/\ell$, this gives $P = \frac{\pi}{4}\,\kappa^3/(m\ell)$. The power radiated must equal the photon frequency times the decay rate, so this classical result implies an ℓ-independent asymptotic decay rate,

$$\Gamma = \tfrac{\pi}{4}\,\kappa^2/m \times \left(1 + \mathcal{O}(\ell^{-1})\right). \tag{7.5}$$

Decay rates from states with fixed n nicely converge to this value as ℓ increases.

7.3.2 Annihilation decay

In addition to radiative decays, two-body bound states having $\ell = 0$ and composed of particle-antiparticle pairs can annihilate into two or more light sector photons. This is a short-distance process, represented by higher dimension operators in our non-relativistic EFT. Annihilation rates are parametrically smaller than dipole-allowed radiative transition rates, and hence only significant for the lowest $\ell = 0$ energy levels. Constituents with masses of order $m_{\rm W}$ have Compton wavelengths which are comparable (for small

N), or larger (for large N), than the compactification size L. Consequently, annihilation rates are most easily calculated using a dimensionally reduced relativistic EFT, having the form (A.2) for W-boson bound states or 2+1 dimensional QED for mesons. The annihilation rate may be expressed as

$$\Gamma_{\rm annih} = (\lim_{v\to 0} \sigma v)\, |\psi(0)|^2\,, \tag{7.6}$$

where σv is the flux-weighted cross-section in two spatial dimensions (a quantity with dimensions of length) and $\psi(\mathbf{x})$ is the wavefunction for relative motion, so $|\psi(0)|^2$ is the 2D probability density for coincident constituents. Parametrically, $\sigma v \sim \lambda^2/m_{\rm W}$ for CP even states which can annihilate to two photons having momenta of order $m_{\rm W}$, while $|\psi(0)|^2 \sim \kappa m$ since this is the inverse mean square size of the lowest $\ell = 0$ two-body bound states. Hence

$$\Gamma_{\rm annih} = \mathcal{O}(\lambda^3\, m_{\rm W})\,, \tag{7.7}$$

which is one power of λ smaller than radiative decay rates.

Evaluating the cross section in the relativistic 2+1D relativistic EFT, we find[28]

$$\sigma_{WW\to 2\gamma} = \frac{11\pi}{64\, v}\, \frac{\kappa^2}{m^3}\, \left[1 + \mathcal{O}(\mathbf{p}^2/m^2)\right] \tag{7.8}$$

for annihilation of W-bosons with mass m and interaction strength $\kappa = \lambda m_{\rm W}/(2\pi^2)$, and

$$\sigma_{q\bar{q}\to 2\gamma} = \frac{5\pi}{128\, v}\, \frac{\kappa^2}{m^3}\, \left[1 + \mathcal{O}(\mathbf{p}^2/m^2)\right] \tag{7.9}$$

for $q\bar{q}$ annihilation with mass m and interaction strength $\kappa = (1-\frac{1}{N})\, \lambda m_{\rm W}/(4\pi^2)$.

For the lowest $n = \ell = 0$ level of our two-body logarithmic quantum mechanics, the probability at the origin is

$$|\psi(0)|^2 = 2.68915\, \kappa\, \widetilde{m} \tag{7.10}$$

with $\widetilde{m}$ the reduced mass of the two constituents. Consequently, for the lightest CP-even glueballs and mesons (with constituent masses equal to $m_{\rm W}$ and $\frac{1}{2}m_{\rm W}$, respectively) we find

$$\Gamma_{\rm annih} = \begin{cases} 5.80815\, m_{\rm W}\, \left(\frac{\lambda}{4\pi^2}\right)^3\,, & \text{glueballs;} \\ 0.660017\, m_{\rm W}\, \left(\frac{\lambda}{4\pi^2}\right)^3 \left(1-\frac{1}{N}\right)^3\,, & \text{mesons.} \end{cases} \tag{7.11}$$

[28] We consider decays from bound states with vanishing total compact momentum and equal mass constituents. Higher KK modes (i.e., heavy photons) may be neglected. For WW annihilation, each W-boson couples to two different $U(1)$ photons and consequently there are three different processes which contribute ($\gamma_A\gamma_A$, $\gamma_B\gamma_B$, and $\gamma_A\gamma_B$). Evaluating the leading order seagull, t, and u-channel diagrams and taking the non-relativistic limit yields the result shown.

8 Discussion

8.1 Adiabatic continuation

Recent studies have shown that it is possible to engineer circle compactifications of 4D $SU(N)$ YM theory and QCD in such a way that symmetry realizations for large and small circle sizes coincide [12–35]. Available evidence is consistent with the natural conjecture that the weakly coupled small-L regime is smoothly connected — that is, without intervening phase transitions — to the strongly coupled large-L regime. The small circle regime offers a rare luxury: controlled analytic calculations in a phase of the theory with confinement and chiral symmetry breaking. Taking advantage of this tractability, we have studied the behavior of glueballs, mesons, and baryons, with a focus on the spectrum of resonances and their decays.

Our results are broadly consistent with the conjecture of continuity between small and large L. Much physics in adiabatically compactified theories depends on the circle size L through the parameter $\eta = NL\Lambda$. To place our small η results into perspective, first recall that when $\eta \gg 1$, the dynamics of QCD-like theories are insensitive to the scale L. (Finite volume effects vanish at least as fast as L^{-2}.) With fundamental representation fermions ($n_{\rm f} \lesssim N$) with a common mass $m_q \ll \Lambda$, at large L there are multiple characteristic scales for the masses of particles: the pseudo-Nambu-Goldstone (pNGB) mass scale $m_{\rm pNGB} \sim \sqrt{m_q \Lambda}$, the glueball and meson mass scale $m_M \sim \Lambda$, and the baryon mass scale $m_B \sim N\Lambda$.[29]

In the weakly coupled regime $\eta \ll 1$, we find a similar picture, but with particle masses depending on L through the combination $\eta = NL\Lambda$. In adiabatically compactified QCD with, e.g., $n_{\rm f} = N$ earlier work [35] found that the pNGB masses lie in the range $m_{\rm pNGB} \sim [\mathcal{O}(1/N)\text{–}\mathcal{O}(1)] \times \eta\sqrt{m_q\Lambda}$ at small η (if double trace deformations stabilize the color-flavor center symmetry). Our results in this paper show explicitly that $m_M \sim \Lambda\eta^{-1}$ and $m_B \sim N\Lambda\eta^{-1}$. This is clearly similar to the large L pattern, apart from the natural appearance of dependence on the parameter η when L is small.[30] In Fig. 8 we sketch a possible simple interpolation of the spectra of light and heavy states as L is varied.

The situation at $n_{\rm f} = 0$ is depicted in Fig. 9. At small L, instead of light pNGB mesons there are now light glueball states involving dual photons and their bound

[29] If $n_{\rm f} \ll N$ and $m_q/\Lambda \ll 1/N \ll 1$, then there is an additional scale $\Lambda N^{-1/2}$ associated with the mass of the η' meson [69].

[30] The dependence of pNGB masses (2.20) at small L on the charge of the particle under cyclic flavor permutations may, at first sight, seem surprising. But such dependence is also present when L is large but finite in adiabatically compactified theories with flavor twisted boundary conditions, as seen explicitly in the results of Ref. [70].

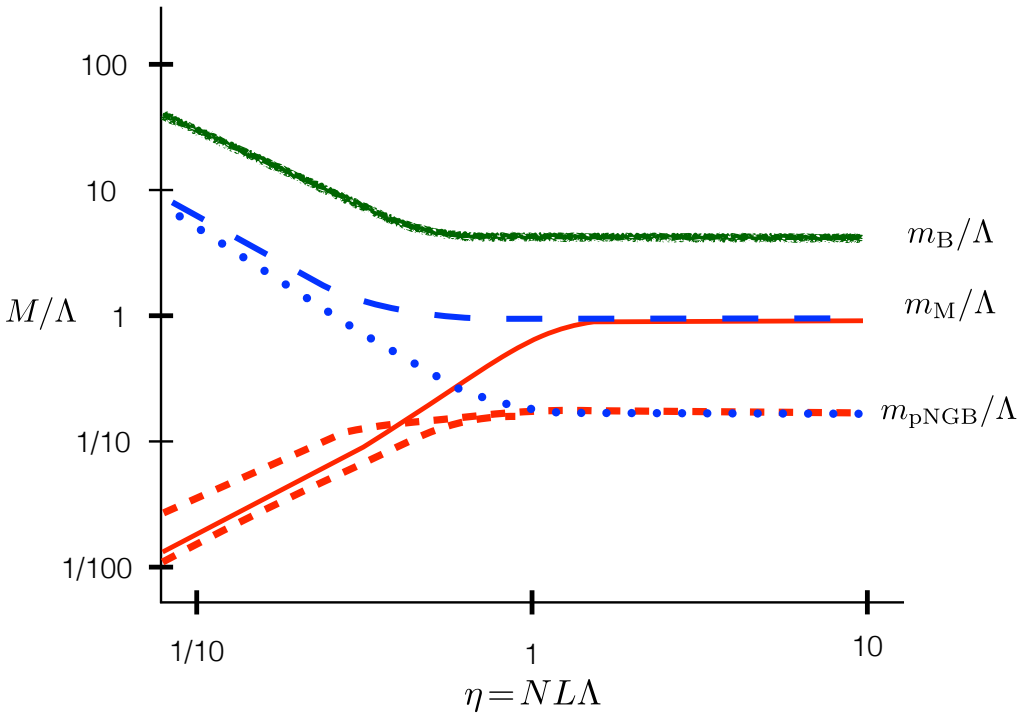

Figure 8. [Color online.] A sketch of a possible interpolation of the spectrum as the circle size L is varied in adiabatically compactified QCD with $n_f = N$ and $0 < m_q \ll \Lambda$. In this log-log cartoon, masses are in units of Λ and the abscissa $\eta \equiv NL\Lambda$. The short-dashed red and dotted blue curves correspond to the neutral and charged pNGBs, respectively. At small L, the neutral pNGBs are dual photons, while the charged pNGBs are non-relativistic quark-antiquark bound states. The large splitting in their masses at small L is due to the partial breaking of flavor symmetry to its Cartan subgroup by our flavor-twisted boundary conditions. The solid red curve represents the lightest flavor singlet meson which, at small L, is a bound state of dual photons. The long-dashed blue curve represents glueballs and other mesons (both flavor singlet and non-singlet) which are not pNGBs and which, at small L, are bound states of W-bosons. The fuzzy green curve at the top of the figure represents the evolution of the mass of a baryon from small to large L.

states, with masses $m_{\rm light} \sim [\mathcal{O}(1/N)\text{–}\mathcal{O}(1)] \times \Lambda\, \eta^{5/6}$ (if double trace deformations stabilize center symmetry). The $N-1$ dual photons are charged under the center symmetry, indicating that they are topologically non-trivial excitations containing flux wrapping the compactified direction. These states cannot be created by topologically trivial local operators (acting on the vacuum) and will have masses which do not asymptote to finite limits at large L but rather grow linearly, $m \sim \sigma L$, with σ the decompactified YM string tension. The bound state of two dual photons with vanishing total center charge is the lightest topologically trivial glueball at small L, and can smoothly connect to the lightest glueball at large L. In the heavy sector at small L, W-boson bound states form

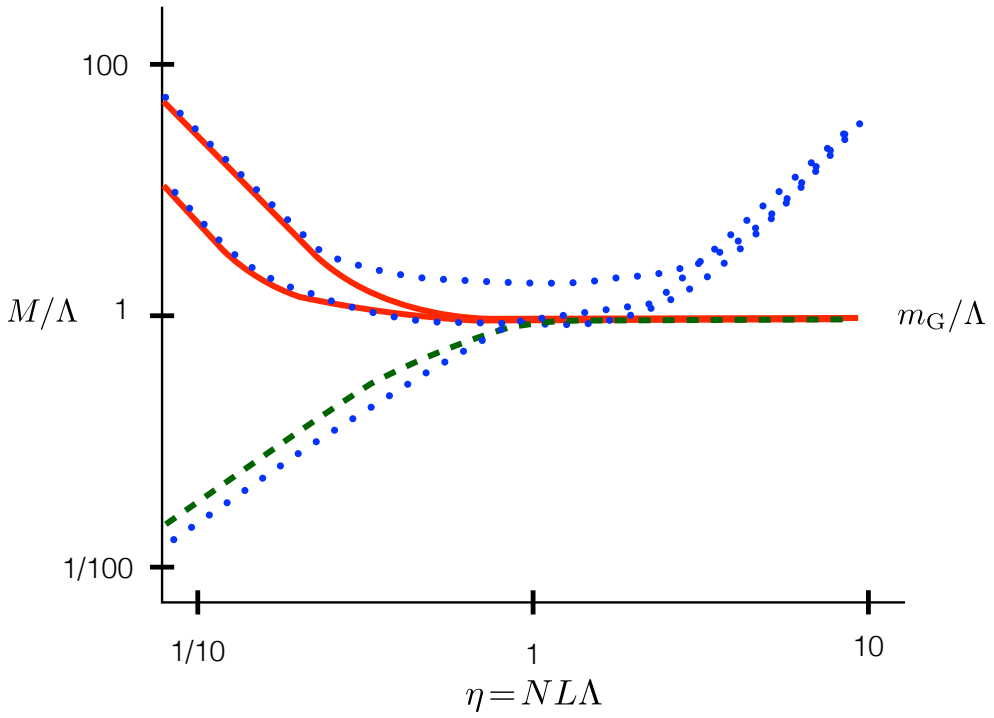

Figure 9. [Color online.] A sketch of a possible interpolation of the spectrum as the circle size L is varied in adiabatically compactified Yang-Mills. The illustration is for $N = 2$ for simplicity. The dashed green curve shows the lightest glueball, with vanishing center charge, which is a bound state of two dual photons at small L. The dotted blue curve with a positive slope at small η corresponds to the lightest topologically non-trivial "glueball" with non-zero center charge. This state is a dual photon at small L and evolves into a state with a linearly growing energy, $m \sim \sigma L$ at large L, where σ is the string tension. The two solid red curves correspond to center-neutral W-boson bound states, which evolve into ordinary glueballs at large L. The dotted blue curves with negative slope at small η correspond to W-boson states with non-zero center charge, which evolve into wrapped-flux states with a linearly diverging mass at large L.

nearly degenerate multiplets containing all values of center charge. Within each such multiplet, the vanishing center charge state can evolve into an ordinary topologically trivial glueball at large L, while the remaining states with non-zero center charge will have linearly diverging masses at large L.

Finally, when $1 \leq n_{\rm f} < N$, the overall picture is the same as the sketch shown in Fig. 8, except that the light sector at small L now contains $n_{\rm f}-1$ pseudo-Nambu-Goldstone bosons, with masses vanishing at $m_q = 0$, as well as non-pNGB states, namely the remaining $N-n_{\rm f}$ dual photons and their bound states. These non-pNGB

states have masses on the order of $m_{\rm light} \sim \Lambda\,\eta^b$ with an exponent $b > 0$ depending on $n_{\rm f}/N$. Whether these states should be described as glueballs or mesons, or some admixture, is not clear. There is no symmetry which clearly delineates a distinction. It should be possible to clarify the situation by computing the amplitudes with which these states are created by local fermion bilinears or Polyakov loop operators, but such an analysis has not yet been performed. In any case, these states can smoothly evolve into ordinary glueballs and mesons as $L \to \infty$. The same is true of the glueballs and mesons in the heavy sector at small L. Due to string breaking by dynamical quarks, none of these states will have masses which diverge as $L \to \infty$.

8.2 Large N behavior

Our analysis has been carried out with N arbitrary but fixed. The usual large N limit involves sending N to infinity while holding fixed the 't Hooft coupling λ (or equivalently the strong scale Λ). If the compactification size L is also held fixed, then the large N limit takes the compactified theory out of the regime $\eta = NL\Lambda \ll 1$ where a weak coupling analysis is possible and into the strongly coupled domain, $\eta \gg 1$, where large N volume independence applies [41, 71–75]. Our small η analysis adds nothing to the understanding of this limit.

However, it is interesting to consider an alternate $N \to \infty$ limit in which $\eta = NL\Lambda$ is held fixed. This is the key parameter which controls the physics of adiabatically compactified QCD-like theories. Viewing Λ as a fixed physical scale, fixing η requires reducing the compactification size as N increases, $L \propto 1/N$, or equivalently holding fixed $m_{\rm W} \equiv 2\pi/(NL)$. If η is fixed at a small value, then a weak coupling analysis remains valid for all N.

8.2.1 Heavy sector

Starting with the heavy non-relativistic sector, our results show that the glueball and meson spectra remain stable as $N \to \infty$ (regardless of whether $n_{\rm f} = N$, or $n_{\rm f} \ll N$). For example, the value of N simply never enters the result (6.24) for two-body glueball binding energies, while the only N dependence in meson binding energies (6.29) comes from the quark-antiquark interaction strength proportional to $1-\frac{1}{N}$. So masses of glueballs and mesons become N-independent at large N. The lightest baryon masses, as one would expect, grow linearly with N, but (based only on results at $N=2$ and $N \gg 1$) the ground state baryon binding energy per quark (6.58) and the shape of the single particle distribution (Fig. 6) are quite insensitive to N.

Similarly, the only N dependence in the glueball and meson radiative decay (7.3) and annihilation rates (7.11) arises from the same $1-\frac{1}{N}$ interaction strength factor for mesons. Given this, one might guess that glueball and meson scattering amplitudes

would also have finite, non-zero large N limits — but this is not entirely correct. If one ignores higher order radiative corrections then, for example, two-body mesons (at small η) may be labeled by the Cartan charge of their constituents. The amplitude for the elastic scattering process $M^a + M^b \to M^a + M^b$ arising from the exchange of one or more Cartan photons will include a trivial factor of δ_{ab} expressing the fact that both mesons must contain constituents charged under the same $U(1)$ factor if they are to scatter via photon exchange. When radiative corrections are included, the actual mass eigenstates are linear combinations of the fixed Cartan charge states which (for $n_{\rm f} = N$) have definite center charge (or more precisely, definite color-flavor center charge, as discussed in Ref. [44]), $\widetilde{M}^p = N^{-1/2} \sum_a \omega^{-ap} M^a$. The resulting scattering amplitude for $\widetilde{M}^p + \widetilde{M}^q \to \widetilde{M}^{p'} + \widetilde{M}^{q'}$, is $\mathcal{O}(1/N)$ for all center charges satisfying $p+q = p'+q'$, instead of $\mathcal{O}(1)$ for coinciding Cartan charges and zero otherwise.

The same argument applies to glueballs. Consider, for simplicity, glueballs which are bound states of two W-bosons, with either $n_{\rm f} = 0$ or $n_{\rm f} = N$ (so the compactified theory has either an ordinary, or intertwined color-flavor center symmetry). As discussed in Sec. 6.3.1, glueballs in our small η regime, before diagonalizing center symmetry, may be labeled by a *single* Cartan index plus the ordered compact momenta of their W-boson constituents. (Subsequent Cartan indices are determined by the mass formula (4.9), which in turn is a consequence of the adjoint Higgs mechanism operative at small η.) The transformation to a mass eigenstate basis with definite center charge involves exactly the same discrete Fourier transform as for mesons, $\widetilde{G}^p = N^{-1/2} \sum_a \omega^{-ap} G^a$. The resulting $2 \leftrightarrow 2$ scattering amplitude for $\widetilde{G}^p + \widetilde{G}^q \to \widetilde{G}^{p'} + \widetilde{G}^{q'}$ is suppressed by $1/N$ for all center charges satisfying $p+q = p'+q'$.

More generally, scattering amplitudes at small η involving K external particles (incoming plus outgoing) scale as $\mathcal{O}(N^{1-\frac{1}{2}K})$. This holds for processes involving any combination of light dual photons and heavy sector bound states (either mesons or glueballs) with $\mathcal{O}(1)$ constituents, provided at least one of the particles in the scattering process is a heavy sector bound state. (Scattering involving only dual photons is discussed below.) This relation shows that decay amplitudes into two particle final states are $\mathcal{O}(N^{-1/2})$, so decay rates to exclusive two particle final states are suppressed by $1/N$. That may appear inconsistent with the $\mathcal{O}(1)$ total radiative and annihilation rates computed in Sec. 7, but inclusive decay rates sum over all accessible final states. Because the splittings between states with differing center charge are parametrically smaller than heavy sector binding or rest energies (by powers of λ for heavy states, or $m_\gamma/m_{\rm W}$ for light dual photons), inclusive $1 \to 2$ decay rates pick up a factor of N from summing over all possible center charges of the final state particles consistent with the

initial state center charge.[31] The same logic shows that while fully exclusive $2 \leftrightarrow 2$ scattering rates are $\mathcal{O}(N^{-2})$, inclusive $2 \leftrightarrow 2$ scattering rates for mesons and glueballs are $\mathcal{O}(N^{-1})$ as $N \to \infty$.

Meson-baryon scattering amplitudes scale as $\mathcal{O}(N^0)$, since a quark (or antiquark) with any given Cartan index can interact with the quark having the same Cartan index in the baryon. The same scaling holds for glueball-baryon scattering (for both heavy sector bound state glueballs, and light dual photons). Baryon-baryon scattering amplitudes are $\mathcal{O}(N)$, since every quark in one baryon can interact via an unbroken $U(1)$ gauge group with one of the quarks in the other baryon.

These large N scaling relations at small η may be compared with conventional large N behavior when Λ and L are held fixed, and hence $\eta \to \infty$. It will be interesting to compare with conventional behavior in both the 't Hooft ($n_{\rm f}$ fixed as $N \to \infty$) and Veneziano ($n_{\rm f}/N$ fixed as $N \to \infty$) limits. In all cases, meson and glueball spectra are stable as $N \to \infty$, while the lightest baryon masses grow linearly with N. One unusual consequence of our flavor-twisted boundary conditions, at small η, is that baryons composed of only a single flavor of quark (or more generally $\mathcal{O}(1)$ different flavors) have masses which grow quadratically with N.

In the standard 't Hooft large N limit, glueball scattering amplitudes scale as $\mathcal{O}(N^{2-K_g})$, with K_g the number of external glueballs (incoming plus outgoing) [68]. For processes involving mesons, possibly with additional glueballs, the scaling of scattering amplitudes becomes $\mathcal{O}(N^{1-K_g-\frac{1}{2}K_m})$, where K_m is the number of external mesons. Hence, meson decay widths are $\mathcal{O}(N^{-1})$ and glueball decay widths to either two glueball, or two meson final states are $\mathcal{O}(N^{-2})$. Rates for two glueballs to scatter into two glueballs, or into two mesons, are $\mathcal{O}(N^{-4})$, while $2 \leftrightarrow 2$ meson scattering rates are $\mathcal{O}(N^{-2})$. Baryon-baryon scattering amplitudes are $\mathcal{O}(N)$ while baryon-meson scattering amplitudes are $\mathcal{O}(1)$ [68].

In the Veneziano large N limit, the additional factors of $n_{\rm f} \propto N$ in sums over final states (assuming a common quark mass for all flavors) make both meson and glueball decay rates $\mathcal{O}(1)$. Hence, except for the lightest states in each symmetry channel, mesons and glueballs remain resonances, with finite lifetimes, as $N \to \infty$. The inclusive rate for two mesons to scatter into two mesons is $\mathcal{O}(N^{-1})$, while two glueballs can scatter into two mesons with an $\mathcal{O}(N^{-2})$ inclusive rate, parametrically faster than the $\mathcal{O}(N^{-4})$ rate for pure glueball scattering.

Comparing these conventional large η scaling relations with our small η results, one sees that for mesons our $\mathcal{O}(N^0)$ total decay rates, $\mathcal{O}(N^{-1})$ inclusive two particle

[31] This assumes the decay channel is not parametrically close to threshold, so that the decay kinematics is insensitive to the splittings between final state particles with differing center charges.

scattering rates, and $\mathcal{O}(N^{-2})$ exclusive two particle rates all coincide with the behavior of mesons in the Veneziano limit. The scaling of our baryon-baryon and baryon-meson scattering amplitudes is the same as in conventional large N limits. But the fact that, at small η, glueball processes have the *same* large N scaling as mesons is quite peculiar.

Two significant features contribute to this change in behavior of glueball dynamics between large and small η. First is the adjoint Higgs mechanism induced by the center-symmetric holonomy at small η. This suppresses fluctuations in off-diagonal components of the $SU(N)$ gauge field, so that only the $N-1$ gluonic degrees of freedom play a singificant role in resonance formation, scattering, and decay. In contrast, at large η there are huge fluctuations in the holonomy and all N^2 gluonic degrees of freedom contribute to every glueball operator. This leads to the familiar $1/N^2$ suppression factors in exclusive decay rates and $2 \to 2$ scattering amplitudes of glueballs. A second essential difference at large and small η is the contribution of states with non-zero center charge. At $n_{\rm f} = 0$, such states have linearly diverging energy as $\eta \to \infty$ (as shown in Fig. 9), and play no role in scattering processes involving $\mathcal{O}(N^0)$ energies. But at small η these topologically non-trivial states become nearly degenerate in energy with vanishing center charge states, and dominate inclusive scattering and decay rates at large N.

8.2.2 Light sector

Turning now to the light sector, when $n_{\rm f} \ll N$, the smallest non-zero dual photon mass is $\mathcal{O}(m_\gamma/N)$. Holding η fixed as $N \to \infty$ implies that the light scale m_γ is also held fixed. Consequently, the lightest (non-Goldstone boson) mass vanishes as $N \to \infty$.

The interpretation and consequences of the vanishing of the mass of the lightest non-Goldstone boson excitations in the small-η large N limit were the focus of Ref. [76]. At very low energies, small compared to m_γ, the theory does not flow to a trivial fixed point. Rather, to all orders in the semi-classical expansion the low energy theory becomes gapless as $N \to \infty$. The low energy dynamics at $N = \infty$ is most naturally written as a *four-dimensional* theory, despite the fact that the "parent" UV theory was compactified on a tiny circle. The fourth dimension in the low energy, large N dynamics is emergent, appearing only on length scales large compared to m_γ^{-1}.

The results in this work are consistent with this picture, but do not shed much additional light on the origin or interpretation of this unexpected phenomena. The quartic interactions of dual photons, shown in Eq. (3.9), may be interpreted in the large N emergent dimension description as momentum-dependent interactions with vertex factors proportional to $1/N$ times the product of photon momenta in the emergent dimension. Consequently, for $\mathcal{O}(N^0)$ momenta (in the original spatial dimensions),

dual photon scattering amplitudes scale as $\mathcal{O}(N^{-1})$ at large N, the same as for heavy sector glueballs.

As shown in Eqs. (3.11) and (3.12), the dual photon binding energies (and momenta) discussed in Sec. 3 vanish exponentially as $N \to \infty$. So these bound states play no significant role at large N, and the emergence of the extra dimension in the light sector of the theory happens just as described in Ref. [76]. To understand how, e.g., the glueballs arising from W-boson bound states fit into the large N emergent dimension picture, recall that the emergent dimension appears as an N-site discretized circle with lattice spacing m_γ^{-1} [76]. A continuum 4D description is only relevant for physics with momenta small compared to m_γ. But at small η, the $\mathcal{O}(m_{\rm W})$ W-boson masses, their $\mathcal{O}(\lambda m_{\rm W})$ binding energies, and the $\mathcal{O}(\lambda^2 m_{\rm W})$ radiative corrections to binding energies are all large compared to m_γ. So the large N bound state dynamics does not involve the low energy emergent dimension, and must be treated using a 3D effective field theory, as done in the present paper.

8.3 Outlook

The analysis and results of this paper raise a number of questions which would be interesting to study in future work. First, as noted near the end of Sec. 7.1, we have not performed the matching calculation necessary to determine the $\mathcal{O}(\lambda)$ corrections to the rest mass parameters of the 3D non-relativistic EFT. Differences in the short distance corrections to the EFT rest masses are needed to determine the relative stability of meson, glueball, and heavy photon resonances whose leading order masses are identical. For example, the lightest glueball resonances with mass near $4m_{\rm W}$ might be composed of two W-bosons each with (tree level) mass $2m_{\rm W}$, or from four of the lightest W-bosons each with mass $m_{\rm W}$. Such glueball states are nearly degenerate with heavy photons having a tree-level mass of $4m_{\rm W}$. The results of a one-loop matching calculation of EFT rest energies would enable one to determine the relative ordering of these states. In particular, this would allow one to answer the interesting question of which near-extremal states are absolutely stable by virtue of minimizing the ratio of mass to compact momentum, $M/|P_3|$.

Second, as emphasized in Sec. 6, the bound state spectra for glueballs, mesons, and baryons have an exponentially rising (Hagedorn) density of states. It is interesting that this Hagedorn scaling emerges as a consequence of a logarithmic potential within the domain of validity of non-relativistic quantum mechanics, in contrast to the common lore that Hagedorn scaling is characteristic of relativistic string dynamics. In any case, the implications of Hagedorn scaling in the density of states for the thermodynamics of adiabatically compactified QCD deserve further study. Previous work [19, 22, 27] considered the $SU(2)$ deformed Yang-Mills theory (see also Refs. [77, 78]), and argued

that a thermal confinement-deconfinement transition occurs near the temperature

$$\beta_c^{-1} \simeq \frac{\lambda m_{\rm W}}{4\pi^2}\,. \tag{8.1}$$

The picture behind this conclusion is that in the regime[32] $\zeta^{1/3} \ll \beta^{-1} \ll m_{\rm W}$, the dilute monopole-instanton gas representation of the 3D Euclidean vacuum effectively reduces to a dilute two-dimensional gas of magnetically charged particles subject to binary logarithmic interactions. At the same time, there is also a thermal gas of electrically charged particles, namely W-bosons. The thermal phase transition is believed to be driven by a competition between the effects of these electrically and magnetically interacting gases. However, in Refs. [19, 22, 27, 77, 78] the electrically-charged component of the gas was treated classically, and the existence of Hagedorn behavior in the density of states was not taken into account. It would be interesting to revisit these calculations in light of our results here, and clarify whether the temperature (8.1) is indeed a correct estimate of the phase transition temperature.

Next, it would be very interesting if lattice gauge theory simulations could be performed in both pure Yang-Mills and QCD exploring the cross-over regions in Figs. 8 and 9, along the lines of Refs. [20, 30]. This would require simulations in a variety of lattice volumes with one dimension having double trace center stabilizing terms and flavor-twisted boundary conditions on quarks.

Last, and perhaps most interesting from a phenomenological perspective, is the possibility of studying multi-baryon states at small L. To motivate this, recall that in the real world there is a wide separation between "nuclear" excitation scales relevant in multi-baryon systems and the energy scales characteristic of single baryons. For example, the saturation binding energy per nucleon of nuclear matter, roughly 14 MeV, is tiny compared to the ≈ 300 MeV energy required to excite a single nucleon beyond its ground state. Or, one may compare nuclear binding scales to nucleon masses of nearly a GeV. Both comparisons indicate a wide separation between nuclear and single-baryon energy scales. Moreover, lattice simulations indicate that the nuclear/hadronic scale separation persists even as quark masses are varied [79–81], and that it also persists when $N = 2$ instead of 3 [82], suggesting that this scale separation is robust feature of QCD. This scale separation is vital for essentially all phenomenological understanding nuclear physics, including the modeling of nuclei as a collection of individual nucleons.

The puzzle is that there is no fundamental explanation for this important experimentally-observed scale separation from QCD. For example, this scale separation is

[32] This temperature range is similar to, but slightly more restrictive than the condition for the validity of our non-relativistic EFT analysis, and is needed to justify the treatment of the monopole-instanton gas as two-dimensional.

not an automatic consequence of either the large N or chiral limits. The adiabatic small-L regime allows one to use straightforward numerical and analytic methods to study multi-baryon systems for any quark mass and any number of colors. Further exploration of QCD phenomenology on a small circle may thus yield useful insights into the long-standing and important puzzle of the separation between nuclear and hadronic energy scales in QCD.

Acknowledgments

We are grateful to M. Ünsal for helpful discussions. This work was supported, in part, by the U. S. Department of Energy via grants DE-FG02-00ER-41132 (A.C.) and DE-SC0011637 (K.A. & L.Y.) and by a Discovery Grant of the National Science and Engineering Research Council of Canada (E.P.). L. Yaffe thanks the University of Regensburg and the Alexander von Humboldt foundation for their generous support and hospitality during completion of this work.

A Non-relativistic EFT derivation

We denote $SU(N)$ indices by a, b, c, d, etc., each running from 1 to N, and define the set of $N \times N$ basis matrices $\{E^{ab}\}$ by $(E^{ab})_{cd} \equiv \delta_{ac}\,\delta_{bd}$. We use an N-dimensional basis for the root vectors β_{ab} ($a \neq b$). The positive roots are $\beta_{ab} = (0, ..., 0, 1, 0, ..., 0, -1, 0, ..., 0)$, $a < b$, with 1 and -1 in the a-th and b-th position, respectively; the negative roots are $\beta_{ba} = -\beta_{ab}$, $a < b$. The indices $\mu = 0, 1, 2$ denote the noncompact spacetime directions and $x^3 \equiv x^3 + L$ is the coordinate of the compact direction. The circumference $L \equiv 2\pi R$. The Cartan generators are denoted by $H^a \equiv E^{aa}$. The overall $U(1)$ photon coupling to $\sum_a H^a$ decouples from the $SU(N)$ dynamics and is introduced solely for the convenience of working with an N-dimensional weight basis. Since all weight vectors are orthogonal to the vector $(1, 1, 1, 1, ..., 1)$, the static interactions discussed below in Appendix B only involve $SU(N)$ charges which are neutral with respect to this overall $U(1)$.

Until otherwise specified [just before Eq. (A.9)], we write Euclidean space expressions in this appendix. The Yang-Mills Lagrangian $L = \frac{N}{4\lambda}\,\mathrm{tr}\,F_{\alpha\beta}^2$, with $F_{\alpha\beta}$ Hermitian. The 't Hooft coupling $\lambda \equiv Ng^2(m_{\rm W})$, where the scale $m_{\rm W} \equiv 1/(NR)$ denotes the lightest W-boson mass. We decompose the gauge field into components along the compact and noncompact directions,

$$A_3 = \sum_{1\le a\le N} A_3^a(x^\mu)\, H^a\,, \tag{A.1a}$$

$$A_\mu = \sum_{1\le a\le N} A_\mu^a(x^\mu, x^3)\, H^a + \sum_{1\le a<b\le N} W_\mu^{ab}(x^\mu, x^3)\, E^{ab} + W_\mu^{ab*}(x^\mu, x^3)\, E^{ba}\,. \tag{A.1b}$$

The expansion (A.1) is written in the unitary gauge, where the only nonzero gauge field components along the S^1 direction are the Cartan components and they have no x^3-dependence. The N real fields A_μ^a describe 3D photons in the Cartan subalgebra, while the $\frac{1}{2}(N^2-N)$ complex fields W_μ^{ab} $(a<b)$ in the off-diagonal elements describe charged W-bosons.

Next, we expand A_3^a around the center symmetric expectation value (2.4) of the holonomy, $A_3^a \equiv \rho^a/(NR) + \phi^a$, so that ϕ^a represents the fluctuations of the holonomy.[33] Plugging the expansion (A.1) into the Yang-Mills Lagrangian one obtains, up to quadratic order in the W-boson fields,

$$\begin{aligned}\mathcal{L}_{2W} = \frac{N}{4\lambda}\Bigg\{ &\sum_{1\le a\le N} F^a_{\mu\nu}\, F^{\mu\nu\, a} + 2\,\partial_\mu\phi^a\,\partial^\mu\phi^a + 2\,\partial_3 A^a_\mu\,\partial^3 A^{\mu\, a} \\ &+ \sum_{1\le a<b\le N} 2\left|\partial_\mu W^{ab}_\nu + i(A^a_\mu - A^b_\mu)\, W^{ab}_\nu - (\mu\leftrightarrow\nu)\right|^2 \\ &+ 4\left|\left(-i\partial_3 + \tfrac{a-b}{RN} + \phi_b - \phi_a\right) W^{ab}_\mu\right|^2 + 2i\left(F^a_{\mu\nu} - F^b_{\mu\nu}\right) W^{ab}_{[\mu}\, W^{ab*}_{\nu]}\Bigg\}\,. \end{aligned} \tag{A.2}$$

The second line shows explicitly that the W-boson field W_μ^{ab} has charge $+1$ and -1 under the a-th and b-th Cartan $U(1)$ gauge groups, respectively. Hereafter, we neglect the fluctuations ϕ^a of the holonomy; as explained in Sec. 4, they play no role in the dynamics to the order that we study. (These neutral fluctuations are gapped by the perturbative center-stabilization mechanism.)

Next, we derive the leading-order EFT valid for momenta $p \ll m_{\rm W}$ (but large compared to the non-perturbatively induced mass gap (2.12), $p \gg m_\gamma$). This EFT describes the interactions of charged massive W-bosons with the (perturbatively) massless Cartan photons and with the "heavy photons," modes in the Kaluza-Klein (KK) tower containing the Cartan photon fields. (See Ref. [83] for a closely related treatment.)

As a final step before considering the $p \ll m_{\rm W}$ non-relativistic limit, we rewrite the Lagrangian (A.2) in a mass (or KK) eigenstate basis. The KK expansions are defined as usual, e.g.,

$$A^a_\mu(x^\nu, x^3) = \sum_{n=-\infty}^{\infty} e^{ix^3 n/R}\, A^{a,n}_\mu(x^\nu)\,, \tag{A.3}$$

with $A^{a,-n}_\mu(x^\nu) = (A^{a,n}_\mu(x^\nu))^*$, and similarly for the W^{ab}_μ fields (without a corresponding reality condition). Inserting these expansions into the 4D Lagrangian (A.2), integrating

[33] Here, $\rho^a = \frac{1}{2}(N+1) - a$ are the components of the Weyl vector in our basis. The expectation value $\langle A_3^a\rangle = \rho^a/(NR)$ corresponds to $\mathbb{Z}_N$ symmetric eigenvalues of the holonomy and produces vanishing traces in the fundamental representation, $\langle \mathrm{tr}_F\, \Omega^k\rangle = 0$ for $k = 1, ..., N-1$.

over x_3 (and neglecting holonomy fluctuations), leads to an effective three-dimensional Lagrangian

$$\mathcal{L}^{3D} = \mathcal{L}_2 + \mathcal{L}_3 + \mathcal{L}'_3 + \cdots\,, \tag{A.4}$$

in which we separate, for convenience, quadratic, cubic, and higher order terms. The quadratic part is given by

$$\mathcal{L}_2 = \frac{NL}{4\lambda}\sum_{n=-\infty}^{\infty}\left(\sum_{1\le a\le N}\left|F^{a,n}_{\mu\nu}\right|^2 + 2\left|m^{aa}_n\,A^{a,n}_\mu\right|^2 + \sum_{1\le a<b\le N} 2\left|\partial_{[\mu}W^{ab,n}_{\nu]}\right|^2 + 4\left|m^{ab}_n\,W^{ab,n}_\mu\right|^2\right), \tag{A.5}$$

with the KK masses

$$m^{ab}_n \equiv m_{\rm W}|a-b+nN|\,, \qquad m_{\rm W}\equiv (NR)^{-1}\,. \tag{A.6}$$

The cubic terms contain the coupling of the Cartan photons to the charge currents of the W-bosons,

$$\mathcal{L}_3 = \frac{NL}{4\lambda}\sum_{m,n=-\infty}^{\infty}\sum_{1\le a<b\le N} 2i\partial_{[\mu}W^{ab,n*}_{\nu]}\left(A^{a,n-m}_{[\mu} - A^{b,n-m}_{[\mu}\right)W^{ab,m}_{\nu]} + (\text{h.c.}), \tag{A.7}$$

as well as their magnetic-moment coupling to the spin of the W-bosons,

$$\mathcal{L}'_3 = \frac{NL}{4\lambda}\sum_{m,n=-\infty}^{\infty}\sum_{1\le a<b\le N} 2i\left(F^{a,n-m}_{\mu\nu} - F^{b,n-m}_{\mu\nu}\right)W^{ab,m}_{[\mu}\,W^{ab,n*}_{\nu]}\,. \tag{A.8}$$

Quartic terms in the Lagrangian, if needed, can be worked out similarly.

We shall eventually return to our Lagrangian of interest, $\mathcal{L}^{3D}$, but first we discuss the construction of a non-relativistic effective field theory (NR EFT) in the simpler case of a single massive charged vector boson. To this end, let W_μ denote a 3D complex vector field with $U(1)$ gauge symmetry, $W_\mu \to e^{i\alpha}W_\mu$, and Lagrangian[34]

$$\begin{aligned} L = &-\frac{1}{4e^2}\left(\partial_{[\mu}A_{\nu]}\right)^2 - \tfrac{1}{2}\left|\partial_{[\mu}W_{\nu]}\right|^2 - M^2\,W_\mu W^{\mu *} \\ &+ i\,A^\mu\left(W^{\nu *}\,\partial_{[\mu}W_{\nu]} - W^\nu\,\partial_{[\mu}W^*_{\nu]}\right) - \tfrac{1}{2}\left|A_{[\mu}W_{\nu]}\right|^2 - \tfrac{i}{2}\,\partial^{[\mu}A^{\nu]}\,W_{[\mu}\,W^*_{\nu]}\,. \end{aligned} \tag{A.9}$$

This charged vector boson Lagrangian contains precisely the kinds of terms appearing in the Lagrangian (A.4)–(A.8) of our full theory. We use e^2 to denote the coupling constant of the massless photon. The leading-order correspondence with our full theory is

$$e^2 = \frac{\lambda}{NL} = \frac{\lambda m_{\rm W}}{2\pi}\,. \tag{A.10}$$

[34] At this point, we revert to Minkowski space expressions using a $(-,+,+)$ metric signature.

Note that the vector field W_μ has a conventional normalization, but we have chosen to scale the charge e out of covariant derivatives and define the photon field A_μ as having dimension 1.

A 3D massive vector field has two polarization states. Define polarization vectors $e^i_\mu(\mathbf{k})$, $i = 1, 2$, obeying $e^i_\mu(\mathbf{k})\, e^{j\,\mu}(\mathbf{k}) = \delta^{ij}$ and $k^\mu\, e^i_\mu(\mathbf{k}) = 0$, for on-shell momenta $k_\mu \equiv (|\mathbf{k}|, \mathbf{k})$. Explicitly,

$$e^1_\mu(\mathbf{k}) \equiv \Big(0, \frac{\widetilde{\mathbf{k}}}{|\mathbf{k}|}\Big)\,, \qquad e^2_\mu(\mathbf{k}) \equiv \Big(\frac{|\mathbf{k}|}{M}, \frac{\mathbf{k}}{|\mathbf{k}|}\frac{\omega_k}{M}\Big)\,, \tag{A.11}$$

where $\omega_k \equiv \sqrt{\mathbf{k}^2 + M^2}$ and $(\widetilde{\mathbf{k}})_i \equiv \epsilon_{ij}(\mathbf{k})_j$ (we use $i, j = 1, 2$ to denote spatial indices and take $\epsilon_{12} = -\epsilon_{21} = 1$). The free mode expansion of the second quantized field is

$$\begin{aligned} W_\mu(t, \mathbf{x}) &= \int \frac{d^2k}{(2\pi)^2\,\sqrt{2\omega_k}} \sum_{i=1}^{2} \left[e^{i(\omega_k t - \mathbf{k}\cdot\mathbf{x})}\, e^i_\mu(\mathbf{k})\, a^i(\mathbf{k})^\dagger + e^{-i(\omega_k t - \mathbf{k}\cdot\mathbf{x})}\, e^i_\mu(\mathbf{k})\, b^i(\mathbf{k})\right], \\ &\equiv W^+_\mu(t, \mathbf{x}) + W^-_\mu(t, \mathbf{x})\,, \end{aligned} \tag{A.12}$$

where $[a^i(\mathbf{k}), a^j(\mathbf{p})^\dagger] = [b^i(\mathbf{k}), b^j(\mathbf{p})^\dagger] = (2\pi)^2\delta^{ij}\,\delta^2(\mathbf{p}-\mathbf{k})$, and all other commutators vanish. It is convenient to denote by $W^\pm_\mu$ the positive frequency ($\propto e^{i\omega_k t}$) and negative frequency ($\propto e^{-i\omega_k t}$) parts, respectively. The $U(1)$ charge operator $Q \equiv \int d^2x\, 2\,\mathrm{Im}\big(W^{\nu\,*}\partial_0 W_\nu\big)$, after normal ordering, becomes $Q = \int \frac{d^2k}{(2\pi)^2} \sum_i \big[a^i(\mathbf{k})^\dagger a^i(\mathbf{k}) - b^i(\mathbf{k})^\dagger b^i(\mathbf{k})\big]$, from which it is evident that the operators $a^i(\mathbf{k})^\dagger$ ($a^i(\mathbf{k})$) are creation (annihilation) operators of positively charged vector bosons while the operators $b^i(\mathbf{k})^\dagger$ ($b^i(\mathbf{k})$) create (annihilate) negatively charged antiparticles. Polarization index i=1 (i=2) refers to particles with transverse (longitudinal) polarization, respectively. The free Hamiltonian $P_0 = \int \frac{d^2k}{(2\pi)^2}\, \omega_k \sum_i \big[a^i(\mathbf{k})^\dagger a^i(\mathbf{k}) + b^i(\mathbf{k})^\dagger b^i(\mathbf{k})\big]$ and has eigenvalue ω_k for all four single-particle states of a given spatial momentum $\mathbf{k}$.

Apart from explaining the physical content of the massive vector boson theory, the mode expansion (A.12) provides an easy way to see that an effective theory describing the dynamics of non-relativistic vector bosons can be expressed solely in terms of the spatial components W_i of the vector field W_μ. For small momenta, $|\mathbf{k}| \ll M$, the longitudinal polarization vector $e^2_\mu(\mathbf{k}) = \big(0, \frac{\mathbf{k}}{|\mathbf{k}|}\big) + \mathcal{O}\big(\frac{|\mathbf{k}|}{M}\big)$, with only spatial components to leading order. Since the transverse polarization vector $e^1_\mu(\mathbf{k})$ is purely spatial, in the non-relativistic limit the time component W_0 can be eliminated, leading to an effective theory for a spatial vector field.

One may construct the Lagrangian of this effective non-relativistic theory by writing all terms consistent with the symmetries and matching the coefficients to terms in the relativistic theory to the desired order in the small coupling and small momentum expansion (treating $\frac{|\boldsymbol{\nabla}|}{M} \sim \frac{|\mathbf{k}|}{M} \ll 1$, where $\boldsymbol{\nabla}$ is a spatial gradient.) To carry out

this procedure, we introduce two different two-component complex fields, $\vec{\phi}_+(t,\mathbf{x})$ and $\vec{\phi}_-(t,\mathbf{x})$. In a second-quantized non-relativistic theory, these fields (and their Hermitian conjugates) annihilate (or create) particles of charges $+1$ and -1, respectively. The two-component vector represents the direction in the two-dimensional polarization space. To leading order in the derivative and small-coupling expansion, the fields $\vec{\phi}_\pm$ can be considered as scalars under $SO(2)$ spatial rotations, with an emergent $SO(2)$ "flavor" symmetry acting as rotations in the polarization space. Magnetic moment interactions explicitly break this $SO(2)\times SO(2)$ symmetry down to the diagonal $SO(2)$. (This is completely analogous to the approximate spin rotation symmetry in light atoms and molecules when spin-orbit interactions can be neglected.)

Temporarily ignoring the gauge field A_μ, to lowest non-trivial order in powers of $\frac{\boldsymbol{\nabla}}{M}$, the Lagrangian of the NR EFT is

$$L_{\rm NR} = \vec{\phi}_+^{\,\dagger}\, i\partial_t\, \vec{\phi}_+ + \vec{\phi}_-^{\,\dagger}\, i\partial_t\, \vec{\phi}_- - M\,|\vec{\phi}_+|^2 - M\,|\vec{\phi}_-|^2 - \frac{|\boldsymbol{\nabla}\vec{\phi}_+|^2}{2m} - \frac{|\boldsymbol{\nabla}\vec{\phi}_-|^2}{2m}\,. \tag{A.13}$$

and the corresponding Hamiltonian is

$$H = \int d^2x\; \vec{\phi}_+(\mathbf{x})^\dagger \cdot \big(M - \tfrac{\boldsymbol{\nabla}^2}{2m}\big)\vec{\phi}_+(\mathbf{x}) + \vec{\phi}_-(\mathbf{x})^\dagger \cdot \big(M - \tfrac{\boldsymbol{\nabla}^2}{2m}\big)\vec{\phi}_-(\mathbf{x})\,. \tag{A.14}$$

The conserved charge $Q = \int d^2x\; (\vec{\phi}_+)^\dagger \cdot \vec{\phi}_+ + (\vec{\phi}_-)^\dagger \cdot \vec{\phi}_-$. Mode expansions of the non-relativistic fields read

$$\phi^i_+(t,\mathbf{x})^\dagger = \int \frac{d^2k}{(2\pi)^2}\, e^{i\varepsilon_k t - i\mathbf{k}\cdot\mathbf{x}}\, a^i(\mathbf{k})^\dagger\,, \quad \phi^i_-(t,\mathbf{x})^\dagger = \int \frac{d^2k}{(2\pi)^2}\, e^{i\varepsilon_k t - i\mathbf{k}\cdot\mathbf{x}}\, b^i(\mathbf{k})^\dagger\,, \tag{A.15}$$

where $\varepsilon_k \equiv M + \mathbf{k}^2/(2m)$, and $a^i(\mathbf{k})^\dagger$ and $b^i(\mathbf{k})^\dagger$ are the same creation operators appearing in the relativistic expansion (A.12) (and its Hermitian conjugate). The fields (A.15) satisfy non-relativistic canonical commutation relations, $[\phi^i_+(t,\mathbf{x}), \phi^j_+(t,\mathbf{y})^\dagger] = [\phi^i_-(t,\mathbf{x}), \phi^j_-(t,\mathbf{y})^\dagger] = \delta^{ij}\,\delta^2(\mathbf{x}-\mathbf{y})$, with other commutators vanishing.

To fix parameters in the NR EFT one demands that physical quantities, computed in the EFT and in the IR limit of the full theory, agree with each other order by order in the low energy and weak coupling expansions. At low orders, the matching is rather straightforward. In the free theory (A.13), single-particle states have energies $\varepsilon_{\mathbf{k}} = M + \frac{\mathbf{k}^2}{2m}$ and charges ± 1. This agrees with the energy and charge of low momentum states in the relativistic theory (A.9) provided both the rest mass parameter M, and the kinetic mass m, appearing in the non-relativistic theory (A.13) equal, at lowest order, the physical mass M of the original theory.

Note that if one ignores the explicit polarization vector dependence in the relativistic expression (A.12), then the operator $\phi^i_+(t,\mathbf{x})^\dagger$ corresponds, in the non-relativistic

limit and after a trivial rescaling by $\sqrt{2M}$, to the positive-frequency part W_i^+ of W_μ, while $\phi^i_-(t,\mathbf{x})^\dagger$ corresponds to the positive frequency part $(W_i^-)^\dagger$ of the conjugate field $W_\mu^\dagger$.

We now proceed to write down the NR EFT Lagrangian describing the theory (A.9) to leading order in the small-λ and derivative expansion. We choose to work in Coulomb gauge for the photon field A_μ. The time component A_0 is not an independent field but is determined by the charge distribution of the W-bosons via Gauss' law. We denote the vector boson charge density by

$$n(t,\mathbf{x}) = iW^{\nu\,*}\,\partial_{[0}W_{\nu]} - iW^\nu\,\partial_{[0}W^*_{\nu]}\,, \tag{A.16}$$

(neglecting higher order "seagull" contributions). Varying the action, the Lagrangian (A.9) gives $A_0(t,\mathbf{x}) = e^2\int d^2y\, G(\mathbf{x}-\mathbf{y})\, n(t,\mathbf{y})$, where the two-dimensional Laplacian Green's function G was defined in Eq. (4.3). Using this result to eliminate A_0 from the action, one obtains the Coulomb energy, $V_C \equiv -\frac{e^2}{2}\int d^2x\, d^2y\, n(t,\mathbf{x})\, G(\mathbf{x}-\mathbf{y})\, n(t,\mathbf{y})$, as a contribution to (minus) the Lagrangian. Ignoring, for the moment, interactions mediated by spatial components of the photons as these are higher order in the non-relativistic limit, our effective theory (A.13) changes, to leading order, only by the inclusion of the Coulomb energy in the action,

$$\begin{aligned} S_{\rm NR} = \int dt\, d^2x \left(\vec\phi_+^\dagger\, i\partial_t\, \vec\phi_+ + \vec\phi_-^\dagger\, i\partial_t\, \vec\phi_- - M\,|\vec\phi_+|^2 - M\,|\vec\phi_-|^2 - \frac{|\boldsymbol{\nabla}\vec\phi_+|^2}{2M} - \frac{|\boldsymbol{\nabla}\vec\phi_-|^2}{2M}\right) \\ + \frac{e^2}{2}\int dt\, d^2x\, d^2y\, n(t,\mathbf{x})\, G(\mathbf{x}-\mathbf{y})\, n(t,\mathbf{y})\,, \end{aligned} \tag{A.17}$$

where $n(t,\mathbf{x}) = \vec\phi_+(t,\mathbf{x})^\dagger\cdot\vec\phi_+(t,\mathbf{x}) - \vec\phi_-(t,\mathbf{x})^\dagger\cdot\vec\phi_-(t,\mathbf{x})$ is the non-relativistic limit of the vector boson charge density (A.16). The corresponding Hamiltonian is just

$$\begin{aligned} H = \int d^2x\, \vec\phi_+(\mathbf{x})^\dagger\cdot\big(M - \tfrac{\boldsymbol{\nabla}^2}{2M}\big)\vec\phi_+(\mathbf{x}) + \vec\phi_-(\mathbf{x})^\dagger\cdot\big(M - \tfrac{\boldsymbol{\nabla}^2}{2M}\big)\vec\phi_-(\mathbf{x}) \\ - \frac{e^2}{2}\int d^2x\, d^2y\, n(\mathbf{x})\, G(\mathbf{x}-\mathbf{y})\, n(\mathbf{y})\,. \end{aligned} \tag{A.18}$$

The action (A.17) or Hamiltonian (A.18) include all leading-order terms in the non-relativistic ($v/c \ll 1$) limit using the systematic power counting rules that we discuss next. (In what follows, $c \equiv 1$.)

Higher order terms which can appear in the NR EFT may be classified and ordered using a suitable power counting scheme for the operators and their matrix elements, evaluated in characteristic bound states.[35] This approach is now well-established for

[35] These are determined by solving the two-particle Schrödinger equation which results from projecting the Hamiltonian (A.18) into the two-particle Hilbert space.

3+1 dimensional Coulombic systems [67]. Compared to such systems, several important differences arise in our 2+1D theory. The first is that a particle of mass M moving in a non-relativistic orbit due to a central force $F \sim e^2/r$ moves at speed $v \sim e/\sqrt{M}$, for any orbit radius, rather than $v \sim e/\sqrt{Mr}$ as in a three dimensional $F \sim e^2/r^2$ central force field. The second is the appearance of $e^2 \ln(e^2/M)$ terms, non-analytic in the coupling, in the ground state energy [as seen in Eq. (6.8)], owing to the scaling properties of the logarithmic potential. Ignoring such logarithmic factors, the appropriate power counting is similar to that detailed in Ref. [67]: the size of bound states is of order $a_0 \sim (e^2 M)^{-1/2}$ and their characteristic binding energy $\Delta E \sim e^2$. For estimating the parametric dependence of matrix elements of arbitrary operators that may arise in the NR EFT Hamiltonian, evaluated in low-lying bound states of the lowest-order theory (A.18), we take[36] the fields $\vec{\phi}_\pm$ to scale as $\sqrt{e^2 M}$, time derivatives $\partial_t \sim e^2$, spatial derivatives $\nabla \sim \sqrt{e^2 M}$, and Coulomb-gauge scalar and vector potentials $eA_0 \sim e^2$ and $e\mathbf{A} \sim e^4/\sqrt{e^2 M}$. Thus, the field strengths scale as $e\mathbf{E} \sim e^2\sqrt{e^2 M}$ and $eB \sim e^4$. (Here, and below, we have rescaled the Maxwell action for the photon by e^2, to give the gauge field a conventional perturbative normalization.) Using these parametric estimates, it follows that all terms in the lowest-order NR Hamiltonian (A.18), excepting the rest-energy terms, are of order e^2, as required.

To assess the relative importance of higher order terms, we begin with the magnetic moment coupling of the vector bosons, the last term in the NR Lagrangian (A.9). Writing the leading terms consistent with the symmetries of the theory which couple the field strength tensor F_{ij} to the NR vector fields ϕ^i and $\phi^{i\,\dagger}$, one finds, to leading order in $1/M$, that there is a unique such term,

$$L_{\rm NR}^{\rm mag} = -\frac{i}{2M}\, eF_{ij}\left(\phi_+^{i\,\dagger}\phi_+^j - \phi_-^{i\,\dagger}\phi_-^j\right), \tag{A.19}$$

whose coefficient follows by matching to the relativistic form (A.9) using relations (A.11), (A.12), and (A.15). The above power counting rules show that magnetic moment interactions will shift bound state energy levels by an amount of order e^4/M, or a relative $\mathcal{O}(e^2/M)$ correction to binding energies.

Given our original choice (A.11) of polarization vectors, the NR fields $\phi_\pm^i$, $i = 1, 2$ annihilate vector bosons which are linearly polarized, either transverse or parallel to their momenta, respectively. However, using operators that create particles in eigenstates of S_z, the spin of the vector boson field $S_z = \int d^2x(\epsilon_{ij}\dot{W}_i W_j^* + \text{h.c.})$, is typically more convenient when discussing bound states in a central potential. Such operators

[36] These power counting rules for $\vec{\phi}_\pm$ follow, e.g., by demanding that $\int d^2x\, \phi^\dagger\phi \sim 1$ in a bound state of size a_0. For the remaining assignments, the arguments are the same as given in Ref. [67]; see also Ref. [84].

can be obtained by redefining our NR field operators as follows:

$$\begin{aligned} \phi^1_\pm &= \tfrac{1}{\sqrt{2}}\big(\phi^\uparrow_\pm + \phi^\downarrow_\pm\big)\,, & \phi^{1\,\dagger}_\pm &= \tfrac{1}{\sqrt{2}}\big(\phi^{\uparrow\,\dagger}_\pm + \phi^{\downarrow\,\dagger}_\pm\big)\,, \\ \phi^2_\pm &= \tfrac{1}{\sqrt{2}i}\big(\phi^\uparrow_\pm - \phi^\downarrow_\pm\big)\,, & \phi^{2\,\dagger}_\pm &= \tfrac{i}{\sqrt{2}}\big(\phi^{\uparrow\,\dagger}_\pm - \phi^{\downarrow\,\dagger}_\pm\big)\,. \end{aligned} \tag{A.20}$$

The new operators $\phi^{\uparrow\,\dagger}_\pm$ and $\phi^\uparrow_\pm$ obey canonical commutation relations and create or destroy vector bosons with $S_z = 1$, similarly, $\phi^{\downarrow\,\dagger}_\pm$ and $\phi^\downarrow_\pm$ create or destroy $S_z = -1$ states. Using these redefined fields, the magnetic moment coupling (A.19) becomes

$$L^{\rm mag}_{\rm NR} = -\frac{eB}{2M}\left(\phi^{\uparrow\,\dagger}_+\phi^\uparrow_+ - \phi^{\downarrow\,\dagger}_+\phi^\downarrow_+ - \phi^{\uparrow\,\dagger}_-\phi^\uparrow_- + \phi^{\downarrow\,\dagger}_-\phi^\downarrow_-\right), \tag{A.21}$$

showing that the magnetic moment couplings split, at order e^4/M, the level degeneracy of $\uparrow\uparrow$ and $\downarrow\downarrow$ bound states. In particular, the magnetic moment interaction term (A.21) leads to the spin-spin hyperfine interaction potential (local in 2D), discussed in Sec. 6.2.2.

Coefficients of further operators in the EFT can be found by matching scattering amplitudes between the full and effective theories, as done in continuum NRQED in Ref. [84]. (See Ref. [67] for matching in NRQCD using lattice gauge theory.) The resulting terms are dimensionally reduced versions of ones listed in the above references and include, for example, $\frac{e}{M^2}\big[C_1\,\nabla\cdot\mathbf{E}\;\phi^{j\,\dagger}_+\phi^j_+ + C_2\,(\partial_i E_j - \frac{1}{2}\delta_{ij}\nabla\cdot\mathbf{E})\,\phi^{i\,\dagger}_+\phi^j_+ + \cdots\big]$, whose coefficients can be found by matching scattering amplitudes in external static electric fields. The contribution of these operators to the bound state energies also scale as e^4/M. Additionally, there are a number of possible contact terms involving four non-relativistic fields, schematically of the form $e^2(\phi^\dagger\phi)^2$, that also contribute $\mathcal{O}(e^4/M)$ energy shifts. There are, of course, also corrections arising from higher orders in the expansion of the relativistic dispersion relation of the form $\phi^{i\,\dagger}_+\frac{\nabla^4}{M^3}\phi^i_+ + \cdots$. According to the power counting rules, these also contribute to bound state energies at order e^4/M. We have not systematically enumerated all possible higher order terms in the NR EFT and leave their detailed study and matching for future work.

To conclude this Appendix, we invite the reader to consider the transition from the non-relativistic effective theory (A.17) for our toy single vector boson model (A.9), to the effective theory (4.2) describing our full theory (A.4)–(A.8). The transition from the toy NR EFT (A.17) to our full EFT (4.2) is largely one of bookkeeping due to the proliferation of fields in the full theory. In brief, in the NR EFT (4.2), the fields $\vec{\phi}^{ab}$ with $a > b$ correspond to the field $\vec{\phi}_+$ of the toy model, while the fields $\vec{\phi}^{ab}$ with $a < b$ correspond to the $\vec{\phi}_-$ field of the single complex vector model. The charge densities (4.10) are the multi-field generalizations of toy model charge density (A.16). The Hamiltonian (A.18) is easily seen to give rise to the complete form (4.12) (with the same normal ordering issues discussed in Sec. 4).

B Light sector details

We start with the quadratic part (A.5) of the 4D action to remind the reader about the 3D photon-scalar duality and the normalization of the dual photon field used in dual description (2.8). The Cartan generators in the fundamental representation have eigenvalues given by the N weight vectors $\boldsymbol{\nu}_A$, $A = 1, ..., N$. In our basis and choice of normalization, the highest weight is $\boldsymbol{\nu}_1 = (1-\frac{1}{N}, -\frac{1}{N}, ..., -\frac{1}{N})$ and coincides with the first fundamental weight vector $\boldsymbol{\mu}_1$ of $su(N)$. Consider a static quark, or fundamental representation probe charge, placed at the origin of $\mathbb{R}^2$ and having some weight vector $\boldsymbol{\nu}$ characterizing its color charge. This adds a source to the 3D (Minkowskian, c.f. footnote 34) Lagrangian for the static (KK index $n = 0$) Cartan components of the gauge field, $-\frac{NL}{4\lambda} F^a_{\mu\nu} F^{\mu\nu\, a} + A^a_0(\mathbf{x})\, \nu^a\, \delta^2(\mathbf{x})$ (where a sum on a is implied, and ν^a is the a-th component of the quark's weight).

The resulting A^a_0 equation of motion, $\frac{NL}{\lambda}\, \nabla^2 A^a_0(\mathbf{x}) = \nu^a\, \delta^2(\mathbf{x})$, implies Gauss' law, $\oint_C dl\, \hat{n}^i \big(\frac{NL}{\lambda} F^a_{i0}\big) = \nu^a$, where the curve C encircles the origin (counterclockwise) and $\hat{n}$ is its outward normal. An N-component dual photon field $\boldsymbol{\sigma}$ may be introduced via the relation $\frac{NL}{\lambda}\, F^a_{i0} = \frac{1}{2\pi}\, \epsilon_{ij}\, \partial_j \sigma^a$ (with $\epsilon_{12} \equiv 1$). The choice of coefficient ensures that $\oint_C dl\, \hat{n}^i\, \epsilon_{ij}\, \partial_j\, \sigma^a = 2\pi\nu^a$, i.e., the monodromy of the dual photon field is 2π times the charge (the weight vector $\boldsymbol{\nu}$). To be consistent with probes in all fundamental representations, the dual photon field is defined to be periodic with a periodicity of 2π times the $su(N)$ weight lattice, generated by the fundamental weights $\{2\pi\boldsymbol{\mu}_A\}$. The 2+1D Lorentz invariant form of the above duality relation is $F^a_{\mu\nu} = \frac{\lambda}{2\pi NL}\, \epsilon_{\mu\nu\lambda}\, \partial^\lambda \sigma^a = \frac{\lambda m_{\rm W}}{4\pi^2}\, \epsilon_{\mu\nu\lambda} \partial^\lambda \sigma^a$ (with $\epsilon_{0ij} \equiv -\epsilon_{ij}$). To implement the duality, we replace the Maxwell part of the quadratic action (A.5) by $-\frac{NL}{4\lambda}\, F^a_{\mu\nu} F^{\mu\nu\, a} + \frac{1}{4\pi}\, \epsilon_{\mu\nu\lambda}\, F^{\mu\nu\, a}\, \partial^\lambda \sigma^a$. Treating σ^a and $F^a_{\mu\nu}$ as independent integration variables and integrating out the field strength $F^a_{\mu\nu}$, the resulting kinetic term for the dual photon is $\frac{\lambda}{8\pi^2 NL}\, (\partial_\lambda \sigma^a)^2 = \frac{\lambda m_{\rm W}}{16\pi^3}\, (\partial_\lambda \sigma^a)^2$, as shown in the light sector action (2.8).

The Coulomb energy V_C of two static charges with weights $\boldsymbol{\lambda}_1$ and $\boldsymbol{\lambda}_2$, separated by a distance r, can also be obtained from the above expressions. One finds $V_C = -\frac{\lambda m_{\rm W}}{4\pi^2}\, (\boldsymbol{\lambda}_1 \cdot \boldsymbol{\lambda}_2)\, \ln r$. The weights for W-bosons are root vectors, and since roots have length two, the interaction energy of oppositely charged static W-bosons is $\frac{\lambda m_{\rm W}}{2\pi^2} \log r$, as shown in Eqs. (6.6) and (6.23). For a fundamental quark and an antiquark of opposite weights, we have $-\boldsymbol{\lambda}_1 \cdot \boldsymbol{\lambda}_2 = \boldsymbol{\nu} \cdot \boldsymbol{\nu} = 1 - \frac{1}{N}$, hence they experience attraction of that strength, as shown in (6.27). On the other hand, a quark with weight $\boldsymbol{\lambda}_1 = \boldsymbol{\nu}$ and antiquark with weight $\boldsymbol{\lambda}_2 = -\boldsymbol{\nu}'$, with $\boldsymbol{\nu} \neq \boldsymbol{\nu}'$, experience repulsion since $-\boldsymbol{\lambda}_1 \cdot \boldsymbol{\lambda}_2 = \boldsymbol{\nu} \cdot \boldsymbol{\nu}' = -\frac{1}{N}$, as shown in Fig. 3. Likewise, it follows that quarks (or antiquarks) of different weights attract with strength $\frac{1}{N}$, as shown in Fig. 4.

Finally, a magnetic monopole-instanton of magnetic charge α (one of the affine

roots), is represented in the dual description by insertions of $e^{i\boldsymbol{\alpha}\cdot\boldsymbol{\sigma}(x)}$ ($x \in \mathbb{R}^3$). Hence the interaction action between two monopole-instantons of charges $\boldsymbol{\alpha}_1$ and $\boldsymbol{\alpha}_2$ can be obtained as $\langle e^{i\boldsymbol{\alpha}_1\cdot\boldsymbol{\sigma}(x_1)} e^{i\boldsymbol{\alpha}_2\cdot\boldsymbol{\sigma}(x_2)}\rangle = \exp\left[-\frac{2\pi^2}{\lambda m_{\rm W}}\frac{\boldsymbol{\alpha}_1\cdot\boldsymbol{\alpha}_2}{|x_1-x_2|}\right]$, where the expectation value was calculated with the free field portion of the $\boldsymbol{\sigma}$-field Lagrangian (2.8). A remark relevant for the thermal case is that, when reduced to two dimensions, the corresponding correlator becomes $e^{\frac{4\pi^2 T}{\lambda m_{\rm W}}\,\boldsymbol{\alpha}_1\cdot\boldsymbol{\alpha}_2\,\ln(|x_1-x_2|T)}$ for $|x_1-x_2| \gg 1/T$.

C Symmetry transformations

Let us choose to work in $A_3 = 0$ gauge, where the holonomy Ω is an independent degree of freedom. Regarding $A_\mu(x)$ as anti-Hermitian, and viewing the quark field q as an $N \times n_{\rm f}$ matrix of spinors, we will define $\Omega_F = \mathrm{diag}(\xi^{1/2}, \xi^{3/2}, \cdots, \xi^{N-1/2})$. Our boundary conditions (in both index-free and component forms) are

$$A_\mu(x_3{+}L) = \Omega\, A_\mu(x_3)\, \Omega^\dagger\,, \qquad A_\mu(x_3{+}L)^{ab} \simeq \omega^{a-b}\, A_\mu(x_3)^{ab}\,, \tag{C.1a}$$

$$q(x_3{+}L) = \Omega\, q(x_3)\, \Omega_F^\dagger\,, \qquad q(x_3{+}L)^{aA} \simeq \omega^{-\frac{N}{2}+(a-\frac{1}{2})}\, \xi^{-(A-\frac{1}{2})}\, q(x_3)^{aA}\,, \tag{C.1b}$$

where $\simeq$ means when Ω has the form (2.4).

Mode expansions

Suppose that Ω has the form (2.4) with negligible fluctuations, let $\mathbf{y} \equiv (y_1, y_2)$ denote the non-compact spatial coordinates, and ignore interactions. Then:

$$A_\mu(t, \mathbf{y}, x_3)^{ab} = \frac{1}{L}\sum_{n\in\mathbf{Z}} \int \frac{d^2p}{(2\pi)^2\sqrt{2\omega}} \Big[e^{-i(\omega t - \mathbf{p}\cdot\mathbf{y} - k_n^{ab} x_3)} e_\mu^i(\vec{p})\, \phi_i(\mathbf{p})_n^{ab} \\ - e^{i(\omega t + \mathbf{p}\cdot\mathbf{y} + k_n^{ab} x_3)}\, e_\mu^i(-\vec{p})^*\, \big(\phi_i(-\mathbf{p})_{-n}^{ba}\big)^\dagger \Big]\,, \tag{C.2}$$

where $\mu = 0, 1, 2$, the compact momentum $k_n^{ab} \equiv \frac{2\pi}{NL}(a - b + nN)$, the 3D spatial momentum $\vec{p} \equiv (p_1, p_2, k_n^{ab})$, and the frequency $\omega \equiv (\mathbf{p}^2 + (k_n^{ab})^2)^{1/2}$ (with dependence on $\mathbf{p}$, n, a and b implicit). The polarization vectors $\{e_\mu^i(\vec{p})\}$, $i = 1, 2$, satisfy 2+1D transversality, $p^\mu e_\mu^i = 0$, with $p^0 \equiv \omega$. This expansion satisfies BCs (C.1a), anti-Hermiticity and transversality of A_μ, and the 4D free wave equation $\Box A_\mu = 0$.

The corresponding mode expansion for the quarks is

$$q(t, \mathbf{y}, x_3)^{aA} = \frac{1}{L}\sum_{n\in\mathbf{Z}+\frac{1}{2}} \int \frac{d^2p}{(2\pi)^2\sqrt{2\omega}} \Big[e^{-i(\omega t - \mathbf{p}\cdot\mathbf{y} - k_n^{aA} x_3)}\, u_s(\vec{p})\, \psi_s(\mathbf{p})_n^{aA} \\ + e^{i(\omega t + \mathbf{p}\cdot\mathbf{y} + k_n^{aA} x_3)}\, u_{-s}(-\vec{p})\, \big(\chi_s(-\mathbf{p})_n^{aA}\big)^\dagger \Big]\,, \tag{C.3}$$

where the quark compact momentum is $k_n^{aA} \equiv \frac{2\pi}{NL}[(a-\frac{1}{2}) - \frac{N}{n_f}(A-\frac{1}{2}) + nN]$, the 3D spatial momentum $\vec{p} \equiv (p_1, p_2, k_n^{aA})$, and the frequency $\omega \equiv (\mathbf{p}^2 + (k_n^{aA})^2)^{1/2}$. The free particle spinors $u_s(\vec{p})$ have helicity $s = \pm 1$ and satisfy $\gamma_\alpha p^\alpha u_s(\vec{p}) = 0$ with $p^\alpha \equiv (\omega, \vec{p})$. In a chiral basis, $\gamma_0 \equiv \left(\begin{smallmatrix} 0 & 1 \\ -1 & 0 \end{smallmatrix}\right)$, $\gamma_i \equiv \left(\begin{smallmatrix} 0 & \sigma_i \\ \sigma_i & 0 \end{smallmatrix}\right)$, $\gamma_5 \equiv -i\gamma_0\gamma_1\gamma_2\gamma_3 = \left(\begin{smallmatrix} 1 & 0 \\ 0 & -1 \end{smallmatrix}\right)$, one has $u_+(\vec{p}) = \left(\begin{smallmatrix} \xi_+(\hat{p}) \\ 0 \end{smallmatrix}\right)$ and $u_-(\vec{p}) = \left(\begin{smallmatrix} 0 \\ \xi_-(\hat{p}) \end{smallmatrix}\right)$, where $\xi_\pm(\hat{p})$ are two-component spinors satisfying $\hat{p} \cdot \vec{\sigma}\, \xi_\pm(\hat{p}) = \pm\xi_\pm(\hat{p})$ with phase convention $\xi_\pm(\hat{p})^* = \pm i\sigma_2\, \xi_\mp(\hat{p})$. The free particle spinors satisfy $\gamma_5\, u_s(\vec{p}) = s\, u_s(\vec{p})$ and $u_s(\vec{p})^* = C u_{-s}(\vec{p})$ with $C \equiv i\gamma_5\gamma_2$ and $C^\dagger \gamma^\alpha C = (\gamma^\alpha)^*$. The above mode expansion satisfies the boundary conditions (C.1b) and the massless Dirac equation $\gamma^\alpha \partial_\alpha q = 0$.

The coordinate space EFT operators are just 2D spatial Fourier transforms of the momentum-space mode operators,

$$\vec{\phi}(\mathbf{y})_n^{ab} \equiv \int \frac{d^2p}{(2\pi)^2}\, e^{i\mathbf{p}\cdot\mathbf{y}}\, \vec{\phi}(\mathbf{p})_n^{ab}\,, \tag{C.4a}$$

$$\psi_\pm(\mathbf{y})_n^{aA} \equiv \int \frac{d^2p}{(2\pi)^2}\, e^{i\mathbf{p}\cdot\mathbf{y}}\, \psi_\pm(\mathbf{p})_n^{aA}\,, \tag{C.4b}$$

$$\chi_\pm(\mathbf{y})_n^{aA} \equiv \int \frac{d^2p}{(2\pi)^2}\, e^{i\mathbf{p}\cdot\mathbf{y}}\, \chi_\pm(\mathbf{p})_n^{aA}\,. \tag{C.4c}$$

Axial $U(1)_A^{n_f}$

Let $\boldsymbol{\theta} = \mathrm{diag}(\theta_1, \cdots, \theta_{n_f})$. The axial transformation is standard:

$$q(x) \to e^{i\gamma_5 \boldsymbol{\theta}} q(x)\,, \qquad\qquad q(x)^{aA} \to e^{i\gamma_5 \theta_A} q(x)^{aA}\,, \tag{C.5}$$

with $\gamma_5 \equiv (\gamma_5)^\dagger$. Non-invariance under the diagonal $U(1)_A$ only appears in the non-perturbative light sector. This transformation is produced by

$$\psi_\pm(\mathbf{p})_n^{aA} \to e^{\pm i\theta_A}\, \psi_\pm(\mathbf{p})_n^{aA}\,, \qquad\qquad \chi_\pm(\mathbf{p})_n^{aA} \to e^{\pm i\theta_A}\, \chi_\pm(\mathbf{p})_n^{aA}\,. \tag{C.6}$$

Building two-component operators, $\psi(\mathbf{p})_n^{aA} \equiv \left(\begin{smallmatrix} \psi_+(\mathbf{p})_n^{aA} \\ \psi_-(\mathbf{p})_n^{aA} \end{smallmatrix}\right)$ and $\chi(\mathbf{p})_n^{aA} \equiv \left(\begin{smallmatrix} \chi_+(\mathbf{p})_n^{aA} \\ \chi_-(\mathbf{p})_n^{aA} \end{smallmatrix}\right)$, this transformation is equivalent to

$$\psi(\mathbf{p})_n^{aA} \to e^{i\theta_A\sigma_3}\, \psi(\mathbf{p})_n^{aA}\,, \qquad\qquad \chi(\mathbf{p})_n^{aA} \to e^{i\theta_A\sigma_3}\, \chi(\mathbf{p})_n^{aA}\,. \tag{C.7}$$

Charge conjugation

Recall that N is assumed odd. Combine the basic charge conjugation transformation, $A_\mu \to A_\mu^*$, with global color and flavor permutations V and V_F, respectively, chosen to preserve the form (2.4) of Ω at the $\mathbb{Z}_N$ symmetric minimum and the quark boundary conditions,

$$V \equiv \|\delta_{a+b,N+1}\| = \|\delta_{\bar{a},b}\|\,, \qquad\qquad V_F \equiv \|\delta_{A+B,n_f+1}\| = \|\delta_{\bar{A},B}\|\,, \tag{C.8}$$

where $\bar{a} \equiv N+1-a$, $\bar{A} \equiv n_{\rm f}+1-A$. Note that $\Omega^* = V\,\Omega\,V^\dagger$ and $\Omega_F^* = V_F\,\Omega_F\,V_F^\dagger$. The action of charge conjugation is

$$\Omega \to V\Omega^* V^\dagger \simeq \Omega\,, \tag{C.9a}$$

$$A_\mu(x) \to V A_\mu(x)^* V^\dagger\,, \qquad A_\mu(x)^{ab} \to (A_\mu(x)^{\bar{a},\bar{b}})^* = -A_\mu(x)^{\bar{b},\bar{a}}\,, \tag{C.9b}$$

$$q(x) \to C(V q(x)^* V_F^\dagger)\,, \qquad q(x)^{aA} \to C(q(x)^{\bar{a}\bar{A}})^*\,, \tag{C.9c}$$

This transformation is produced by

$$\vec{\phi}(\mathbf{p})_n^{a\,b} \to -\vec{\phi}(\mathbf{p})_n^{\bar{b}\,\bar{a}}\,, \qquad \psi_s(\mathbf{p})_n^{aA} \to \chi_s(\mathbf{p})_{-n}^{\bar{a}\bar{A}}\,, \qquad \chi_s(\mathbf{p})_n^{aA} \to \psi_s(\mathbf{p})_{-n}^{\bar{a}\bar{A}}\,. \tag{C.10}$$

x_3 reflection

Let $y \equiv (x^0, x^1, x^2, L-x^3)$ denote the reflected coordinates. Combine the basic reflection, $A_\mu(x) \to A_\mu(y)$ (recall $A_3 \equiv 0$), with the global color and flavor permutations V and V_F defined above. Then the action of x_3 reflection is

$$\Omega \to V\Omega^\dagger V^\dagger \simeq \Omega\,, \tag{C.11a}$$

$$A_\mu(x) \to V A_\mu(y) V^\dagger\,, \qquad A_\mu(x)^{ab} \to A_\mu(y)^{\bar{a}\bar{b}}\,, \tag{C.11b}$$

$$q(x) \to R_3(V q(y) V_F^\dagger)\,, \qquad q(x)^{aA} \to R_3\, q(y)^{\bar{a}\bar{A}}\,, \tag{C.11c}$$

where R_3 satisfies $R_3^\dagger \gamma^\alpha R_3 = (1-2\delta_3^\alpha)\gamma^\alpha$ and in our chiral basis $R_3 = \gamma_5\gamma_3$. The free particle spinors satisfy $R_3 u_s(\vec{p}\,') = s u_{-s}(\vec{p})$ where $\vec{p}\,' \equiv (p_1, p_2, -p_3)$. This transformation is produced by

$$\vec{\phi}(\mathbf{p})_n^{ab} \to \vec{\phi}(\mathbf{p})_{-n}^{\bar{a}\bar{b}}\,, \qquad \psi_s(\mathbf{p})_n^{aA} \to -s\,\psi_{-s}(\mathbf{p})_{-n}^{\bar{a}\bar{A}}\,, \qquad \chi_s(\mathbf{p})_n^{aA} \to s\,\chi_{-s}(\mathbf{p})_{-n}^{\bar{a}\bar{A}}\,. \tag{C.12}$$

$\mathbb{Z}_N$ center

Assume here that either $n_{\rm f} = 0$, or $n_{\rm f} = N$. Combine the basic $\mathbb{Z}_N$ center transformation, $\Omega \to \omega\,\Omega$, with global color and flavor permutations P and P_F chosen to preserve the form (2.4) of Ω and the quark boundary condition,

$$P \equiv \|\delta_{a,b-1}\|\,, \qquad P_F \equiv \|\delta_{A,B-1}\|\,, \tag{C.13}$$

with color and flavor indices regarded as defined modulo N. Note that $P^\dagger \Omega P = \omega\,\Omega$ when Ω has the form (2.4), and similarly $P_F^\dagger \Omega_F P_F = \omega\,\Omega_F$. The action of a $\mathbb{Z}_N$ center transformation is

$$\Omega \to \omega\, P\Omega P^\dagger \simeq \Omega\,, \tag{C.14a}$$

$$A_\mu(x) \to P A_\mu(x) P^\dagger\,, \qquad A_\mu(x)^{ab} \to A_\mu(x)^{a-1,b-1}\,, \tag{C.14b}$$

$$q(x) \to P q(x) P_F^\dagger\,, \qquad q(x)^{aA} \to q(x)^{a-1,A-1} \tag{C.14c}$$

This transformation is produced by

$$\vec{\phi}_n^{ab}(\mathbf{p}) \to \vec{\phi}_{n-\delta_a+\delta_b}^{a-1,b-1}(\mathbf{p})\,, \quad \psi_n^{aA}(\mathbf{p}) \to \psi_{n-\delta_a+\delta_A}^{a-1,A-1}(\mathbf{p})\,, \quad \chi_n^{aA}(\mathbf{p}) \to \chi_{n-\delta_a+\delta_A}^{a-1,A-1}(\mathbf{p})\,, \quad \text{(C.15)}$$

where $\delta_a = 1$ if $a = 1$, otherwise 0. This is equivalent to relations (5.7) and (5.9).

References

[1] S. Scherer, *Introduction to chiral perturbation theory*, *Adv. Nucl. Phys.* **27** (2003) 277, [hep-ph/0210398].

[2] O. Aharony, S. S. Gubser, J. M. Maldacena, H. Ooguri, and Y. Oz, *Large N field theories, string theory and gravity*, *Phys. Rept.* **323** (2000) 183–386, [hep-th/9905111].

[3] E. Witten, *Anti-de Sitter space, thermal phase transition, and confinement in gauge theories*, *Adv. Theor. Math. Phys.* **2** (1998) 505–532, [hep-th/9803131].

[4] J. M. Maldacena and C. Nunez, *Towards the large N limit of pure $\mathcal{N} = 1$ superYang-Mills*, *Phys. Rev. Lett.* **86** (2001) 588–591, [hep-th/0008001].

[5] I. R. Klebanov and M. J. Strassler, *Supergravity and a confining gauge theory: duality cascades and χSB resolution of naked singularities*, *JHEP* **08** (2000) 052, [hep-th/0007191].

[6] J. Polchinski and M. J. Strassler, *The string dual of a confining four-dimensional gauge theory*, hep-th/0003136.

[7] T. Sakai and S. Sugimoto, *Low energy hadron physics in holographic QCD*, *Prog. Theor. Phys.* **113** (2005) 843–882, [hep-th/0412141].

[8] M. Mia, K. Dasgupta, C. Gale, and S. Jeon, *Five easy pieces: the dynamics of quarks in strongly coupled plasmas*, *Nucl. Phys.* **B839** (2010) 187–293, [arXiv:0902.1540].

[9] P. van Baal, *QCD in a finite volume*, hep-ph/0008206.

[10] M. Unsal, *Abelian duality, confinement, and chiral symmetry breaking in QCD(adj)*, *Phys.Rev.Lett.* **100** (2008) 032005, [arXiv:0708.1772].

[11] M. Unsal, *Magnetic bion condensation: a new mechanism of confinement and mass gap in four dimensions*, *Phys. Rev.* **D80** (2009) 065001, [arXiv:0709.3269].

[12] M. Unsal and L. G. Yaffe, *Center-stabilized Yang-Mills theory: confinement and large N volume independence*, *Phys. Rev.* **D78** (2008) 065035, [arXiv:0803.0344].

[13] M. Shifman and M. Unsal, *QCD-like theories on $R_3 \times S_1$: a smooth journey from small to large $r(S_1)$ with double-trace deformations*, *Phys. Rev.* **D78** (2008) 065004, [arXiv:0802.1232].

[14] M. Shifman and M. Unsal, *Multiflavor QCD* on $R_3 \times S_1$: studying transition from Abelian to non-Abelian confinement*, *Phys. Lett.* **B681** (2009) 491–494, [arXiv:0901.3743].

[15] M. Unsal and L. G. Yaffe, *Large-N volume independence in conformal and confining gauge theories*, *JHEP* **08** (2010) 030, [arXiv:1006.2101].

[16] M. Shifman and M. Unsal, *On Yang-Mills theories with chiral matter at strong coupling*, *Phys. Rev.* **D79** (2009) 105010, [arXiv:0808.2485].

[17] G. Cossu and M. D'Elia, *Finite size phase transitions in QCD with adjoint fermions*, *JHEP* **07** (2009) 048, [arXiv:0904.1353].

[18] J. C. Myers and M. C. Ogilvie, *Phase diagrams of $SU(N)$ gauge theories with fermions in various representations*, *JHEP* **07** (2009) 095, [arXiv:0903.4638].

[19] D. Simic and M. Unsal, *Deconfinement in Yang-Mills theory through toroidal compactification with deformation*, *Phys. Rev.* **D85** (2012) 105027, [arXiv:1010.5515].

[20] H. Vairinhos, *Phase transitions in center-stabilized lattice gauge theories*, *PoS* **LATTICE2011** (2011) 252, [arXiv:1111.0303].

[21] E. Thomas and A. R. Zhitnitsky, *Topological susceptibility and contact term in QCD. A toy model*, *Phys. Rev.* **D85** (2012) 044039, [arXiv:1109.2608].

[22] M. M. Anber, E. Poppitz, and M. Unsal, *2d affine XY-spin model/4d gauge theory duality and deconfinement*, *JHEP* **04** (2012) 040, [arXiv:1112.6389].

[23] E. Poppitz, T. Schäfer, and M. Unsal, *Continuity, deconfinement, and (super) Yang-Mills theory*, *JHEP* **10** (2012) 115, [arXiv:1205.0290].

[24] E. Poppitz, T. Schäfer, and M. Ünsal, *Universal mechanism of (semi-classical) deconfinement and theta-dependence for all simple groups*, *JHEP* **03** (2013) 087, [arXiv:1212.1238].

[25] P. C. Argyres and M. Unsal, *The semi-classical expansion and resurgence in gauge theories: new perturbative, instanton, bion, and renormalon effects*, *JHEP* **08** (2012) 063, [arXiv:1206.1890].

[26] P. Argyres and M. Unsal, *A semiclassical realization of infrared renormalons*, *Phys. Rev. Lett.* **109** (2012) 121601, [arXiv:1204.1661].

[27] M. M. Anber, S. Collier, E. Poppitz, S. Strimas-Mackey, and B. Teeple, *Deconfinement in $\mathcal{N} = 1$ super Yang-Mills theory on $\mathbb{R}^3 \times \mathbb{S}^1$ via dual-Coulomb gas and "affine" XY-model*, *JHEP* **11** (2013) 142, [arXiv:1310.3522].

[28] G. Cossu, H. Hatanaka, Y. Hosotani, and J.-I. Noaki, *Polyakov loops and the Hosotani mechanism on the lattice*, *Phys. Rev.* **D89** (2014), no. 9 094509, [arXiv:1309.4198].

[29] M. M. Anber, E. Poppitz, and B. Teeple, *Deconfinement and continuity between thermal and (super) Yang-Mills theory for all gauge groups*, *JHEP* **09** (2014) 040, [arXiv:1406.1199].

[30] G. Bergner and S. Piemonte, *Compactified $\mathcal{N} = 1$ supersymmetric Yang-Mills theory on the lattice: continuity and the disappearance of the deconfinement transition*, *JHEP* **12** (2014) 133, [arXiv:1410.3668].

[31] X. Li and M. B. Voloshin, *Metastable vacuum decay in center-stabilized Yang-Mills theory at large N*, *Phys. Rev.* **D90** (2014), no. 10 105028, [arXiv:1408.3054].

[32] M. M. Anber, E. Poppitz, and T. Sulejmanpasic, *Strings from domain walls in supersymmetric Yang-Mills theory and adjoint QCD*, *Phys. Rev.* **D92** (2015), no. 2 021701, [arXiv:1501.6773].

[33] M. M. Anber and E. Poppitz, *On the global structure of deformed Yang-Mills theory and QCD(adj) on* $\mathbb{R}^3 \times \mathbb{S}^1$, *JHEP* **10** (2015) 051, [arXiv:1508.0910].

[34] T. Misumi and T. Kanazawa, *Adjoint QCD on* $\mathbb{R}^3 \times S^1$ *with twisted fermionic boundary conditions*, *JHEP* **06** (2014) 181, [arXiv:1405.3113].

[35] A. Cherman, T. Schäfer, and M. Ünsal, *Chiral lagrangian from duality and monopole operators in compactified QCD*, *Phys. Rev. Lett.* **117** (2016), no. 8 081601, [arXiv:1604.6108].

[36] Y. B. Rumer, *Negative and limiting temperatures*, *Soviet Physics JETP* **11** (1960), no. 6 1365.

[37] R. Hagedorn, *Statistical thermodynamics of strong interactions at high-energies*, *Nuovo Cim. Suppl.* **3** (1965) 147–186.

[38] D. J. Gross, R. D. Pisarski, and L. G. Yaffe, *QCD and instantons at finite temperature*, *Rev. Mod. Phys.* **53** (1981) 43.

[39] N. Weiss, *The Wilson line in finite temperature gauge theories*, *Phys. Rev.* **D25** (1982) 2667.

[40] J. C. Myers and M. C. Ogilvie, *New phases of* $SU(3)$ *and* $SU(4)$ *at finite temperature*, *Phys. Rev.* **D77** (2008) 125030, [arXiv:0707.1869].

[41] P. Kovtun, M. Unsal, and L. G. Yaffe, *Volume independence in large* N_c *QCD-like gauge theories*, *JHEP* **06** (2007) 019, [hep-th/0702021].

[42] T. Azeyanagi, M. Hanada, M. Unsal, and R. Yacoby, *Large-N reduction in QCD-like theories with massive adjoint fermions*, *Phys. Rev.* **D82** (2010) 125013, [arXiv:1006.0717].

[43] S. Catterall, R. Galvez, and M. Unsal, *Realization of center symmetry in two adjoint flavor large-N Yang-Mills*, *JHEP* **1008** (2010) 010, [arXiv:1006.2469].

[44] A. Cherman, S. Sen, M. Unsal, M. L. Wagman, and L. G. Yaffe, *Order parameters and color-flavor center symmetry in QCD*, arXiv:1706.5385.

[45] H. Kouno, Y. Sakai, T. Makiyama, K. Tokunaga, T. Sasaki, and M. Yahiro, *Quark-gluon thermodynamics with the* $Z(N_c)$ *symmetry*, *J. Phys.* **G39** (2012) 085010.

[46] Y. Sakai, H. Kouno, T. Sasaki, and M. Yahiro, *The quarkyonic phase and the* Z_{N_c} *symmetry*, *Phys. Lett.* **B718** (2012) 130–135, [arXiv:1204.0228].

[47] H. Kouno, T. Makiyama, T. Sasaki, Y. Sakai, and M. Yahiro, *Confinement and* $\mathbb{Z}_3$ *symmetry in three-flavor QCD*, *J. Phys.* **G40** (2013) 095003, [arXiv:1301.4013].

[48] H. Kouno, T. Misumi, K. Kashiwa, T. Makiyama, T. Sasaki, and M. Yahiro, *Differences and similarities between fundamental and adjoint matters in SU(N) gauge theories*, *Phys. Rev.* **D88** (2013), no. 1 016002, [arXiv:1304.3274].

[49] T. Iritani, E. Itou, and T. Misumi, *Lattice study on QCD-like theory with exact center symmetry*, *JHEP* **11** (2015) 159, [arXiv:1508.7132].

[50] H. Kouno, K. Kashiwa, J. Takahashi, T. Misumi, and M. Yahiro, *Understanding QCD at high density from a Z_3-symmetric QCD-like theory*, *Phys. Rev.* **D93** (2016), no. 5 056009, [arXiv:1504.7585].

[51] T. Hirakida, H. Kouno, J. Takahashi, and M. Yahiro, *Interplay between sign problem and Z_3 symmetry in three-dimensional Potts models*, *Phys. Rev.* **D94** (2016), no. 1 014011, [arXiv:1604.2977].

[52] T. Hirakida, J. Sugano, H. Kouno, J. Takahashi, and M. Yahiro, *Sign problem in Z_3-symmetric effective Polyakov-line model*, arXiv:1705.0665.

[53] H. Shimizu and K. Yonekura, *Anomaly constraints on deconfinement and chiral phase transition*, arXiv:1706.6104.

[54] A. M. Polyakov, *Quark confinement and topology of gauge groups*, *Nucl. Phys.* **B120** (1977) 429–458.

[55] F. J. Wegner and E. K. Riedel, *Logarithmic corrections to the molecular-field behavior of critical and tricritical systems*, *Phys. Rev. B* **7** (Jan, 1973) 248–256.

[56] M. J. Stephen, E. Abrahams, and J. P. Straley, *Logarithmic corrections to the mean-field theory of tricritical points*, *Phys. Rev. B* **12** (Jul, 1975) 256–262.

[57] R. D. Pisarski, *Tricritical logarithms in three dimensions*, *Physics Letters A* **85** (1981), no. 6 356 – 358.

[58] R. D. Pisarski, *Fixed point structure of ϕ^6 in three-dimensions at large N*, *Phys. Rev. Lett.* **48** (1982) 574–576.

[59] H. W. Hammer and D. T. Son, *Universal properties of two-dimensional boson droplets*, *Phys. Rev. Lett.* **93** (2004) 250408, [cond-mat/0405206].

[60] D. B. Kaplan, *Five lectures on effective field theory*, 2005. nucl-th/0510023.

[61] M. A. Shifman, *Theory of preasymptotic effects in weak inclusive decays*, in *Workshop on Continuous Advances in QCD Minneapolis, Minnesota, February 18-20, 1994*, pp. 249–286, 1994. hep-ph/9405246.

[62] D. Lee, *Large-N droplets in two dimensions*, *Phys. Rev.* **A73** (2006) 063204, [physics/0512085].

[63] C. B. Thorn, *Quark confinement in the infinite momentum frame*, *Phys. Rev.* **D19** (1979) 639.

[64] O. Atabek, C. Deutsch, and M. Lavaud, *Schrödinger equation for the two-dimensional coulomb potential*, *Phys. Rev. A* **9** (Jun, 1974) 2617–2624.

[65] C. Quigg and J. L. Rosner, *Quantum mechanics with applications to quarkonium*, *Phys. Rept.* **56** (1979) 167–235.

[66] J. Boyd, *Chebyshev and Fourier Spectral Methods: second revised edition*. Dover Books on Mathematics. Dover Publications, 2001.

[67] G. P. Lepage, L. Magnea, C. Nakhleh, U. Magnea, and K. Hornbostel, *Improved nonrelativistic QCD for heavy quark physics*, *Phys. Rev.* **D46** (1992) 4052–4067, [hep-lat/9205007].

[68] E. Witten, *Baryons in the* $1/N$ *expansion*, *Nucl.Phys.* **B160** (1979) 57.

[69] E. Witten, *Large N chiral dynamics*, *Annals Phys.* **128** (1980) 363.

[70] A. Cherman, S. Sen, M. L. Wagman, and L. G. Yaffe, *Exponential reduction of finite volume effects with twisted boundary conditions*, *Phys. Rev.* **D95** (2017), no. 7 074512, [arXiv:1612.0403].

[71] T. Eguchi and H. Kawai, *Reduction of dynamical degrees of freedom in the large N gauge theory*, *Phys. Rev. Lett.* **48** (1982) 1063.

[72] G. Bhanot, U. M. Heller, and H. Neuberger, *The quenched Eguchi-Kawai model*, *Phys. Lett.* **B113** (1982) 47–50.

[73] A. Gonzalez-Arroyo and M. Okawa, *A twisted model for large N lattice gauge theory*, *Phys. Lett.* **B120** (1983) 174–178.

[74] A. Gonzalez-Arroyo and M. Okawa, *The twisted Eguchi-Kawai model: a reduced model for large N lattice gauge theory*, *Phys. Rev.* **D27** (1983) 2397.

[75] M. Garcia Perez, A. Gonzalez-Arroyo, and M. Okawa, *Volume independence for Yang-Mills fields on the twisted torus*, *Int. J. Mod. Phys.* **A29** (2014), no. 25 1445001, [arXiv:1406.5655].

[76] A. Cherman and E. Poppitz, *Emergent dimensions and branes from large-N confinement*, *Phys. Rev.* **D94** (2016), no. 12 125008, [arXiv:1606.1902].

[77] G. V. Dunne, I. I. Kogan, A. Kovner, and B. Tekin, *Deconfining phase transition in (2+1)-dimensions: the Georgi-Glashow model*, *JHEP* **01** (2001) 032, [hep-th/0010201].

[78] Y. V. Kovchegov and D. T. Son, *Critical temperature of the deconfining phase transition in (2+1)-d Georgi-Glashow model*, *JHEP* **01** (2003) 050, [hep-th/0212230].

[79] S. R. Beane, E. Chang, S. Cohen, W. Detmold, H. W. Lin, K. Orginos, A. Parreno, M. J. Savage, and B. C. Tiburzi, *Magnetic moments of light nuclei from lattice quantum chromodynamics*, *Phys. Rev. Lett.* **113** (2014), no. 25 252001, [arXiv:1409.3556].

[80] A. Parreno, M. J. Savage, B. C. Tiburzi, J. Wilhelm, E. Chang, W. Detmold, and K. Orginos, *Octet baryon magnetic moments from lattice QCD: approaching experiment from a three-flavor symmetric point*, *Phys. Rev.* **D95** (2017), no. 11 114513, [arXiv:1609.3985].

[81] M. L. Wagman, F. Winter, E. Chang, Z. Davoudi, W. Detmold, K. Orginos, M. J. Savage, and P. E. Shanahan, *Baryon-baryon interactions and spin-flavor symmetry from lattice quantum chromodynamics*, arXiv:1706.6550.

[82] W. Detmold, M. McCullough, and A. Pochinsky, *Dark nuclei. II. Nuclear spectroscopy in two-color QCD*, *Phys. Rev.* **D90** (2014), no. 11 114506, [arXiv:1406.4116].

[83] M. M. Anber, *The Abelian confinement mechanism revisited: new aspects of the Georgi-Glashow model*, *Annals Phys.* **341** (2014) 21–55, [arXiv:1308.0027].

[84] T. Kinoshita and M. Nio, *Radiative corrections to the muonium hyperfine structure. 1. The $\alpha^2(Z\alpha)$ correction*, *Phys. Rev.* **D53** (1996) 4909–4929, [hep-ph/9512327].